CRC Report No. E-129-2

Alternative Oxygenate Effects on Emissions

November 2022

The Coordinating Research Council, Inc. (CRC) is a non-profit corporation supported by the petroleum and automotive equipment industries. CRC operates through the committees made up of technical experts from industry and government who voluntarily participate. The four main areas of research within CRC are: air pollution (atmospheric and engineering studies); aviation fuels, lubricants, and equipment performance; heavy-duty vehicle fuels, lubricants, and equipment performance (e.g., diesel trucks); and light-duty vehicle fuels, lubricants, and equipment performance (e.g., passenger cars). CRC's function is to provide the mechanism for joint research conducted by the two industries that will help in determining the optimum combination of petroleum products and automotive equipment. CRC's work is limited to research that is mutually beneficial to the two industries involved. The final results of the research conducted by, or under the auspices of, CRC are available to the public.

CRC Project E-129-2

Alternative Oxygenate Effects on Emissions

Jonathan Burton, Matthew Ratcliff, Cameron Hays, Earl D. Christensen, Peter C. St John, Gina M. Fioroni, Robert L. McCormick

National Renewable Energy Laboratory

October 2022

Executive Summary

Introduction and Methodology

The study described in this report extends the investigation of project E-129 to add key information to explain ethanol effects on particulate matter (PM) emissions and to examine additional oxygenates of interest. There were 19 fuels studied in the current project, see Table ES-1. The fuels covered a wide range of particulate matter index (PMI), from 1 to 2.75. Three hydrocarbon fuels were included, a certification gasoline and two base fuels into which oxygenates were splash blended. These were Fuel C (PMI=1.21) and Fuel D (PMI=2.75). Fuel C was originally developed as a low PMI fuel for CRC Project E-94-2 (*1*), and was used as the base fuel for CRC Project E-129 (*2*). Fuel D was developed as a high PMI fuel for CRC Project E-94-2 (*1*).The oxygenates blended at 3.7 and/or 5.5 wt% oxygen were methanol, ethanol, 1-propanol, isobutanol, dimethoxymethane (DMM), methyl-tert-butyl ether (MTBE), and ethyl-tert-butyl ether (ETBE). The fuels were characterized by detailed hydrocarbon analysis (DHA) that was used to calculate PMI as well as the NREL Sooting Index (*3*) and particulate matter emissions (+) index developed by CRC (*4*). DHA results produced at NREL were compared to results from Gage Products for all the fuels and to results from Separation Systems International (SSI) for two of the fuels. PMI values differed by an average of 0.22 PMI units between laboratories. PMI was well correlated with the NREL PM Index (R^2=0.94) and PME (R^2=0.86) such that there was no significant difference in the ability of these indices to predict fuel effects on emissions. A broad range of additional fuel properties were also measured including heat of vaporization and distillation.

Table ES-1. Fuels evaluated in this program.

Blendstock	Designation	PMI (measured at NREL)	Nominal Oxygen wt%	Nominal Oxygenate vol%
Cert Fuel*	--	1.29	0	0
Fuel C*	--	1.21	0	0
Fuel D	--	2.75	0	0
Methanol	D-MeOH-7	2.56	3.7	7
Methanol	D-MeOH-10	2.44	5.5	10.4
Ethanol*	C-EtOH-10	1.11	3.7	10
Ethanol*	C-EtOH-15	1.05	5.5	15
Ethanol	D-EtOH-10	2.46	3.7	10
Ethanol	D-EtOH-15	2.31	5.5	15
MTBE*	C-MTBE-19	1.00	3.7	19
MTBE	D-MTBE-19	2.29	3.7	19
n-Propanol	D-PrOH-13	2.47	3.7	13
n-Propanol	D-PrOH-20	2.28	5.5	19.5
i-Butanol*	C-iBu-16	1.06	3.7	16
i-Butanol	D-iBu-16	2.34	3.7	16
ETBE	D-ETBE-24	2.08	3.7	24
ETBE	D-ETBE-35	1.75	5.5	35
DMM	D-DMM-8	2.47	3.7	8
DMM	D-DMM-12	2.40	5.5	12

*Fuels also used in E-129 study.

The project evaluated these fuels in a single cylinder engine (SCE), with full control of fuel injection timing and of fuel spray impingement on the piston. Two engine operating conditions were examined: Condition A, a high speed, high load point (2500 rpm, 12.5 bar gross indicated mean effective pressure [gIMEP]) and Condition B an intermediate speed, high load point (1500 rpm, 12 bar gIMEP). At each condition, start of injection (SOI) was varied from later in the intake stroke where the piston has moved well away from top dead center (Figure ES-1 and Figure ES-2 – lower right) to earlier in the intake stroke where the piston is closer to top dead center and spray impingement on the piston is likely to occur (Figure ES-2 – upper right). Figure ES-1 shows example injector current traces which denote SOI (leading edge of the injection current) and end of injection (EOI, trailing edge of the current profile).

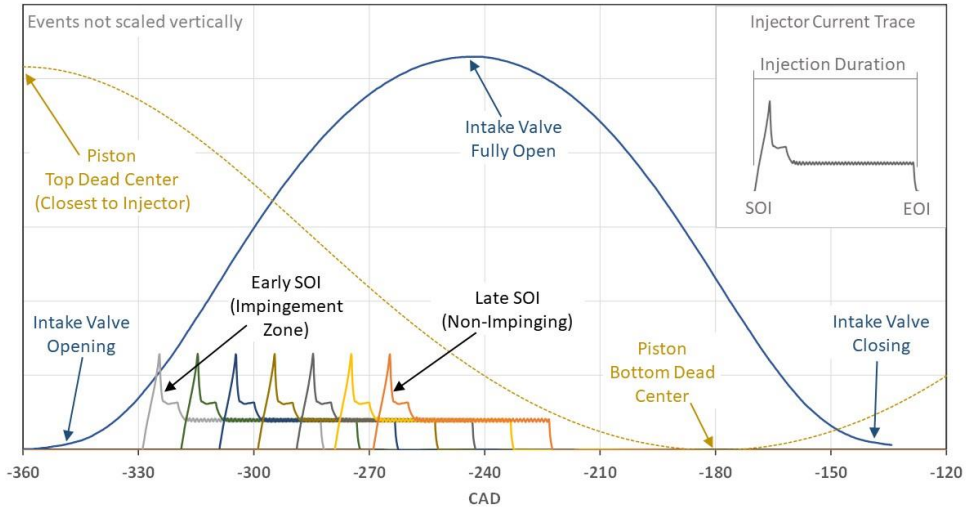

Figure ES-1. SOI sweep compared to intake valve opening/closing and piston position of the engine.

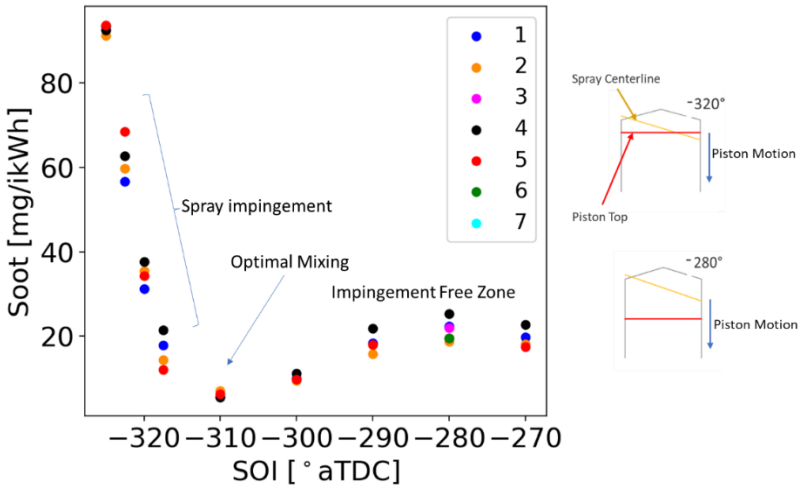

Figure ES-2. Example soot emissions for an SOI sweep (left). Seven replications are shown (not all replications extend over the entire SOI sweep) for fuel D-PrOH-13. Simple representations of piston and fuel spray (right).

Soot emissions for an example SOI sweep are shown in Figure ES-2 (left). At the most retarded injection point of -270° crank angle degrees (CAD) after top dead center (aTDC) shown in Figure ES-2, there is no impingement and soot emissions are relatively low. Moving to earlier (more advanced) injection first leads to a drop in soot as there is more time for mixing before spark. Beyond this point the spray impinges on the top of the piston. The CAD for the transition to spray impingement varies with fuel properties and engine operating conditions. Advancing SOI beyond the transition point, the soot emissions begin to rapidly increase because fuel spray impingement increasingly deposits fuel onto the piston as a film or pool. Fuel films or pools can burn in a diffusion flame that produces high levels of soot, rather than the nearly premixed combustion that occurs in the impingement free zone.

Measurements acquired from each sweep were brake specific soot and gaseous (NOx, CO, and hydrocarbons) emissions in mass per indicated kilowatt-hour (mg/ikWh for soot or g/ikWh for gases) in the spray impingement zone, the transition point location in CAD °aTDC between the impingement and non-impingement zones, and brake specific soot and gaseous emissions in the non-impingement zone. The results were interpreted in terms of the theory of competing effects of dilution of the heavy aromatic soot precursors by the oxygenate blendstocks versus the evaporative cooling effects of the high heat of vaporization (HOV) alcohols which may slow evaporation leading to rich zones that form soot. Vapor-liquid equilibria (VLE) effects that cause aromatics to evaporate later in the evaporation process may also be important for the lowest molecular weight alcohols that form high non-ideal solutions when blended with gasoline (*5*).

Important Observations

The observations described below represent statistically significant differences based on repeatability estimates.

Hydrocarbon fuels:

- Soot emissions in the non-impingement and impingement zones, and the transition to impingement generally trended with PMI. However, at a few non-impingement SOIs soot emissions overlapped within the measurement errors.

Fuel C blends:

- The MTBE blend shows the dilution of aromatics effect with the lowest soot under both engine speed conditions and the most advanced transition to impingement.
- Ethanol blends show no apparent dilution effect in the non-impingement zone as they produced similar soot emissions to Fuel C. This suggests that HOV/VLE effects counterbalanced dilution effects in these blends. The isobutanol blend shows similar dilution effect to MTBE in non-impingement.
- The E15 and isobutanol blends show the earliest transition to impingement and highest soot emissions in the impingement zone, while E10 is similar to Fuel C.

In the original CRC E-129 study these fuels were examined in four light-duty gasoline vehicles over the LA92 cycle. For the change in PM emissions averaged over the fleet of cars, relative to Fuel C the

ranking of the fuels was: Fuel C ≈ C-EtOH-10 > C-EtOH-15 > C-MTBE-19 ≈ C-iBu-16 (1). For these results, taken over a drive cycle covering a wide range of speed load conditions, the dilution effect to reduce soot was observed for E15, isobutanol, and MTBE – but not for E10 where the relatively low level of dilution may have been too small to measurably reduce PM – or alternatively, HOV/VLE effects may have been dominant at this relatively low dilution level. Also, dilution effects do not fully explain the E15 result as ethanol was present at significantly higher molar concentration than isobutanol or MTBE and therefore diluted aromatics to a greater extent than these oxygenates. Thus, a combination of dilution and HOV/VLE effects appear to have been occurring.

In the present study for non-impinging conditions the fuel ranking is:

- Condition A: Fuel C ≈ C-EtOH-15 ≈ C-EtOH-10 > C-iBu-16 > C-MTBE-19
- Condition B: Fuel C ≈ C-EtOH-15 > C-EtOH-10 > C-iBu-16 ≈ C-MTBE-19

As noted, E15 has the highest dilution of aromatics on a molar basis for this set of blends, yet consistently produces just as much soot as the base fuel for non-impinging conditions – which we attribute to the effect of ethanol's higher HOV or non-ideal VLE. E10, the isobutanol blend, and the MTBE blend all have similar levels of dilution on a molar basis, yet E10 has consistently higher soot emissions, likely for the same reasons as E15. These trends are not in line with PMI but can be explained based on dilution and HOV/VLE effects.

For impinging conditions, the following ranking was observed:

- Condition A: C-iBu-16 > Fuel C ≈ C-EtOH-10 > C-MTBE-19[1]
- Condition B: C-EtOH-15 > C-iBu-16 > Fuel C ≈ C-EtOH-10 > C-MTBE-19

The observation that the isobutanol blend moves from being one of the lowest soot forming fuels under non-impinging conditions to one of the highest soot forming fuels under impinging conditions clearly points to a change in the controlling physics for this fuel. Isobutanol's higher viscosity relative to other gasoline blending components, which translated into higher viscosity for the isobutanol blend, may be an important factor (*6*). Impinging condition results are clearly not in line with results of CRC E-129 suggesting that spray impingement on the piston is not widespread over the LA92 drive cycle.

Fuel D alcohol blends:

- Under high engine speed conditions (condition A) no dilution effects are observed in the non-impingement zone with the high-level methanol and ethanol blends showing increased soot, and other blends showing similar soot to the base fuel. At this engine speed there is also little difference between the fuels for the transition point to impingement. In the impingement zone alcohol blends generally showed similar or higher soot than the base fuel.
- At the lower engine speed conditions (condition B) dilution effects are observed in the non-impingement zone with increasing alcohol levels producing less soot and the correlation of soot

[1] Note that the experiment with C-EtOH-15 was not completed at this condition.

emissions with PMI is R^2=0.77. At this lower engine speed there is more time for heat transfer, evaporation, and mixing which may overcome HOV/VLE effects. At this condition D-iBu-16 had the most retarded transition point, similar to what was observed for C-iBu-16. In the impingement zone most alcohol blends increased soot relative to the base fuel.

Fuel D ether blends:

- At the high-speed condition (condition A) and non-impingement, MTBE and ETBE both reduced soot while the DMM blends caused soot to increase. All ethers slightly advanced the transition point with D-MTBE-19 having the most advanced and the lowest soot emissions in impingement – even though the ETBE blends had significantly more aromatics dilution on a molar basis. In the impingement zone the ETBE and DMM blends showed similar levels of soot, slightly lower than the base fuel.
- At the lower speed conditions of condition B, all fuels showed dilution effects in the non-impingement zone and there was a strong correlation of soot with PMI (R^2=0.93). MTBE showed the most advanced transition and lowest soot level in the impingement zone. D-DMM-8 showed the most retarded transition and highest soot, while other fuels were similar to the base fuel.

Key Findings

The present study varied SOI to achieve both non-impinging and impinging conditions. If engine calibrators primarily avoid spray impinging conditions, results at non-impinging conditions may be more representative. For Fuel C blends with ethanol under this condition, E15 showed similar soot emissions to the base fuel, with E10 showing the same or lower emissions. These results imply that HOV/VLE effects can produce fuel-rich zones even when the spray is not impinging on the piston. In this study, some spray may impinge on the cylinder liner, intake valves and cylinder head, and/or HOV/VLE effects may be large enough to slow droplet evaporation to the point that fuel rich zones exist in the gas phase at the time the charge is ignited. This contrasts with the apparent dominance of dilution in the original E-129 study. For Fuel D ethanol blends soot emissions increased relative to the base fuel at the high engine speed condition. However, at the lower engine speed condition dilution effects dominated such that ethanol blends reduced soot formation. Taken together, these results show that both HOV/VLE and dilution effects can impact soot formation from ethanol blends, depending on engine operating conditions and the properties of the base fuel. Lower engine speeds that provide more time for heat transfer, evaporation, and mixing favor dilution effects and hence lower soot.

The other oxygenates examined exhibited a wide range of behaviors. At the slow engine speed condition for non-impingement both alcohols and ethers showed a strong aromatics dilution effect to reduce soot formation, with moderate to strong correlations with PMI (Figure ES-3). However, at high speed and non-impingement HOV/VLE effects appeared to be dominant for alcohols, causing increased soot for methanol and ethanol, or the same soot as the base fuel for propanol and isobutanol in Fuel D, and therefore poor correlations with PMI. In the much lower PMI Fuel C, isobutanol showed dilution effects. These effects do not show a strong correlation with HOV, likely because dilution, HOV, and VLE

effects are of a different magnitude for each alcohol, and all affect the results. For the ethers, at high engine speed MTBE and ETBE reduce soot, while DMM blends increase soot. Additionally, soot levels for the ETBE blends, while reduced relative to the base Fuel D, were higher than observed for MTBE despite the much higher molar concentration (greater aromatics dilution) for the ETBE blends. Because these effects were not observed at low engine speeds, some aspects of ETBE and DMM properties appear to be inhibiting fuel evaporation and mixing enough to create fuel rich regions at high engine speed. To capture trends in PM emissions for the very wide range of oxygenate blends considered in this study new indices that more accurately represent both HOV/VLE effects as well as fuel property effects on the fuel spray will need to be developed.

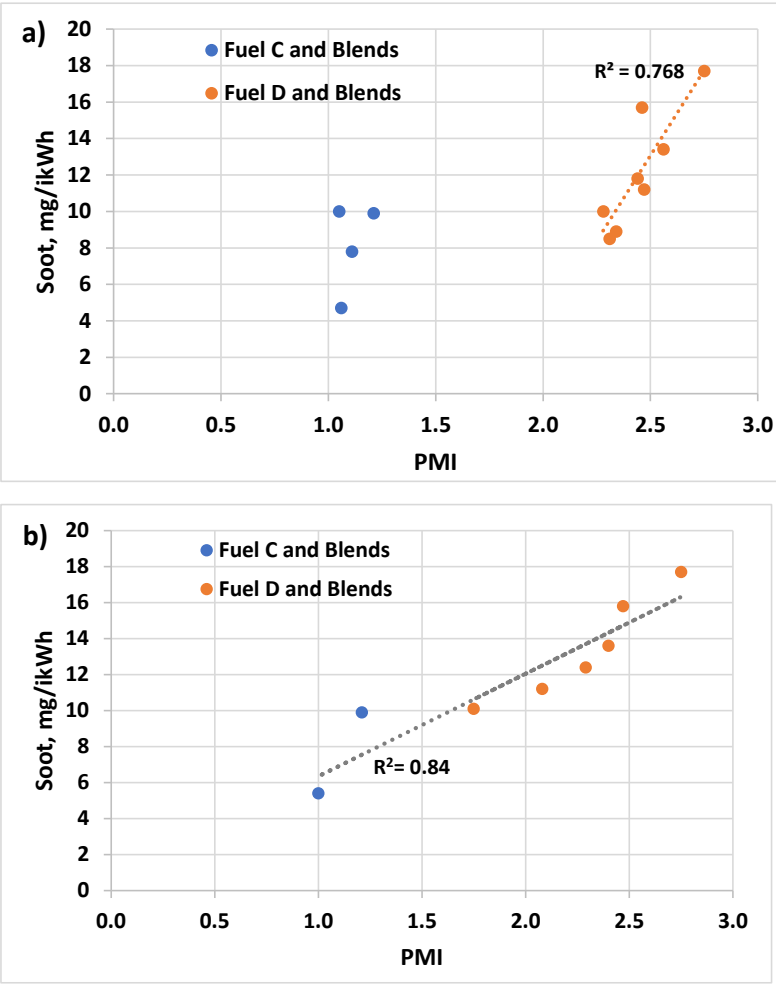

Figure ES-3. Soot emissions versus PMI for condition B, non-impingement a) alcohol blends where regression line is for Fuel D and blends only, correlation coefficient for soot with PMI for Fuel C and blends is <0.2, and b) ether blends where regression is for all fuels, correlation coefficient for Fuel D and blends only is 0.93.

Similar to the results for this study, specific questions that arise from the prior E-129 and E-94-2 studies would appear to be explainable by the interplay between aromatics dilution and HOV/VLE effects. In particular:

- Why does 10% ethanol fuel increase PM emissions in comparison to E0 fuels of equal PMI value in E-94-2? This result was observed at both low (1.4) and high (2.6) PMI values (*1*).
    - For the vehicles and test conditions used in E-94-2 the results suggest that HOV/VLE effects were more important than dilution effects.
- Why does 15% ethanol fuel not display the same emissions behavior as 10% ethanol in the E-129 study? In the E-129 study 10% ethanol had no statistically significant effect on PM, implying that any dilution effect was too small to be measured and/or that HOV/VLE effects were dominant over dilution (*2*).
    - Ethanol blends containing 15% reduced PM significantly, but not as much as isobutanol and MTBE blends. The result for E15 appears to be caused by a combination of dilution (PM emissions went down) and HOV/VLE effects (i.e., based on molar dilution only, PM emissions should have been lower than observed for isobutanol and MTBE).
- Why do the 15% ethanol, isobutanol and MTBE blends follow the PMI trend line for E0 fuels that was established in the prior CRC E-94-2 study, rather than being offset above like the 10% ethanol fuel?
    - The rationale is the same as for the question above. For E10 the effect of dilution is too small to see, or the result is dominated by HOV/VLE effects. While for E15 dilution effects reduce PM because of the higher blend level, but not as much as expected because of HOV/VLE.

A recommendation for future studies of oxygenates blended into base fuels is to perform a DHA on the base fuels, and then for the oxygenate blends to carefully measure the oxygenate content using an oxygenate-specific method. The DHA of the oxygenate blends can then be calculated from a material balance. While this clearly requires significantly fewer resources than measuring DHA for a large fuel set, it may also be more accurate as hydrocarbon species at relatively low concentrations are diluted by blending the oxygenate, making them even harder to quantify in the oxygenate blends. In addition, this approach obviates the need to quantify oxygenates using the DHA, which can be fraught with challenges.

A second recommendation is to measure a complete set of fuel properties for the fuels used in this or future studies. In particular, viscosity and surface tension can have a significant impact on fuel spray penetration, spray angle, and droplet mean diameter – all of which can impact spray impingement and fuel evaporation. Examination of how ethers impact aromatics evaporation may explain ether results that did not conform to the dilution theory. This could be conducted by DSC/TGA/MS, for example (*7*). Simulation of the evaporation of fuels from liquid films or pools with varying fuel properties may also provide insight.

The effects of much higher fuel injection pressure and split injections, which separately or combined can significantly reduce soot emissions, would be worthy of further investigation. Especially at condition A where high levels of methanol and ethanol increased soot relative to base fuel D and the ETBE blends did not significantly reduce soot. Similarly, condition B, where isobutanol retarded the transition point

and increased soot in the impingement zone, may be beneficially impacted by changing these injection parameters. Another interesting study to consider is the independent effect of fuel temperature on soot emissions and the onset of flash boiling impacts on soot – flash boiling occurs when the cylinder pressure during fuel injection is below the saturation vapor pressure of the fuel, producing radically different fuel atomization and mixing than in a standard spray (*8*).

The complex nature of the interaction between flow in the injector, spray physics, fuel evaporation (HOV/VLE), and aromatics dilution may require development or application of a high-performance computational model of fuel injection and evaporation.

It is important to note that this study was conducted using a warmed-up engine under steady-state conditions while real world vehicle operation, as well as emissions compliance testing, includes cold starting along with transient operation and complex speed-load changes. While the present results can provide insights into the physical phenomena governing fuel effects on soot emissions, predicted fuel impacts must be validated using full vehicle tests over complete driving cycles.

Contents

Executive Summary iii
Introduction and Methodology iii
Important Observations v
Hydrocarbon fuels: v
Fuel C blends: v
Fuel D alcohol blends: vi
Fuel D ether blends: vii
Key Findings vii
Contents xi
List of Figures xiii
List of Tables xv
List of Acronyms xvi
Introduction 1
Methods 3
Fuels Storage and Handling 3
Fuel Analysis 4
Detailed hydrocarbon analysis 4
Calculation of PM Indices and other Properties. 4
Standard fuel properties 6
Heat of vaporization 7
Engine Operation and Emissions 7
Results 10
Fuel Properties 10
Hydrocarbon base fuels 10
Fuel C blends 10
Fuel D blends 10
Fuel Properties Summary 14
Detailed Hydrocarbon Analysis and Calculated Properties 16
DHA and PIONA 16
HOV calculated from DHA 18
Particulate matter index and other soot formation metrics. 19
Engine Emissions 23
Hydrocarbon base fuels 26
Fuel C Blends 29
Fuel D Blends 33

Emissions Study Summary 40
Conclusions and Recommendations 47
References 50
Appendix A: Injection Pressure and λ Sweep Results 54
Appendix B: Fuel Test Order 59
Appendix C: Emissions Results Data 60
Fuel C Blends at Condition A 60
Fuel C Blends at Condition B 61
Fuel D Blends at Condition A 62
Fuel D Blends at Condition B 63
Appendix D: Discussion of Gaseous Emissions 64

List of Figures

Figure ES-1. SOI sweep compared to intake valve opening/closing and piston position of the engine..... iv
Figure ES-2. Example soot emissions for an SOI sweep (left), seven replications are shown (not all replications extend over the entire SOI sweep) for fuel D-PrOH-13. Simple representations of piston and fuel spray (right)..... iv
Figure ES-3. Soot emissions versus PMI for condition B, non-impingement a) alcohol blends where regression line is for Fuel D and blends only, correlation coefficient for soot with PMI for Fuel C and blends as <0.2, and b) ether blends where regression is for all fuels, correlation coefficient for Fuel D and blends only is 0.93..... viii
Figure 1. Volumetric energy density for fuels used in this study..... 14
Figure 2. Oxygenate content in the fuel blends in weight percent. 15
Figure 3. Oxygenate content in the fuel blends in mole percent. 15
Figure 4. Heat of vaporization for the study samples (calculated from DHA at 25°C and measured by DSC/TGA at 10°C). 16
Figure 5. Comparison of target oxygenate content with measured content, vol%, for Fuel C and Fuel D blends (parity line shown as dashed line)..... 18
Figure 6. Comparison of oxygenate analysis from Gage and NREL (parity line shown as dashed line). 18
Figure 7. HOV measured versus HOV calculated from DHA (parity line shown as dashed line). 19
Figure 8. Comparison of PMI values calculated by NREL, Gage Products, and SSI (parity line shown)..... 21
Figure 9. Impact of oxygenate blending on PMI (NREL measurements). 21
Figure 10. Comparison of NREL PM Index with PMI (linear regression line shown). 22
Figure 11. Comparison of PME with PMI (linear regression line shown). 23
Figure 12. SOI sweep compared to intake valve opening/closing and piston position of the engine..... 24
Figure 13. Example SOI sweep (left), seven replications are shown (not all replications extend over the entire SOI sweep) for fuel D-PrOH-13. Simple representations of piston and fuel spray (right). 24
Figure 14. Example of SOI sweep at Condition A for Fuel D showing injection spray to piston impingement transition point and lines/markers used to for calculations. 26
Figure 15. Soot emissions over SOI sweeps at condition A for base hydrocarbon fuels (error bars are 95% confidence interval based on several replications). 27
Figure 16. Soot emissions over SOI sweeps at condition B for base hydrocarbon fuels (error bars are 95% confidence interval based on several replications). 28
Figure 17. Soot emissions over SOI sweeps at condition A for Fuel C and blends. 30
Figure 18. Soot emissions over SOI sweeps at condition B for Fuel C and blends. 31
Figure 19. Injection duration for Fuel C and oxygenate blends for condition A (top) and condition B (bottom). Fuel volumetric energy content at right. 33
Figure 20. Soot emissions over SOI sweeps at condition A for Fuel D and alcohol blends. 34
Figure 21. Soot emissions over SOI sweeps at condition B for Fuel D and alcohol blends. 36
Figure 22. Injection duration for Fuel D alcohol blends for condition A (top) and condition B (bottom). Fuel volumetric energy content at right. 37
Figure 23. Soot emissions over SOI sweeps at condition A for Fuel D and ether blends. 38
Figure 24. Soot emissions over SOI sweeps at condition B for Fuel D and ether blends. 39

Figure 25. Injection duration for Fuel D ether blends for condition A (top) and condition B (bottom). Fuel volumetric energy content at right. 40
Figure 26. Impingement zone soot emissions, condition A, compared to a) PMI (r^2=0.67), b) NREL Index (r^2=0.54), PME (r^2=0.68). 43
Figure 27. Impingement zone soot emissions , condition B, compared to a) PMI (r^2=0.51), b) NREL Index (r^2=0.40), PME (r^2=0.63). 44
Figure 28. SOI transition point, condition A, compared to a) PMI (r2=0.76), b) NREL Index (r2=0.62), PME (r2=0.73). 44
Figure 29. SOI transition point, condition B, compared to PMI (r2=0.37), b) NREL Index (r2=0.34), PME (r2=0.41) 45
Figure 30. Non-impingement zone soot emissions, condition A, compared to a) PMI (r^2=0.72), b) NREL Index (r^2=0.71), PME (r^2=0.61). 46
Figure 31. Non-impingement zone soot emissions, condition B, compared to a) PMI (r^2=0.52), b) NREL Index (r^2=0.61), PME (r^2=0.24). 46

List of Tables

Table ES-1. Fuels evaluated in this program. iii
Table 1. Fuels evaluated in this program. 3
Table 2. Single-cylinder engine specifications. 7
Table 3. Engine operating conditions for start of injection sweeps. 8
Table 4. Selected properties of hydrocarbon base fuels (Fuel C D86 results, and Cert Fuel and Fuels C wt% C and wt% H results from (*1*)). 10
Table 5. Selected properties of Fuel C and blends with oxygenates. 11
Table 6. Selected properties for Fuel D and oxygenate blends. 12
Table 7. Paraffins, isoparaffins, olefins, naphthenes, and aromatics (PIONA) in wt% measured for Fuel C and Fuel D base fuels by Gage Products, SSI and by NREL. 16
Table 8. Carbon number distribution in wt% of aromatics measured for Fuel C and Fuel D by Gage Products, SSI, and by NREL. 17
Table 9. PMI values for all fuels. 20
Table 10. Values for PMI, NREL PM Index, PME, and YSI (YSI calculated as mole weighted average using predicted values of pure components from reference (*30*). 21
Table 11. Analytical results from condition A (95% confidence interval for soot based on 4 to 10 replications). 27
Table 12. Analytical results from condition B (95% confidence interval for soot based on 4 to 10 replications). 28
Table 13. Analytical results from fuel C blends at condition A (95% confidence interval for soot based on 4 to 10 replications). 30
Table 14. Analytical results from fuel C blends at condition B (95% confidence interval for soot based on 4 to 10 replications). 31
Table 15. Analytical results from fuel D and alcohol blends at condition A (95% confidence interval for soot based on 4 to 10 replications). 34
Table 16. Analytical results from fuel D and alcohol blends at condition B (95% confidence interval for soot based on 4 to 10 replications). 36
Table 17. Analytical results from fuel D and ether blends at condition A (95% confidence interval for soot based on 4 to 10 replications). 38
Table 18. Analytical results from fuel D and ether blends at condition B (95% confidence interval for soot based on 4 to 10 replications). 39

List of Acronyms

aTDC –	after top dead center
CAD –	crank angle degrees
DHA –	detailed hydrocarbon analysis
DI –	direct injection
DMM –	dimethoxymethane
DSC/TGA –	Differential Scanning Calorimeter/Thermogravimetric Analyzer
DVPE –	dry vapor pressure equivalent
EOI –	end of injection
ETBE –	ethyl-tert-butyl ether
E10 –	10 vol% ethanol ≡ EtOH-10
E15 –	15 vol% ethanol ≡ EtOH-15
EtOH –	ethanol
FID –	flame ionization detector
GC –	gas chromatograph
gIMEP –	gross indicated mean effective pressure
HCE5 –	Hydrocarbon Expert 5
HOV –	heat of vaporization
iBu –	i-butanol / isobutanol
ikWh –	indicated kilowatt-hr
MeOH –	methanol
MON –	motor octane number
MSD –	mass-selective detector
MSS –	Micro-Soot Sensor
MTBE –	methyl-tert-butyl ether
NMHC –	non-methane hydrocarbons
PIONA –	paraffins, isoparaffins, olefins, naphthenes, aromatics
PM –	particulate matter
PME –	particulate matter emissions (an index)
PMI –	particulate matter index
PrOH –	n-propanol
RF –	response factor
RON –	research octane number
RVP –	Reid vapor pressure
SCE –	single cylinder engine
SIDI –	spark ignition direct injection
SOI –	start of injection
SSI –	Separation Systems International
THC –	total hydrocarbons
VLE –	vapor-liquid equilibria
YSI –	yield sooting index

Introduction

Regulations and consumer demand for increasingly efficient gasoline engines has led to a dramatic increase in the market share of engines employing downsizing, down speeding, turbocharging and direct injection (DI) as strategies for improved thermal efficiency (*9*). At the same time, criteria pollutant emission standards for vehicles have continued to tighten (*10*), requiring engine designs and calibrations that meet fuel economy, greenhouse gas, and criteria pollutant requirements using conventional petroleum fuels as well as biofuel blends. Direct injection is critical for improving engine efficiency by effectively increasing the fuel's knock resistance to allow increasing compression ratio while maintaining optimal combustion phasing (*11*). However, DI can also lead to increased emissions of particulate matter (PM). For example, in a study of 82 vehicles including both port fuel injection and DI vehicles that covered several levels of emission standards, DI PM emissions were on average twice the level from port fuel injection engines (*12*). This is believed to occur because of impingement of the fuel spray on the top of the piston or the cylinder walls which can slow fuel evaporation leading to combustion in fuel rich zones or even pool fires on the top of the piston that produce high levels of PM (*13*,*14*).

In the United States today almost all gasoline contains 10 vol% ethanol (*15*), while blends up to 15 vol% are approved for 2001 and newer vehicles (*16*). Because the source of gasoline PM emissions is high boiling aromatic compounds in the fuel, it is expected that blending of ethanol would reduce PM by diluting the concentration of these aromatic compounds – yet some studies have shown blending of ethanol to increase PM. For example, in a study of 15 port fuel injection cars, tested on 27 fuels, ethanol blends up to 20 vol% increased PM on average (*17*). Studies from the Coordinating Research Council (CRC) in vehicles equipped with DI engines showed a consistent increase in PM for E10 blends in both match and splash blended fuels with respect to E0 (*1*,*18*). Two studies conducted in single cylinder DI engines (SCE) have also shown increased PM for ethanol blends under some conditions – with conditions leading to spray impingement on the piston favoring higher PM (*19*,*20*). Both studies suggested that the increase was caused by ethanol's high heat of vaporization (HOV – over 900 kJ/kg for ethanol and roughly 350 kJ/kg for hydrocarbon gasoline) which reduced the evaporation rate of low-volatility aromatic compounds. Ratcliff and coworkers showed that both cooling (HOV) effects and non-ideal vapor-liquid equilibrium (VLE) effects could cause aromatic compounds to evaporate more slowly or later in the fuel evaporation process for ethanol blends (*5*). They further showed that at the relatively low engine speed of 1500 rpm ethanol blending had no effect on PM for fuels with matched aromatic content (aromatics had the same volume concentration in both E30 and E0 fuels) – presumably because adequate time was available for fuel evaporation and mixing. At 2500 rpm the E30 blend showed significantly higher soot than the E0 reference, because of evaporative cooling and non-ideal VLE effects.

The above studies observed increased PM emissions for DI engines trending with an increasing ethanol content, however, the mechanism for increased particulate formation remains unclear as ethanol itself is not thought to be a PM precursor (*21*). It has been theorized that the presence of ethanol contributes to a charge cooling effect in direct injection engines, increasing particulate formation from other fuel

components. Other potential explanations include shifts in distillation characteristics, changes in volatility, and decreasing energy content (which requires longer injection duration to meet load).

CRC project E-129 was developed to evaluate tailpipe emissions of four spark ignition direct injection (SIDI) vehicles operated on a set of eight fuels formulated by splash-blending 3 oxygenates (ethanol, methyl tert-butyl ether (MTBE), and isobutanol) at different concentrations into a base hydrocarbon non-oxygenated gasoline. The base fuel was re-blended to conform to Fuel C from the CRC No. E-94-2 test program, having a low PMI (*1*). One of the goals of this program was to provide better understanding on whether the observed trend of increasing PM with increasing ethanol content held for higher ethanol concentrations and to begin investigating potential mechanisms for the PM increase. The project evaluated the tailpipe emissions of four model year 2012-2013 light-duty gasoline vehicles equipped direct-injected engines with various size, charge-air, and transmission configurations from a range of automotive manufacturers. The addition of oxygenates reduced the four-vehicle, fleet average emission rates of THC, CO, NOx, NMHC, N2O and PM in comparison to the non-oxygenated base fuel (Fuel C). The fuel containing 10% ethanol was observed to have a much smaller influence on a change in fleet average tailpipe emissions when compared to the effects associated with the other five oxygenated test fuels. E10 had no effect on PM (no dilution effect), while E15 and other oxygenates all showed PM reductions roughly proportional to their volumetric concentration in the fuel (16). While some trends are clear from the results of the program, three fuel effects are still not understood at present:

- Why does 10% ethanol fuel increase PM emissions in comparison to E0 fuels of equal PMI value?
- Why does 15% ethanol fuel not display the same emissions behavior as 10% ethanol?
- Why do the 15% ethanol isobutanol and MTBE blends follow the PMI trend line for E0 fuels that was established in the prior CRC E-94-2 study, rather than being offset above like the 10% ethanol fuel?

The purpose of the study described in this report is to extend the investigation of project E-129 to add key information to explain the ethanol effects on PM emissions and evaluate additional oxygenates of interest methanol, 1-propanol, ethyl-tert-butyl ether (ETBE) and dimethoxy methane (DMM). The project evaluated these fuels in an SCE, which offers better control of key operating parameters known to affect vehicle PM emissions – especially fuel spray impingement on the piston. Two steady-state engine operating conditions were used – a low and an intermediate speed, both at relatively high load, to discern some effects of engine operating conditions on engine-out PM emissions. At each condition, fuel start of injection (SOI) timing was systematically varied (swept) from approximately the middle of the intake stroke when the piston was far away from the injector, to very early in the intake stroke where fuel spray was clearly impinging on the piston. All other parameters were held constant during these injection timing sweeps.

Methods

Fuels Storage and Handling

There were 19 fuels or fuel blends studied in the current project and these are listed in Table 1. Note that fuel designation or name uses the target vol% oxygenate for the blends – actual vol% may be slightly different, and actual values are shown in Tables 5 and 6. The fuels marked with asterisk are identical to the fuels used in the original CRC E-129 study (*2*). Because these fuels were more than 2 years old at the start of the present study, some effort was made to determine if the fuels had weathered significantly. DVPE values from 2018 were available for the certification fuel and Fuel C, having values of 8.74 and 7.33 psi, respectively. DVPE measured in early 2021 gave values of 8.84 and 7.31 psi, suggesting that little weathering had occurred. T10 values from D86 distillation were very similar for the certification fuel, Fuel C, and all oxygenate blends.

Base Fuel D was developed for the CRC E-94-2 study (*1*) and was formulated to have a much higher PMI than base Fuel C so that the present study could cover the full range of PMI of commercial fuels. Fuel D was also blended with a much wider range of oxygenates, including *n*-propanol, ethyl-tert-butyl ether (ETBE) and dimethoxy methane (DMM, also known as methylal). The oxygenates were blended at 3.7 and 5.5 wt%, equivalent to oxygen levels in E10 and E15 blends.

All fuels were stored in climate-controlled storage facilities.

Table 1. Fuels evaluated in this program.

Fuel				Nominal Oxygen wt%	Nominal Oxygenate vol%
Blendstock	**Designation**	**PMI**	**Oxygen**		
Cert Fuel*	--	(report)	none	0	0
Fuel C*	--	low	none	0	0
Fuel D	--	high	none	0	0
Methanol	D-MeOH-7	high	low	3.7	7
Methanol	D-MeOH-10	high	high	5.5	10.4
Ethanol*	C-EtOH-10	low	low	3.7	10
Ethanol*	C-EtOH-15	low	high	5.5	15
Ethanol	D-EtOH-10	high	low	3.7	10
Ethanol	D-EtOH-15	high	high	5.5	15
MTBE*	C-MTBE-19	low	low	3.7	19
MTBE	D-MTBE-19	high	low	3.7	19
n-Propanol	D-PrOH-13	high	low	3.7	13
n-Propanol	D-PrOH-20	high	high	5.5	19.5
i-Butanol*	C-iBu-16	low	low	3.7	16
i-Butanol	D-iBu-16	high	low	3.7	16
ETBE	D-ETBE-24	high	low	3.7	24
ETBE	D-ETBE-35	high	high	5.5	35
DMM	D-DMM-8	high	low	3.7	8
DMM	D-DMM-12	high	high	5.5	12

Fuel Analysis

Detailed hydrocarbon analysis. Detailed hydrocarbon analysis was conducted by NREL, as well as by Gage Products, SwRI, and for a few samples by Separation Systems International (SSI). At NREL the enhanced DHA was performed following the parameters detailed in ASTM method D6729 (*22*) and D6730-X1/CRC AVFL-29 (*23*,*24*). An Agilent 7890A gas chromatograph (GC) equipped with a flame ionization detector (FID) and a liquid nitrogen cryogenic oven cooling valve was utilized for analysis. The GC was coupled with an Agilent 5975C mass-selective detector (MSD) for compound identification. Compound separations were achieved using a Rtx-100 DHA (Restek, Bellefonte, PA) column of dimensions 100 m x 0.25 mm, 0.5 µm d_f. An active post column flow splitter was used to divide the analytical column effluent between the FID and MS for simultaneous qualitative and quantitative analysis. The helium carrier gas was set to a flow rate of 2.3 mL/min constant flow. Inert capillary restrictors were used to deliver flow from the splitter to each detector; 4 m x 0.18 mm to the MSD and 2.5 m x 0.20 mm to the FID. These dimensions allowed for a retention time offset between detectors of < 0.01 minutes. The flow splitter was set to a constant pressure of 3 psi (~1.7 mL/min flow to the MSD). The GC oven was set to an initial hold of 0°C for 15 minutes, followed by a ramp of 1°C/min to 50°C, then 2°C/min to 130°C, and finally 4°C/min to 270°C with a 5 min hold. The FID and MS transfer line temperatures were set to 300°C. The MSD was operated in constant scan mode from m/z 29-400 with source temperature held at 230°C and quadrupole at 150°C. The injection port was set to 250°C and samples were injected neat at 1.0 µL volume with a split ratio of 100:1.

The FID response was verified using a standard of hydrocarbons ranging from C5 to C15 (Supelco Cat# 48879). This 15-component mixture containing *n*-paraffins, isoparaffins, and aromatics is representative of gasoline components. Response factors (RF) of individual components were determined and compared to the RF of *n*-heptane (relative response factor, RRF) (*25*). Each RRF was verified to be within +/- 10% of the theoretical RRF derived from effective carbon numbers. This analysis is used to confirm the injection parameters do not impart significant biases in mass-based response across the carbon number range of gasoline (*26*). Oxygenates were determined from mass response factors as described in ASTM D6729-20 A1. Mass response factors were calibrated using gravimetric mixtures of oxygenates and hydrocarbons following ASTM D4626.

Compound identifications were made based on retention indices using Separation Systems Hydrocarbon Expert 5 (HCE5) software. Assigned compound IDs were then verified using the MS signal via library matching using NIST MS Search 2.0 software and the NIST 2014 spectral database. Quantification of peaks was also done using the FID signal via HCE5 software.

Calculation of PM Indices and other Properties. Once the components were identified and quantified, an Excel spreadsheet containing each component name and the wt% amount present was generated for calculation of PMI and HOV. PMI was calculated as in Aikawa et. al. (*27*).

$$PMI = \sum_{i=1}^{n} \left[\frac{(DBE_i + 1)}{VP(443K)_i} \times Wt_i \right] \quad (1)$$

Where DBE is the double bond equivalent of the individual compound defined as:

$$DBE = (2C + 2 - H)/2 \quad (2)$$

VP is the vapor pressure at 443K, and Wt_i is the wt% of each component detected in the DHA. Vapor pressures at 443 K were estimated following the Lee and Kesler method (*28*).

$$P^{sat} = P_r^{sat} * P_c \quad (3)$$

$$lnP_r^{sat} = (lnP_r^{sat})^{(0)} + \omega(lnP_r^{sat})^{(1)} \quad (4)$$

$$(lnP_r^{sat})^{(0)} = 5.92714 - \frac{6.09648}{T_r} - 1.28862\, lnT_r + 0.169347\, T_r^6 \quad (5)$$

$$(lnP_r^{sat})^{(1)} = 15.2518 - \frac{15.6875}{T_r} - 13.4721\, lnT_r + 0.43577\, T_r^6 \quad (6)$$

Where P^{sat} is the vapor pressure at a desired temperature, T_r is the reduced temperature (desired temperature/critical temperature), P_c is the critical pressure, and ω is the acentric factor. Critical properties for individual compounds were taken from literature sources (*29*,*30*).

Heats of vaporization of individual compounds were predicted following the method proposed by Reid et al. (*31*).

$$\frac{\Delta H_v}{RT_c} = 7.08(1 - T_r)^{0.354} + 10.95\omega(1 - T_r)^{0.456} \quad (7)$$

Where ΔH_v is the heat of vaporization (HOV), R is the gas constant (0.008314 kJ/mol K), T_c is the critical temperature, T is the desired temperature, T_r is the reduced temperature (T/T_c), and ω is the acentric factor for the individual compound. The HOV of the gasoline was calculated as the weighted average of the HOV of individual components.

The NREL sooting index (*3*) which uses the distillation curve, fuel density, and a component-level sooting term to predict emissions trends, was also calculated for all fuels. Measured densities and T70 distillation temperatures were combined with yield sooting indices (YSI) calculated for each component using a group contribution model (*32*), HOV, and Vp for each component. The overall index was obtained with the following regression:

$$\log PM \sim a\, T_{70} + b\rho + c \sum_i^n \frac{YSI_i\, \Delta H_{v,i}}{V_{p,i}} x_i \quad (8)$$

In Eq. 8, ρ represents the density at 15°C and x_i represents the mol fraction of a given component in the fuel. The *a*, *b*, and *c* parameters were previously estimated using linear regression for a large sample of vehicle emissions data generated in the EPAct/V2/E-89 Tier 2 Gasoline Fuel Effects Study (*17*). Uncertainty in these estimated parameters is propagated to uncertainty in the final emissions index prediction.

The particulate matter emissions (PME) index (*4*) was calculated using equation 9:

$$PME = \left(\frac{43.4}{LHV}\right)\ [N_{TECH}\ \cdot \sum_i wt\%_i\ \cdot yTerm_i/VP_i^{\alpha}]^{\beta} \quad (9)$$

Where LHV is lower heating value (or net heat of combustion) for the bulk fuels, and for a direct injection engine and ASTM DHA:

$$N_{TECH} = 0.00597 \quad (10)$$

$$wt\%_i = wt\%\ of\ component\ i \quad (11)$$

$$yTerm_i = (C + O - 1) \cdot (1 + 1.7\ DBE_{NON} + 5.6\ ArRing_{First} + 5.1\ ArRings_{ADD}) \quad (12)$$

$$DBE_{NON} = DBE\ for\ double\ bonds\ not\ in\ aromatic\ rings, plus\ 1\ for\ each\ non - aromatic\ ring\ plus\ 2\ for\ each\ triple\ bond$$

$$ArRing_{First} = Contribution\ for\ first\ aromatic\ ring\ (equal\ to\ 1\ or\ 0)$$

$$ArRing_{ADD} = number\ or\ aromatic\ rings\ beyond\ the\ first\ (regardless\ of\ whether\ seperate\ or\ fused)$$

$$VP_i = vapor\ pressure\ of\ component\ i\ at\ 443K \quad (13)$$

$$\alpha = \alpha_0 + \Delta\alpha_{OX} \cdot OX_{VOL\%} \quad (14)$$

$$\beta = 1.17$$

$$\alpha_0 = 0.456$$

For E10:

$$\Delta\alpha_{OX} = \Delta\alpha_{E10} = -0.003 \quad (15)$$

For higher levels of ethanol or for other oxygenates:

$$\Delta\alpha_{OX} = \Delta\alpha_{E10} \cdot HOV_{OX}/HOV_{E10} \quad (16)$$

using either measured or calculated fuel HOV of the finished gasoline blends.

Standard fuel properties. Fuel properties including density (D4054), kinematic viscosity (D7042), surface tension (D1331 Method C), dry vapor pressure equivalent (DVPE, D5191), research octane number (RON, D2699), motor octane number (MON, D2700), net heat of combustion (D240), distillation curve (D86), and weight percent carbon and hydrogen (D5291) were measured using ASTM standard methods. Viscosity and surface tension were measured for the base fuels and the high oxygenate blend level fuels as these were expected to exhibit the largest differences for these properties.

Heat of vaporization. Heat of Vaporization (HOV) was measured utilizing a Q600 series Differential Scanning Calorimeter/Thermogravimetric Analyzer (DSC/TGA) from TA Instruments as recently described (*33*). The instrument was calibrated per manufacturer's specifications prior to sample analysis. The instrument cell was further characterized with deionized water, run in triplicate, to obtain a correction factor that was applied to all sample measurements. To maintain tighter and sub-ambient temperature control, the instrument was placed inside of a custom-built cold chamber which was maintained at 10°C +/- 3°C. Employing an open and tared aluminum sample pan (110 µL), 20 µL of sample was introduced directly into the pan using a gas-tight syringe and the experiment was immediately started. Samples were stored in the freezer prior to introduction in the instrument to ensure no loss of volatile components. The heat flow, temperature, and weight loss curves were simultaneously recorded for the duration of the experiment. The total HOV is computed by calculating the area under the curve using the trapezoid method to find the total heat lost during the evaporation process and then dividing by the initial sample mass recorded by the instrument. This result is then corrected for using the cell correction factor found from deionized water.

Engine Operation and Emissions

A single-cylinder engine based on a 2009 model year General Motors Ecotec 2.0 L LNF-series engine was used for these experiments. The engine's combustion system features direct injection (DI) of fuel through a side mounted injector, a centrally mounted spark plug and a piston bowl shaped to guide the fuel spray; specifications are listed in Table 2. The injector is a 6-hole design with nozzle diameter of 0.23 mm. The engine is connected to a 75 hp AC dynamometer, utilizing a DRIVVEN Inc. engine controller allowing full control of fuel injection timing, duration and pressure, spark timing, camshaft phaser positions, as well as intake pressure and exhaust back-pressure.

Table 2. Single-cylinder engine specifications.

Displacement (L)	0.5
Bore (mm)	86.0
Stroke (mm)	86.0
Compression ratio	9.2
Number of valves	4
Combustion System	Side-mounted DI

Start of injection (SOI) sweep experiments were performed to study the various fuel effects on soot emissions. Table 3 details the SOI timing ranges for the two operating conditions used in the study, as well as other key engine parameters. Engine inlet coolant and oil temperatures were nominally 90°C, with a 37°C intake air temperature, 0.95 bar exhaust pressure and stoichiometry at $\lambda = 1.0$ for both conditions. Fuel pressure was fixed at 68 bar and the fuel rail surface temperature was monitored and

moderately controlled by a vortex air cooler to a range of 38 – 45°C. Preliminary λ and injection pressure sweeps were conducted for most fuels and are shown in Appendix A. These indicate operation well away from any inflection points. Intake valve closing time was fixed at -134° after top dead center (aTDC) and a short valve overlap period of 24° (-355° aTDC intake valve opening to -331° aTDC exhaust valve closing) was chosen to minimize trapped exhaust residual gases. Baseline SOIs were defined as -280° aTDC and -270° aTDC for conditions A and B, respectively. These points were repeated regularly to check for system drift.

Table 3. Engine operating conditions for start of injection sweeps.

	Test Condition A	**Test Condition B**
Speed – Load (rpm, bar gIMEP)	2500 – 12.5	1500 – 12
Intake Manifold Pressure (bar abs)	1.25	1.0
Intake Manifold Temperature (°C)	37	
Fuel Rail Pressure (bar)	68	
Fuel Rail Surface Temperature (°C)	38 – 45	
Exhaust Manifold Pressure (bar abs)	0.95	
Stoichiometry (λ)	1.0	
Engine Inlet Coolant Temperature (°C)	90	
Intake Valve Opening (° aTDC)	-355	
Intake Valve Closing (° aTDC)	-134	
Intake – Exhaust Valve Overlap (°)	24	
Start of Injection Sweep (° aTDC)	-270 to -340	-260 to -340
Injection Duration (°)	45 – 50	26 – 30
Injection Duration (ms)	3.0 – 3.35	2.9 – 3.35
Spark Timing (° aTDC)*	-8	-4

* Spark timing was retarded (delayed) for the two DMM fuel blends due to their low octane which results in excessive engine knock. Spark was retarded 1.5° for condition A and 3.0° for condition B.

Soot emissions were measured in the raw exhaust stream by an AVL Micro-Soot Sensor (MSS). Exhaust gas emissions were also measured in the raw exhaust stream by a Horiba MEXA-1 emissions bench, which includes measurements of nitric oxides (NO_X), total hydrocarbons (THC), carbon dioxide (CO_2), carbon monoxide (CO) and oxygen (O_2). A Bosch wide-band oxygen sensor with an ETAS module was used to monitor real-time combustion stoichiometry, lambda (λ), which was also verified by emission measurement calculations.

Engine controls and high-speed combustion measurements were made with the integrated independent engine controller. In-cylinder pressure was measured at 0.1 crank angle degree increments. This measurement was then used to calculate parameters like engine load, knock and heat release. Gross indicated mean effective pressure (gIMEP) was used as the measure of engine load, meaning that only the compression and combustion (or power) strokes were used in the calculation. The pumping loop (exhaust and intake strokes) were not used for the gIMEP calculation.

Soot emissions results are presented in mg/ikWh units, which represents milligrams of soot per indicated kilo-watt hours of energy. The “indicated” parts denotes that power was derived from in-cylinder pressure measurements on a gross basis, as described in the previous paragraph. Total hydrocarbons, CO and NOx emissions are reported using a similar specific mass per energy basis, where grams (rather than milligrams) are used.

A standard fuel swap procedure was developed to purge every element of the fuel system. This was followed by running the engine at mid-load until at least 2 liters of the new fuel had passed through the entire system before commencing experiments. The SOI sweeps on each day always began with engine condition A sweeps, starting with injection at SOI = -270° aTDC. Once steady-state operation was attained, data sets were collected for 30 second intervals. SOI was then advanced in 10° steps, collecting data at each step until the soot emissions began to increase (because of fuel spray impingement on the piston). The SOI steps were then reduced to ≈2°, advancing until exhaust soot levels reached ≈30 mg/m^3. At this soot level SOI direction was reversed and swept back to -270° aTDC while collecting replicate sets of data. SOI sweeps at engine condition B were then performed in a similar manner. Multiple replicates (at least three) of these sweeps were performed over the course of two or more days. Each parameter measured within each 30 second data set was averaged, and the replicates of these averaged data sets were compiled and analyzed.

Results

Fuel Properties

Hydrocarbon base fuels. Hydrocarbon fuel properties are shown in Table 4. Major differences in bulk properties between these gasolines are the significantly higher RON and MON of the certification fuel and the significantly higher T90 and final boiling point of Fuel D, consistent with its higher PMI (as shown below).

Table 4. Selected properties of hydrocarbon base fuels (Fuel C D86 results, and Cert Fuel and Fuels C wt% C and wt% H results from (*2*)).

Property	Test Method	Certification Fuel	Fuel C	Fuel D
Density at 15°C, g/mL	D4054	0.7398	0.7389	0.7390
Kinematic viscosity at 20°C, cSt	D7042	0.6545	0.6827	0.6798
Surface tension at 10°C, dynes/cm	D1331	22.354	22.262	22.062
DVPE, psi	D5191	8.84	7.31	7.4
Distillation T10, °C	D86	63.4	60.4	62.2
Distillation T50, °C	D86	106.9	105.6	106.7
Distillation T90, °C	D86	147.2	146.9	171.7
Final boiling point, °C	D86	198.6	193.2	212.4
RON	D2699	96.7	91.7	92.1
MON	D2700	88.3	84.6	85.0
Net heat of combustion, MJ/kg	D240	43.37	43.51	43.60
Volumetric energy density, MJ/L	Calculated	32.09	32.15	32.19
Carbon, wt%	D5291	86.4	85.93	86.28
Hydrogen, wt%	D5291	13.61	14.07	13.72
Heat of vaporization, kJ/kg at 10°C	DSC/TGA	370	353	333
Heat of vaporization, kJ/kg at 25°C	Calculated	352	355	353

Fuel C blends. Results are shown in Table 5. As expected, blending of the oxygenates ethanol, isobutanol, and MTBE increases fuel density and RON, while decreasing volumetric energy density. The lower volumetric energy density indicates that injection duration will be longer at identical speed and load. Blending of ethanol and isobutanol increases heat of vaporization as well as viscosity. Surface tension values for the base fuel and alcohol blends are very similar. The relatively high blend level for MTBE on a volumetric or mass basis (19 vol% or wt%) will dilute aromatics in the base fuel to a greater extent than the other blends – however on a molar basis the greatest dilution is from E15.

Fuel D blends. Fuel D blend property results are shown in Table 6. These fuels present a broad range of properties based on the very broad range of oxygenates blended. Methanol blends produced a large increase in DVPE and a large decrease in T10. Methanol has the highest HOV of the blendstocks which is reflected in the blends. Ethanol blending also increased DVPE and suppressed T10 as well as T50 at the higher blend level. These blends, made to have the same oxygen content as the methanol blends, show similarly high HOV. Propanol and isobutanol blends show progressively less effect on the

blend properties relative to methanol and ethanol. MTBE blending had no effect on DVPE but suppressed T50. ETBE has the lowest oxygen content of all the blendstocks and thus was blended at the highest vol% or wt% level to achieve the fuel oxygen targets. ETBE blends at 24 and 36 vol% dilute the aromatic compounds in the base gasoline much more than blends of other blendstocks on this basis. However, on a molar basis, E15 at 30.7 mol% is the second highest dilution. From a property perspective blending ETBE reduces DVPE and suppressed T50. DMM is the smallest polyether containing two oxygens with a central methylene group, it also has the lowest boiling point of the oxygenates considered (42°C). The highly volatile blendstock increased DVPE to a level in between what was observed for methanol and ethanol, and depressed T10 more than any other blendstock except methanol. It was blended at similar vol% as methanol, but on a molar basis is present at much lower concentration. Viscosity was significantly higher than that of the base fuel for the alcohol blends, but essentially unchanged for the ether blends that were tested. Surface tension of oxygenate blends was essentially the same as that of the base fuel, with the exception of the high level ETBE blend whose surface tension was 5% lower.

Table 5. Selected properties of Fuel C and blends with oxygenates.

Property	Test Method	Fuel C	C-EtOH-10	C-EtOH-15	C-iBu-16	C-MTBE-19
Oxygenate, vol%	D6729	--	9.8	14.6	16.0	18.6
Oxygenate, wt%	D6729		10.4	15.4	17.1	18.6
Oxygenate, mol%	Calculated		19.9	28.1	21.6	20.4
Density at 15°C, g/mL	D4054	0.7398	0.7389	0.7438	0.7492	0.7404
Kinematic viscosity at 20°C, cSt	D7042	0.6827	--	0.761	0.7965	--
Surface tension at 10°C, dynes/cm	D1331	22.262	--	22.307	22.165	--
DVPE, psi	D5191	7.31	8.26	8.27	6.72	7.58
Distillation T10, °C	D86	63.4	56.6	57.6	66.8	59.0
Distillation T50, °C	D86	106.9	101.7	75.2	97.4	92.3
Distillation T90, °C	D86	147.2	144.7	144.1	142.6	141.4
Final boiling point, °C	D86	198.6	198.9	193.7	194.0	194.2
RON	D2699	91.7	96.5	98.2	95.7	97.4
MON	D2700	84.6	86.8	87.3	85.8	87.7
Net heat of combustion, MJ/kg	D240	43.51	41.67	40.78	41.69	41.91
Volumetric energy density, MJ/L	Calculated	32.15	30.99	30.46	31.24	31.03
Carbon, wt%	D5291	83.203	82.713	81.258	80.140	80.133
Hydrogen, wt%	D5291	13.338	13.687	13.381	13.154	13.187
Heat of vaporization, kJ/kg at 10°C	DSC/TGA	353	411	425	410	346
Heat of vaporization, kJ/kg at 25°C	Calculated	355	423	456	397	351

Table 6. Selected properties for Fuel D and oxygenate blends.

Property	Test Method	Fuel D	D-MeOH-7	D-MeOH 10	D-EtOH-10	D-EtOH-15	D-PrOH-13	D-PrOH-20	D-iBu- 16	D-MTBE-19	D-ETBE-24	D-ETBE-35	D-DMM-8	D-DMM-12
Oxygenate, vol%	D6729	--	6.7	9.7	10.7	16.0	12.1	18.7	15.3	18.4	23.7	35.2	8.0	11.9
Oxygenate, wt%	D6729		7.1	10.3	11.3	16.9	13.0	19.7	16.4	18.4	24.3	36.0	7.8	11.9
Oxygenate, mol%	Calculated		19.5	26.5	21.8	30.7	20.0	29.2	21.1	20.5	24.0	35.6	10.1	15.1
Density at 15°C, g/mL	D4054	0.7390	0.7438	0.7437	0.7437	0.7460	0.7472	0.7514	0.7484	0.7403	0.7409	0.7418	0.7474	0.7517
Kinematic viscosity at 20°C, cSt	D7042	0.6798	--	--	--	0.7136	--	0.8224	0.7973	--	--	0.6546	--	0.6512
Surface tension at 10°C, dynes/cm	D1331	22.062	--	--	--	21.936	--	22.26	22.202	--	--	20.943	--	22.184
DVPE, psi	D5191	7.4	10.81	10.88	8.40	8.30	7.10	7.00	6.70	7.38	6.80	6.50	8.70	9.20
Distillation T_{10}, °C	D86	62.2	48.8	48.9	56.7	57.2	64.2	65.7	66.7	58.0	64.8	65.2	53.7	50.3
Distillation T_{50}, °C	D86	106.7	104.7	102.5	102.0	77.8	89.1	81.2	96.8	91.8	93.1	87.1	103.1	100.1
Distillation T_{90}, °C	D86	171.7	171.2	170.2	171.4	169.2	170.1	168.6	167.4	167.4	166.4	159.5	169.7	169.9
Final boiling point, °C	D86	212.4	212.8	209.0	211.6	209.2	211.7	209.8	210.9	208.1	211.7	204.6	212.4	208.6
RON	D2699	92.1	95.7	97.3	96.9	98.4	96.4	97.9	96.1	98.0	98.0	99.4	90.8	89.8
MON	D2700	85.0	86.4	86.8	87	87.9	86.6	87	86.3	88.5	89.2	91.1	83.4	82.4
Net heat of combustion, MJ/kg	D240	43.56	42.11	41.22	41.78	40.94	41.90	41.01	41.78	41.88	41.71	41.00	41.94	41.19
Volumetric energy density, MJ/L	Calculated	32.19	31.32	30.66	31.07	30.54	31.31	30.81	31.27	31.00	30.90	30.41	31.35	30.96
Carbon, wt%	D5291	86.28	82.48	80.68	82.48	80.68	82.44	80.59	82.55	82.39	82.47	80.61	82.90	81.24
Hydrogen, wt%	D5291	13.72	13.76	13.73	13.83	13.82	13.80	13.77	13.70	13.87	13.78	13.80	13.49	13.40
Heat of vaporization, kJ/kg at 10°C	DSC/TGA	333	410	423	423	427	380	440	410	325	346	342	345	359

Heat of vaporization, kJ/kg at 25°C	Calculated (DHA)	353	416	444	418	449	404	431	394	349	341	337	353	355

Fuel Properties Summary. The certification gasoline and the two hydrocarbon base fuels used in this project have similar volumetric energy density. Because the oxygenate blends are at two oxygen levels (3.7 and 5.5 wt%), these fuels fall into two groups for energy density as shown in Figure 1. There is significant variation within each group because of differences in mass density and molecular weight for the oxygenates, experimental errors in blending, heat of combustion, hydrogen content, and mass density – all of which go into calculating volumetric energy density. Overall, we would expect slightly longer injection duration to maintain constant load for the oxygenate blends than for the hydrocarbon base fuels – which may imply less time for mixing and higher soot emissions.

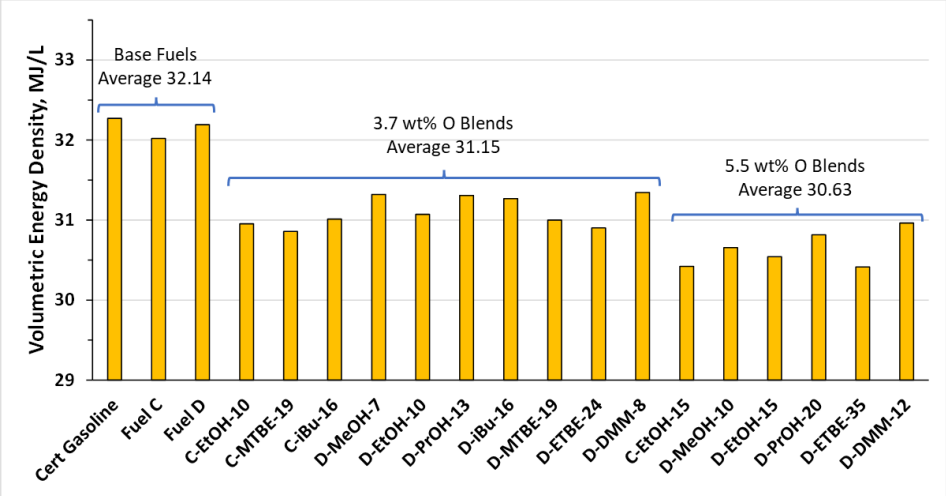

Figure 1. Volumetric energy density for fuels used in this study.

The oxygenates were also blended at a wide range of oxygenate content, because of the wide range of carbon to oxygen ratio for the oxygenates (ranging from 1:1 to 6:1). An important factor in oxygenate blending for PM emissions is dilution of the high boiling aromatics in the fuel by the oxygenate. As shown in Figure 2, dilution ranges over a factor of five, from 7% to 36%. The highest level of 36 wt% for ETBE in Fuel D at 5.5 wt% oxygen level would reduce total aromatics from 34.9 wt% in the base fuel (according to DHA described below) to 22.3 wt%.

While weight and volume percent are commonly used in fuel studies, mole percent (mol%) is much more relevant to outcomes based on chemical reactions such as soot formation. This is particularly important for blending of low molecular weight oxygenates such as methanol and ethanol where mol% values can be more than two times wt% values. Mole percent oxygenate is shown in Figure 3. On this basis the 15 wt% ethanol blends have the second highest levels of dilution at nominally 30 mol%, followed by 20 wt% propanol, 10 wt% methanol, and 24 wt% ETBE at nominally 25 mol%. A large group of blends are at nominally 20 mol%, while the two DMM blends are at 15 and 10 mol%.

A third factor that could affect PM emissions is HOV. All alcohols have higher HOV than ethers or hydrocarbons leading to the sharp break in Figure 4 between these groups of fuels. On the other hand, ETBE has a slightly lower HOV than gasoline and so slightly reduces blend HOV. Differences between

calculated and measured values are typically less than 5% but look larger at the expanded scale of Figure 4.

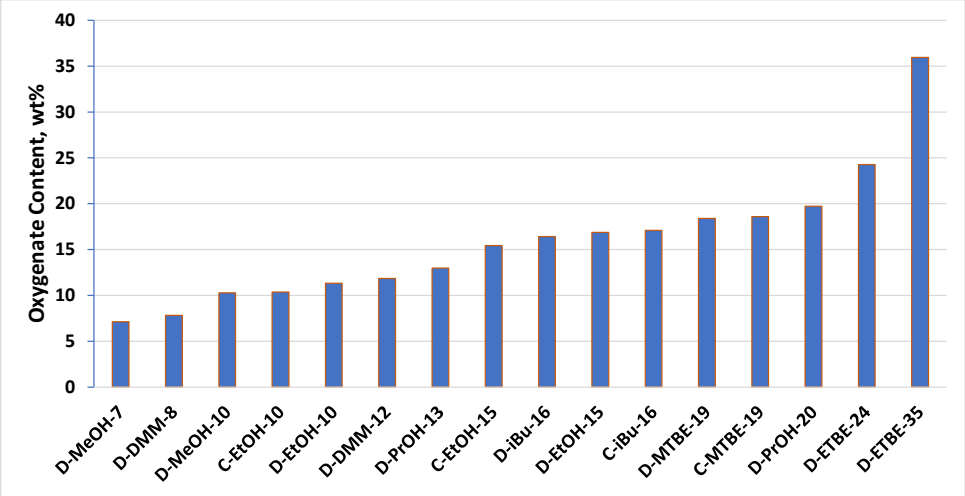

Figure 2. Oxygenate content in the fuel blends in weight percent.

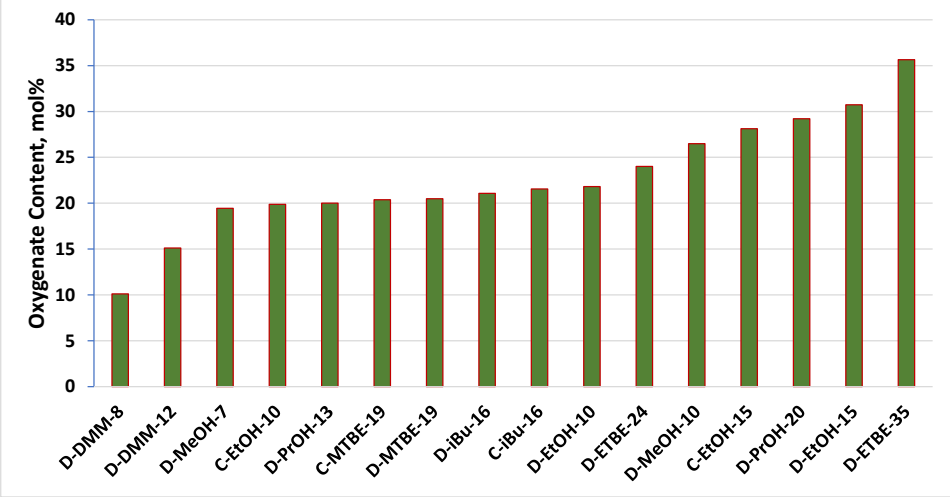

Figure 3. Oxygenate content in the fuel blends in mole percent.

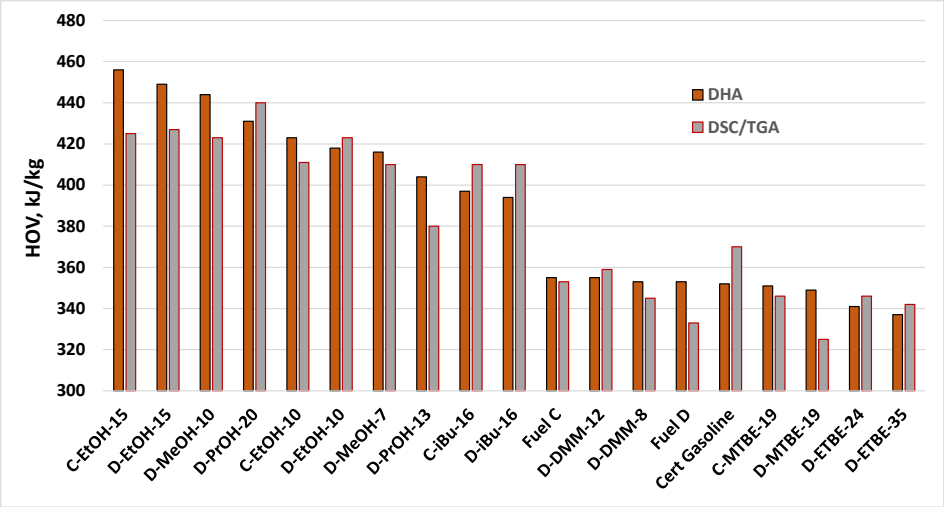

Figure 4. Heat of vaporization for fuel blends (calculated from DHA at 25°C and measured by DSC/TGA at 10°C).

Detailed Hydrocarbon Analysis and Calculated Properties

DHA and PIONA. NREL performed DHA on all the fuels examined in this study using the version of the ASTM D6729 and D6730 procedures outlined in the Methods section. Full DHA results have been supplied to CRC as digital files. The DHA results can be used to calculate the paraffins, isoparaffins, olefins, naphthenes, aromatics content, and these results for the base Fuels C and D are shown in Table 7. For Fuel C, the results are in good agreement with DHA from the original E-129 study. (*2*) For Fuel D, results from Gage Products and from Separation Systems International (SSI) are also shown. NREL found roughly 3% higher total aromatics and slightly lower levels of all other components relative to Gage and SSI.

Table 7. Paraffins, isoparaffins, olefins, naphthenes, and aromatics (PIONA) in wt% measured for Fuel C and Fuel D base fuels by Gage Products, SSI and by NREL.

	Certification Gasoline	Fuel C		Fuel D		
Group	**NREL**	**E-129**	**NREL**	**Gage**	**SSI**	**NREL**
Paraffins	2.05	7.9	7.8	9.5	9.4	8.9
IsoParaffins	52.88	43.5	41.8	49.4	50.2	48.6
Aromatics	38.40	34.9	34.0	31.6	31.84	34.9
Naphthenes	5.57	5.6	7.0	4.0	2.7	2.7
Olefins	0.86	6.8	8.8	5.3	5.4	4.9
Unknowns	0.24	1.2	0.6	0.0	0.5	0.0

Table 8 shows the carbon number distribution of aromatics which provide some insight into the PIONA results for Fuel D. NREL reported ~1% higher toluene (C7) compared to the other labs for Fuel D. This is because NREL employed ASTM D6729 as the method for DHA, as opposed to D6730. The key difference between these two techniques is D6730 employs a pre-column prior to the analytical column which is

used to separate coelutions which can occur with D6729, a key coelution being between toluene and 2,3,3-trimethylpentane. NREL utilizes this technique to provide greater flexibility in instrumentation, while D6730 largely requires a dedicated GC. There is partial separation of these two components with D6729 but due to partial overlap this resulted in an overestimation of toluene concentration. However, a 1% difference in C7 has only a very small impact on calculated PMI or other soot formation metrics. NREL also detects marginally higher levels of C8 – C10 aromatics, much higher levels of C11 aromatics than the other laboratories, while detecting lower levels of C12. These differences speak to the interlaboratory variabilities in DHA analyses, which translate to the precision of PMI values.

Oxygenate blends with the base fuels show dilution of the hydrocarbon components as expected. Figure 5 compares measured oxygenate levels in vol% with target levels. There is generally an excellent agreement. Figure 6 compares oxygenate analysis results from NREL and Gage Products, overall showing excellent agreement.

Table 8. Carbon number distribution in wt% of aromatics measured for Fuel C and Fuel D by Gage Products, SSI, and by NREL.

	Certification Gasoline	Fuel C		Fuel D		
Carbon	**NREL**	**E-129**	**NREL**	**Gage**	**SSI**	**NREL**
C6	0.002	0.396	0.392	0.694	0.691	0.685
C7	22.123	15.721	15.894	7.396	7.302	8.439
C8	0.102	12.622	12.513	6.287	6.294	6.444
C9	11.508	1.868	1.762	7.997	7.986	8.457
C10	3.613	2.193	2.059	6.281	5.503	6.486
C11	1.048	0.842	0.926	1.763	1.892	3.682
C12	0.009	0.351	0.488	1.086	2.043	0.498
C13	--	0.11	--	0.107	0.086	0.172
C14	--		--	--	0.037	--
C15	--		--	--	0.008	--
Total C# %wt		34.103	34.034	31.611	31.842	34.865

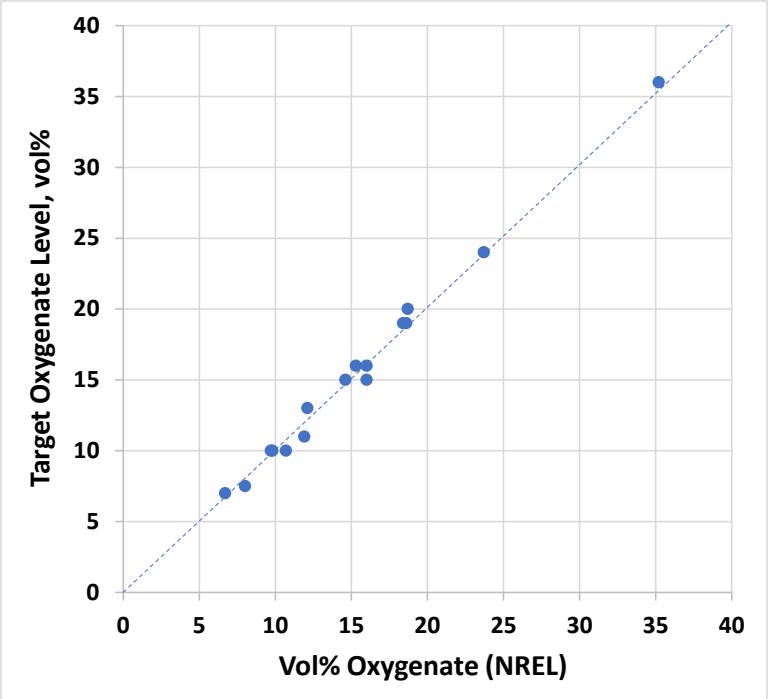

Figure 5. Comparison of target oxygenate content with measured content, vol%, for Fuel C and Fuel D blends, R^2=0.99 (parity line shown as dashed line).

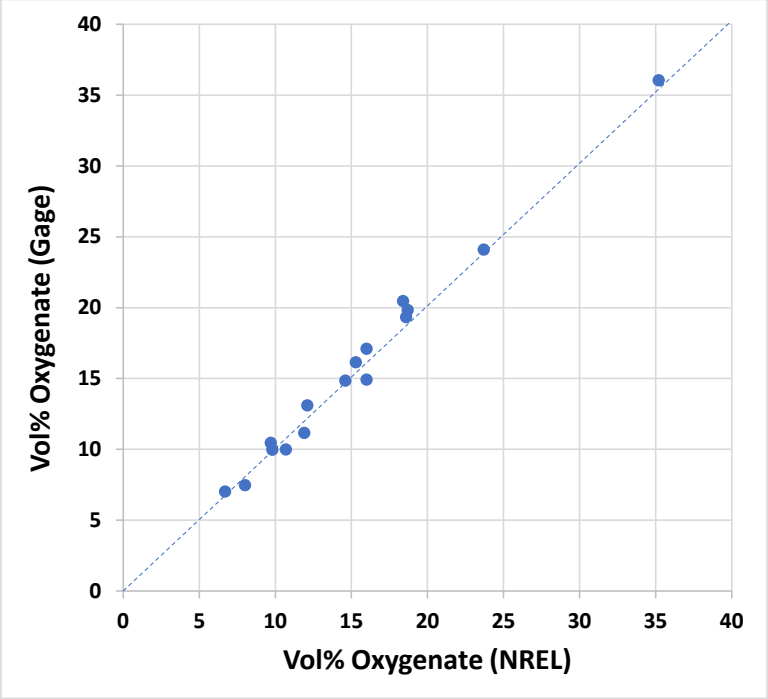

Figure 6. Comparison of oxygenate analysis from Gage and NREL, R^2=0.99 (parity line shown as dashed line).

HOV calculated from DHA. As described in the Methods section HOV can be calculated from DHA as well as measured using DSC/TGA. Figure 7 compares total HOV values for all the fuels from both

methods. The average absolute error between DHA and DSC/TGA was 3.3% (note the expanded scale of Figure 7).

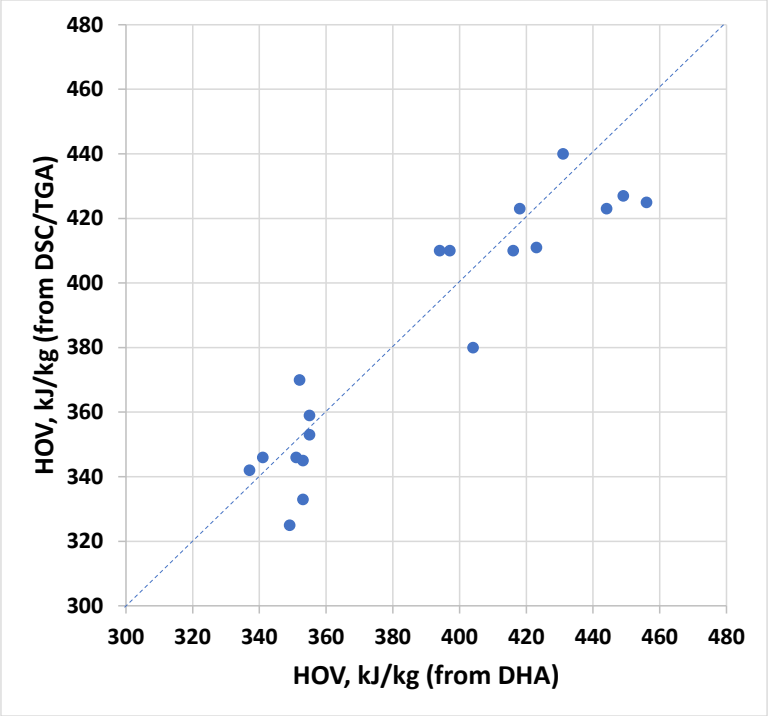

Figure 7. HOV measured versus HOV calculated from DHA, R^2=0.86 (parity line shown as dashed line).

Particulate matter index and other soot formation metrics. A table of PMI values calculated for the study fuels by NREL, Gage Products, and for two samples by Separation Systems International (SSI) is shown in Table 9 and these values are compared graphically in Figure 8. Values from NREL are very similar to values from Gage Products for Fuel C and blends with an average absolute difference of only 0.04 PMI units. For Fuel D and blends NREL's results are on average 0.22 PMI units higher, but for Fuel D and the 7 vol% methanol blend the differences is 0.32 and 0.34 PMI units, respectively. These differences arise because of the somewhat higher aromatic content measured by NREL, and the difference diminishes as larger volumes of oxygenates are blended into Fuel D. Two samples were also analyzed by SSI. SSI's value is 0.08 PMI units lower than NREL's for both Fuel D and for the highest volume percent oxygenate blend, D-ETBE-35. These differences seem to be well within the observed interlaboratory variability for combined DHA and PMI calculation. PMI values trend down with increasing level of oxygenate blending, as shown in Figure 9.

Table 10 shows NREL PMI, the NREL Sooting Index (*3*), and PME (*4*) for the test fuels, as well as calculated YSI values. Figure 10 compares PMI and the NREL Sooting index. These values are highly correlated and thus we would not expect one to be a significantly better predictor PM emissions than the other. Figure 11 compares PME with PMI. PME values are bimodally distributed with a group

around 2 (the Fuel D blends) and a second group around 1.3 (the Fuel C blends). The correlation between PME and PMI is not as strong as for the NREL Index and PMI, but it is still high.

Table 9. PMI values for all fuels.

Fuel	NREL	Gage	SSI
Certification Fuel	1.29	1.27	
Fuel C	1.21	1.30	
C-EtOH-10	1.11	1.16	
C-EtOH-15	1.05	1.08	
C-iBu-16	1.06	1.07	
C-MTBE-19	1.00	1.04	
Fuel D	2.75	2.43	2.67
D-MeOH-7	2.56	2.22	
D-MeOH-10	2.44	2.26	
D-EtOH-10	2.46	2.30	
D-EtOH-15	2.31	2.14	
D-PrOH-13	2.47	2.22	
D-PrOH-20	2.28	2.10	
D-iBu-16	2.34	2.20	
D-MTBE-19	2.29	1.84	
D-ETBE-24	2.08	1.95	
D-ETBE-35	1.75	1.59	1.66
D-DMM-8	2.47	2.27	
D-DMM-12	2.40	2.18	

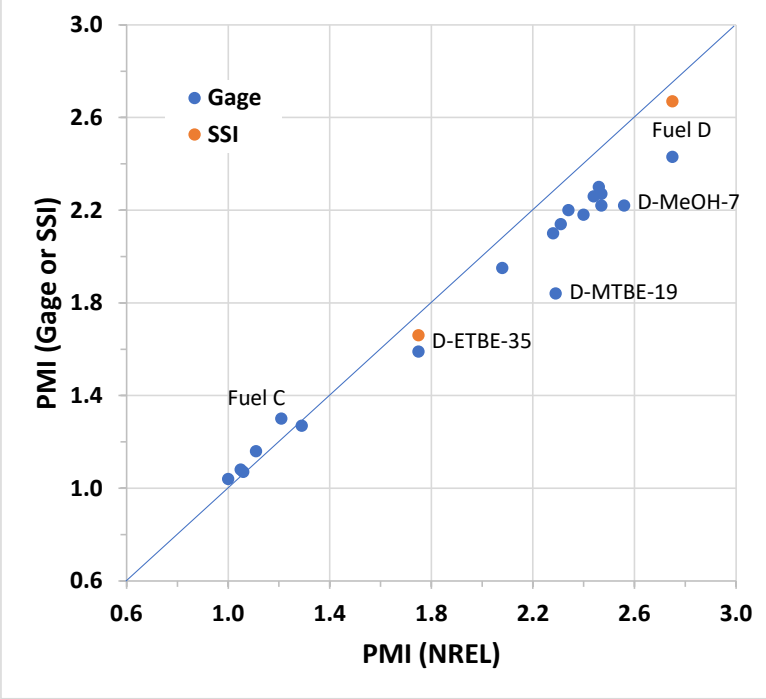

Figure 8. Comparison of PMI values calculated by NREL, Gage Products, and SSI. R^2=0.98 for correlation with Gage data (parity line shown).

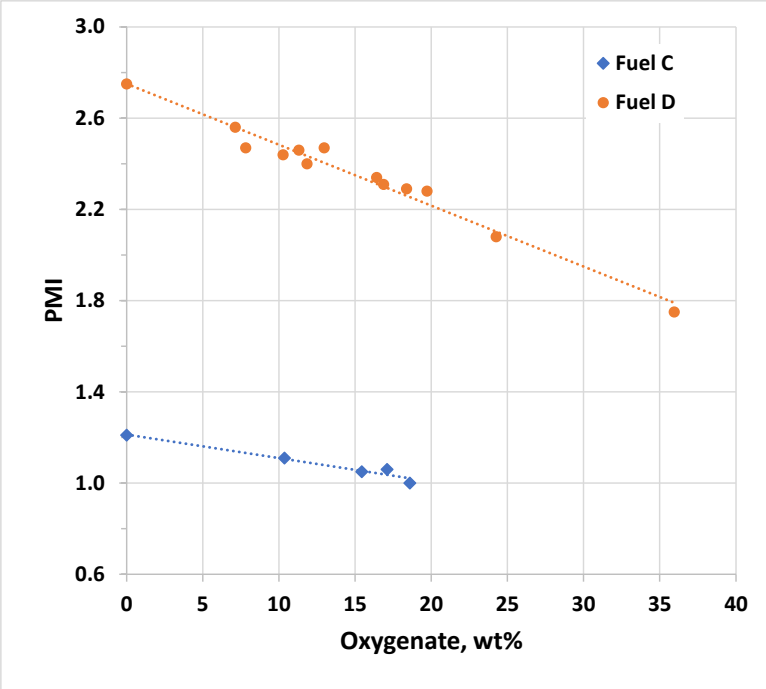

Figure 9. Impact of oxygenate blending on PMI (NREL measurements).

Table 10. Values for PMI, NREL Sooting Index, PME, and YSI (YSI calculated as mole weighted average using predicted values of pure components from reference (*32*).

Fuel	NREL PMI	NREL Sooting Index	PME	YSI
Certification Fuel	1.29	-0.30	1.23	108.4
Fuel C	1.21	-0.12	1.19	99.72
C-EtOH-10	1.11	-0.31	1.25	78.80
C-EtOH-15	1.05	-0.38	1.27	70.66
C-iBu-16	1.06	-0.41	1.35	84.63
C-MTBE-19	1.00	-0.42	1.29	86.18
Fuel D	2.75	1.22	1.84	111.5
D-MeOH-7	2.56	0.85	1.93	91.19
D-MeOH-10	2.44	0.65	1.95	83.12
D-EtOH-10	2.46	0.79	1.98	89.67
D-EtOH-15	2.31	0.58	2.04	81.82
D-PrOH-13	2.47	0.90	1.99	94.04
D-PrOH-20	2.28	0.32	2.04	84.69
D-iBu-16	2.34	0.63	2.01	94.27
D-MTBE-19	2.29	0.67	1.93	95.72

D-ETBE-24	2.08	0.47	1.89	90.57
D-ETBE-35	1.75	0.02	1.87	82.19
D-DMM-8	2.47	1.06	1.88	100.0
D-DMM-12	2.40	1.00	1.95	95.84

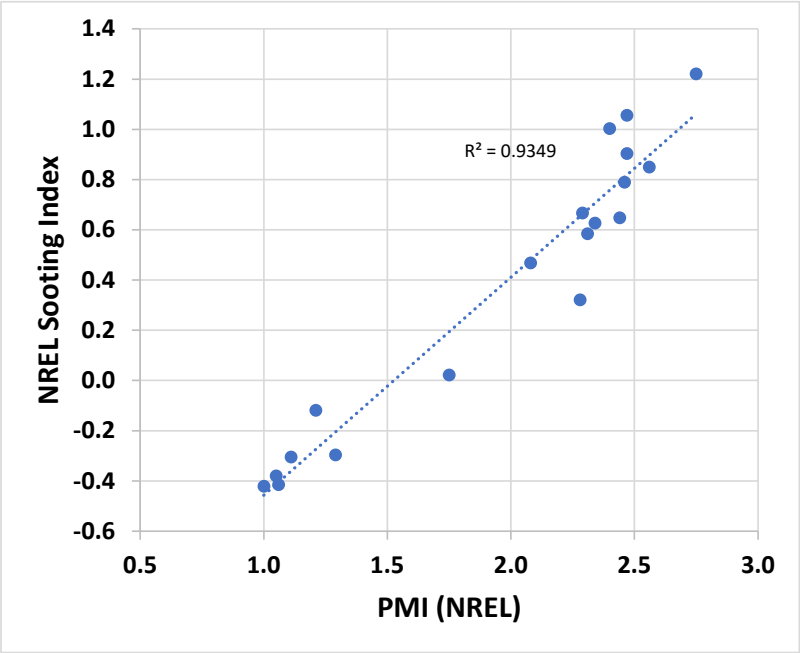

Figure 10. Comparison of NREL Sooting Index with PMI (linear regression line shown).

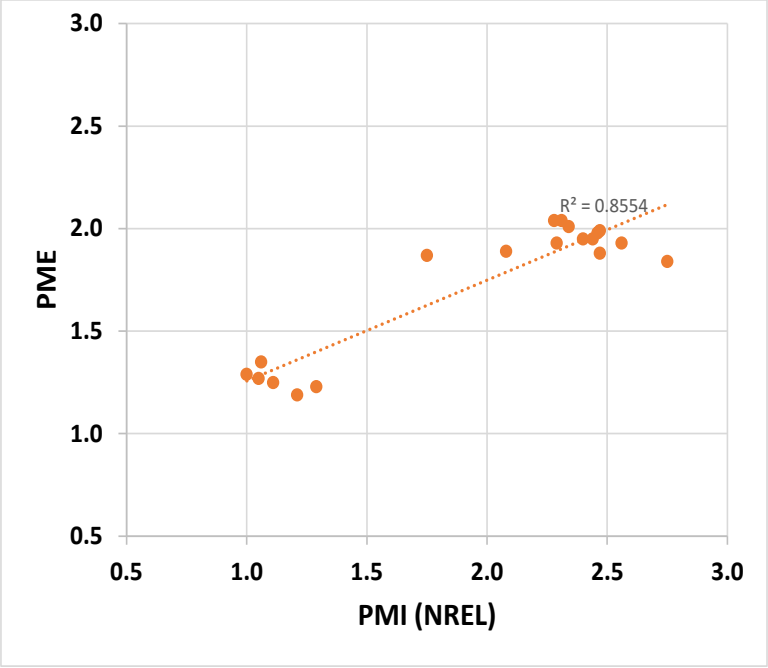

Figure 11. Comparison of PME with PMI (linear regression line shown).

Engine Emissions

Two engine operating conditions were examined: Condition A, a high speed, high load point (2500 rpm, 12.5 bar gross indicated mean effective pressure [gIMEP]) and Condition B an intermediate speed, high load point (1500 rpm, 12 bar gIMEP). At each condition start of injection (SOI) sweeps were conducted by varying SOI from later in the intake stroke where the piston has moved well away from top dead center (Figure 12 and Figure 13 – lower right) to earlier in the intake stroke where the piston is closer to top dead center and spray impingement on the piston is likely to occur (Figure 13 – upper right). Figure 12 shows example injector current traces at the bottom of the chart which denote SOI (leading edge of the injection current) and end of injection (EOI, trailing edge of the current profile). The SOI defined in this report refers to the commanded (i.e., set point) SOI. There is a small but constant time delay between commanded SOI and the actual start of fuel injection. Only one injection event per cycle was used for both A and B conditions. The multiple injection events shown in Figure 12 are examples of some possible SOI sweep timings.

Soot emissions for an example SOI sweep are shown in Figure 13 (left). At the most retarded injection point of -270° crank angle degrees (CAD) after top dead center (aTDC) shown in Figure 13, there is no impingement and soot emissions are relatively low. Moving to earlier (more advanced) injection first leads to a drop in soot as there is more time for mixing before spark. Beyond this point the spray impinges on the top of the piston. The CAD for the transition to spray impingement varies with fuel properties and engine operating conditions. Advancing SOI beyond the transition point, the soot emissions begin to rapidly increase because fuel spray impingement increasingly deposits fuel onto the piston as a film or pool. Fuel films or pools can burn in a diffusion flame that produces high levels of soot, rather than the nearly premixed combustion that occurs in the impingement free zone.

SOI sweep experiments were carried out by starting at the latest SOI condition (farthest away from the piston impingement), then stepping forward in 10 CAD increments until a piston impingement transition zone was noticed. At this transition CAD increments were decreased to 2.5 degrees to achieve higher resolution. SOI was advanced in the piston impingement zone until a predetermined soot threshold was achieved. Then the same SOI steps were immediately repeated in reverse order. Data were recorded at 1 Hz for 30 seconds at each SOI step. This entire sweep up and back down typically took about 40 minutes to accomplish. The full sweep was then repeated a minimum of one time, or 4 data recording intervals for each SOI step. In many cases additional sweeps were performed, moreover the non-impingement base points (either -270° aTDC or -280° aTDC) were repeated frequently as checks for system drift. The average for each recording interval was calculated, then the average of the replicated recording intervals at each SOI CAD was used for analysis and presented in this report.

Note that during injection the piston is always moving away from the fuel spray. Injection durations at condition A were nominally 48 CAD and at condition B 28 CAD, but injection times in milliseconds were

similar (Table 3). The difference is in engine speed – at the high speed of condition A the piston moves a greater distance during injection than for the low-speed condition. It is important to note that for what we are calling the SOI impingement zone, only a fraction of the fuel is impinging on the piston top. For the most advanced (most negative) SOI values employed, the difference between SOI and the transition point is only about 10 CAD, so that impingement is only occurring over 20 to 35% of the injection duration in CAD. This also means that fuels with longer injection duration are not depositing more fuel on the piston but may have higher soot emissions because of less time for mixing after injection ends.

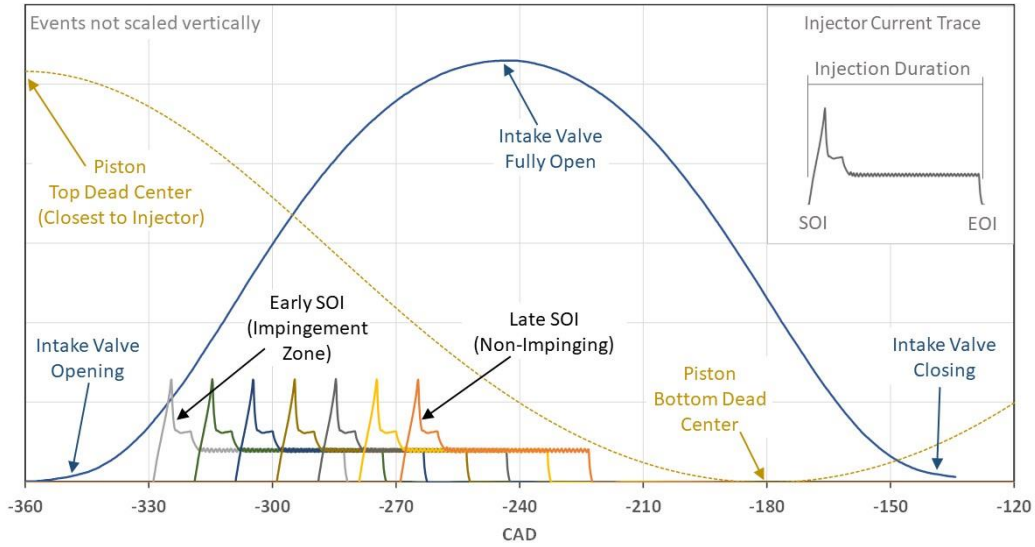

Figure 12. SOI sweep compared to intake valve opening/closing and piston position of the engine.

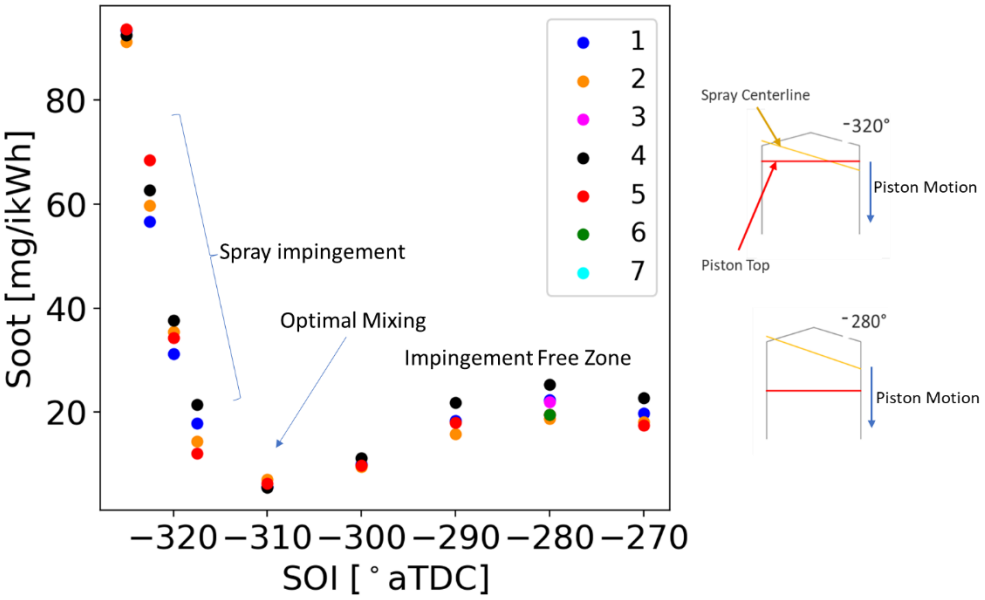

Figure 13. Example SOI sweep (left), seven replications are shown (not all replications extend over the entire SOI sweep) for fuel D-PrOH-13. Simple representations of piston and fuel spray (right).

The main analysis of fuel effects on soot emission is based on three measurements from the SOI sweep data for each of the fuels studied. The first of these is soot emissions in the non-impingement zone at a base condition, -280° SOI for condition A and -270° SOI for condition B. The second is the computed SOI for the transition point from non-impingement to the impingement zone, and the third is soot emissions in the impingement zone at a specific SOI.

The method for computing the spray impingement transition point for each fuel blend is shown in Figure 14, Fuel D is used as the example. A horizontal line is calculated through the minimum soot value over the SOI sweep (minimum of the calculated mean data by SOI), which occurs at the optimal mixing point shown in Figure 13. A second line is a linear curve fit for calculated mean data in the impingement zone. The intersection of these two lines is defined as the transition point, shown as the red dot in Figure 14.

For the results comparing soot emissions in the impingement zone, an SOI is chosen to provide the largest differences between the fuels. In a few cases, an extrapolation of the soot emissions to more negative (more advanced) SOI is required, and these are noted in the write up. Figures 15–22 show the SOI CAD chosen with a vertical dashed line. This procedure is intended to provide a ranking of the fuels for soot formation. Soot emissions from different SOIs for the different fuel groups in the impingement zone are not necessarily similar and caution should be used when comparing the results to other fuel groups.

All three of these parameters: soot level in the non-impingement zone, soot level in the impingement zone, and the transition point are to some extent based on arbitrary choices made by the data analyst in terms of showing the largest differences between fuels or defining the linear region of the impingement zone soot emissions. Thus, these parameters are intended to provide a relative ranking of the fuels.

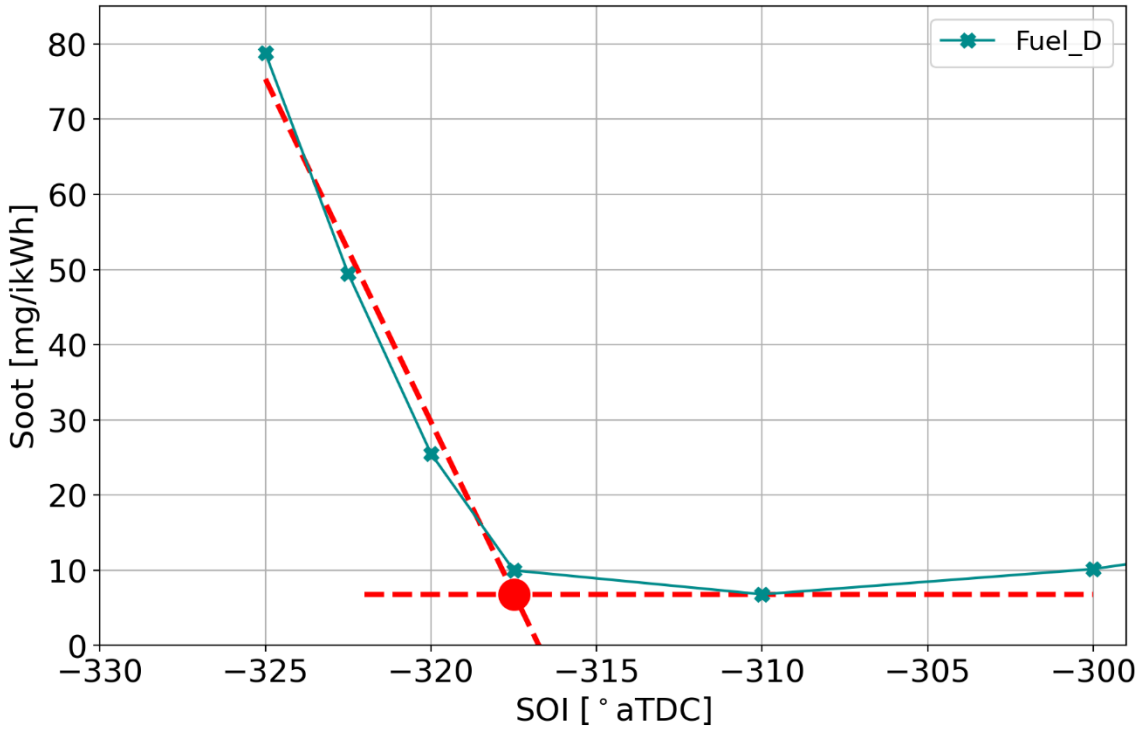

Figure 14. Example of SOI sweep at Condition A for Fuel D showing injection spray to piston impingement transition point and lines/markers used to for calculations.

The order used for testing the fuels is shown in Appendix B. Fuel D and the certification fuel were both repeated three times at various stages of the study to act as benchmarks to ensure that engine and fuel injection parameters were not changing over the course of the study. The fuel injector was changed out with one of the exact same brand and model during the experiments for fuel C blended with 15% ethanol. Later review of the data showed that this altered the results and so all data collected prior to the injector swap was discarded. This means that the first dataset for Fuel D was excluded, as well as data for C-EtOH-15 at advanced SOI (only data for the -280°aTDC SOI point is available).

All emissions results are shown in Appendix C, including gaseous emissions. Fuels showed only minor impacts on gaseous emissions, which are described in Appendix D.

Hydrocarbon base fuels. SOI sweeps for the base fuels are shown in Figures 15 and 16 for condition A and B, respectively; and parameters extracted from these charts are shown in Tables 11 and 12. Given the large range in PMI for these fuels (1.21 to 2.75), it seems unexpected how similar the soot levels are in the non-impingement zone for condition A, but this is likely because in this zone fuel and air are reasonably well mixed. The transition point (where soot emissions begin to sharply increase) occurs at later (less negative CAD, or more retarded) SOIs for fuels with increasing PMI. This means that the onset of diffusion combustion occurs when the piston is farther down the bore and a greater distance from the injector for higher PMI fuels; or put another way. In the impingement zone, at -325° SOI, soot emissions vary by a factor of 10 and are well correlated to PMI (r^2=0.98).

At condition B, the overall later SOIs for the transition points (compared to condition A) are the result of similar loads (therefore similar injection durations) combined with the slower engine speed such that at a given SOI crank angle and injection duration, the dwell time of the piston is longer at the piston position for that crank angle. The intensity of the charge-air motion (e.g., tumble and swirl) is also probably lower at the lower engine speed, which can inhibit fuel spray break-up and evaporation. Thus, there is more opportunity for liquid fuel spray to contact the piston. On the other hand, previous research at fixed SOI and without spray impingement on the piston suggested that at the slower engine speed the impact of fuel evaporation was minimized because of the additional time available for evaporation and mixing (5). Soot emissions are clearly higher for Fuel D in the non-impingement zone, consistent with its PMI; yet are very similar for the other fuels. The transition point and soot in the impingement zone are also well aligned with PMI for these fuels.

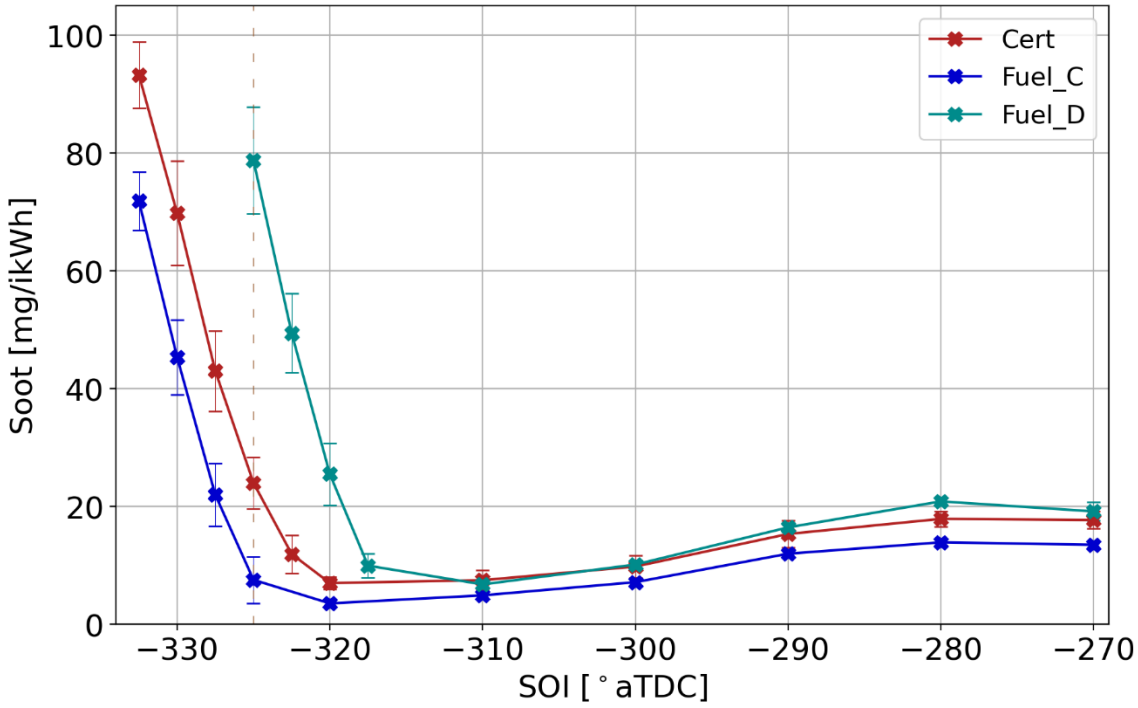

Figure 15. Soot emissions over SOI sweeps at condition A for base hydrocarbon fuels (error bars are 95% confidence interval based on several replications).

Table 11. Analytical results from condition A (95% confidence interval for soot based on 4 to 10 replications).

Fuel	PMI	-325° aTDC Soot (mg/ikWh)	Transition Point SOI (°aTDC)	-280° aTDC Soot (mg/ikWh)
C	1.21	7.6 ± 4	-325.7	13.9 ± 0.6
Cert	1.29	24 ± 4	-322.5	17.9 ± 1.3
D	2.75	79 ± 9	-317.5	20.9 ± 0.6

Considering the properties of the hydrocarbon fuels (Table 4), density, DVPE, energy density, carbon content, heat of vaporization, and total aromatics (Table 7) are all similar. Literature sources also

suggest that other properties that would influence the fuel spray such as viscosity and surface tension do not vary widely for hydrocarbon fuels (*34*,*35*) – which is confirmed by results reported in Table 4. Density, viscosity, and surface tension appear to be the primary factors affecting spray penetration and spray angle suggesting that these spray metrics will not be different for these fuels. Additionally, for flash boiling to occur the ambient (or cylinder) pressure must be less than the fuel saturation vapor pressure. Intake air and fuel temperatures are close to 38°C, the temperature used to measure DVPE. DVPE for these fuels ranged from 7.3 psi (50.3 kPa) to 8.8 psi (60.7 kPa) while for these experiments cylinder pressure during fuel injection was always above 85 kPa.

Primary differences between the fuels include the higher RON and MON of the certification fuel, but this is not likely relevant to soot formation. (*1*) Fuel D has significantly higher T90 and final boiling point, as well as significantly higher concentrations of C10 and C11 aromatics – and consequently higher PMI. Given these facts, the more retarded SOI for transition to spray impingement for Fuel D may be caused by the fuel being more difficult to evaporate from the piston surface than to differences in spray properties.

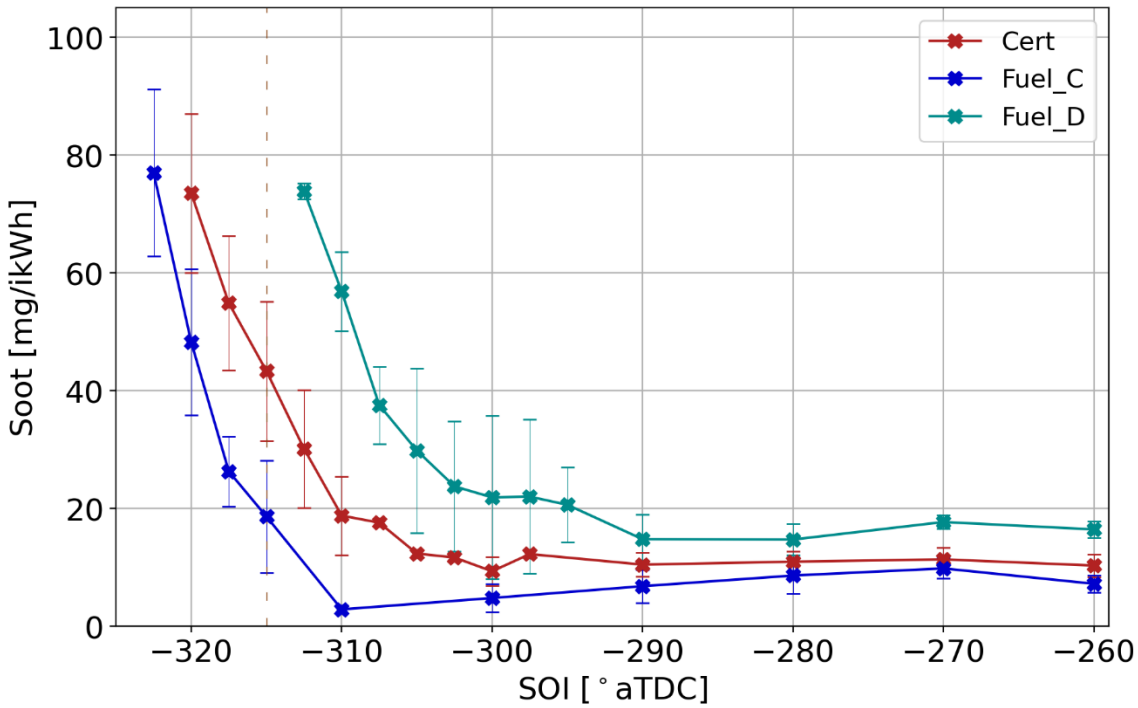

Figure 16. Soot emissions over SOI sweeps at condition B for base hydrocarbon fuels (error bars are 95% confidence interval based on several replications).

Table 12. Analytical results from condition B (95% confidence interval for soot based on 4 to 10 replications).

Fuel	PMI	-315° aTDC Soot (mg/ikWh)	Transition Point SOI (°aTDC)	-270° aTDC Soot (mg/ikWh)
C	1.21	19 ± 10	-311.3	9.9 ± 1.7
Cert	1.29	43 ± 12	-308.5	11.4 ± 2.0
D	2.75	91*± 1.4	-298.8	17.7 ± 1.1

*By extrapolation

Fuel C Blends. SOI sweeps at condition A are shown in Figure 17. Examining the non-impingement zone, Fuel C and the E10 blend emit similar levels of soot, while the levels from isobutanol are significantly lower, and lowest from the MTBE blend. For E10 this indicates that the expected effects of diluting aromatics with high soot forming potential were either too small to observe at this blend level or counter-balanced by the inhibitory effects on fuel evaporation arising from ethanol's higher HOV (see Figure 4) and vapor-liquid equilibrium (VLE) effects that can concentrate aromatics in the evaporating fuel droplets (*5*). However, the isobutanol blend produced the most retarded (least negative CAD) transition point of all the C blends (see Table 13). The transition zone for isobutanol was also more gradual than for the other fuels. This different transition behavior may be an effect of isobutanol's high viscosity, which could impact the spray or droplet atomization. A previous study found that blending of 15 vol% isobutanol increased viscosity at 20°C from 0.6478 to 0.7586 cSt – about 17% (*6*). For the fuels used here, viscosity increased from 0.6827 to 0.7965 cSt for the isobutanol blend versus the base fuel, Fuel C. E10's transition point is slightly retarded relative to Fuel C consistent with an HOV effect on evaporating fuel. Throughout the entire SOI sweep, the MTBE blend consistently produced lower soot emissions than the base fuel C or alcohol blends – even though the E10 blend diluted aromatics to the same extent on a molar basis (about 20%). Correlations of soot emissions with PMI are poor in both impingement and non-impingement zones.

Note that the 15% ethanol blend results at condition A for transition point and impingement are absent because of an oversight early in the experimental campaign that was not noticed until much later. Replicate data at -280° aTDC was obtained with the new injector, producing soot essentially the same as from the 10% ethanol blend in the non-impingement zone (see Table 13).

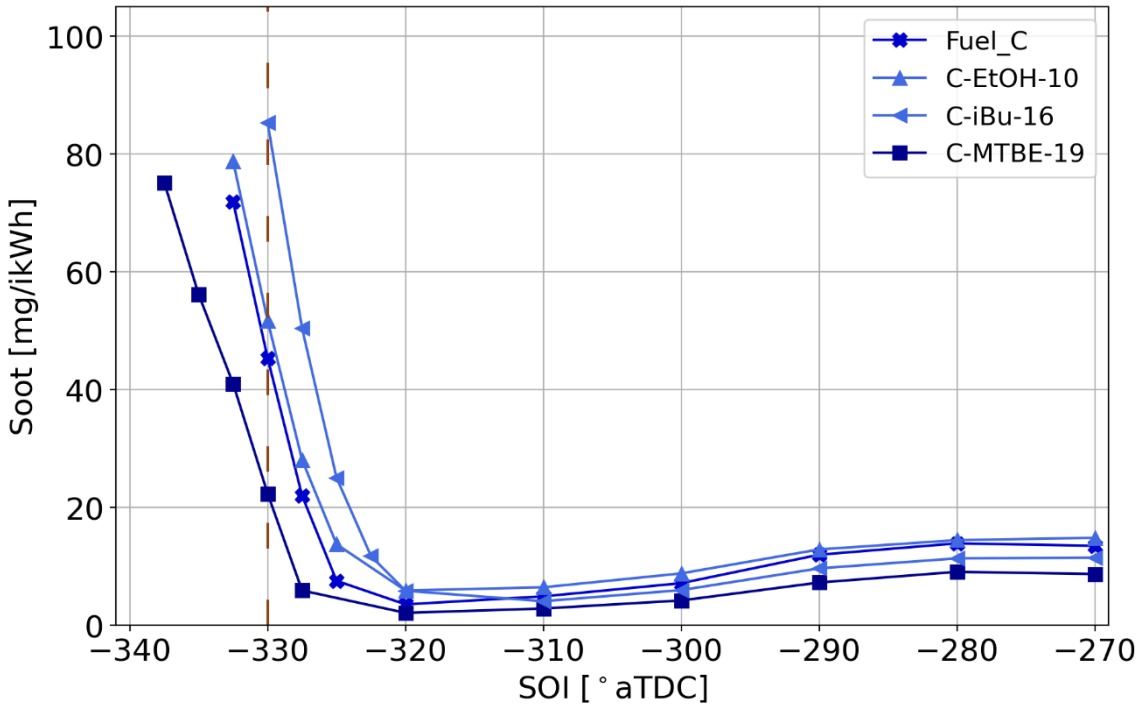

Figure 17. Soot emissions over SOI sweeps at condition A for Fuel C and blends.

Table 13. Analytical results from fuel C blends at condition A (95% confidence interval for soot based on 4 to 10 replications).

Fuel	PMI	-330° aTDC Soot (mg/ikWh)	Transition Point SOI (°aTDC)	-280° aTDC Soot (mg/ikWh)
C	1.21	45 ± 6	-325.7	13.9 ± 0.6
C-EtOH-10	1.11	52 ± 4	-324.5	14.5 ± 1.9
C-EtOH-15	1.05	NA	NA	14.9 ± 1.1
C-iBu-16	1.06	85 ± 8	-323.4	11.4 ± 1.3
C-MTBE-19	1.00	22 ± 5	-327.0	9.1 ± 0.4
PMI Regression R^2		<0.1	<0.1	0.34

The overall soot emission trends from the fuel C blends at condition B (Figure 18) are similar to those at condition A. It is interesting that the isobutanol blend again significantly reduced soot emissions in the non-impingement zone, then had the most retarded transition point at SOI = -299.2° aTDC (Table 14). Soot emissions for the ethanol blends in the non-impingement zone are not significantly different from those for Fuel C. However, unlike the 10% ethanol blend which produced a transition point similar to that for base fuel C, the 15% ethanol blend's transition point occurred at a much more retarded SOI despite its lower PMI. We attribute this to its significantly higher heat of vaporization – in line with the idea that the transition point is determined by how difficult it is for fuel to evaporate after being deposited on the piston. The slightly higher viscosity of the E15 blend may also have contributed to this effect. In the impingement zone the E15 and isobutanol blends show the highest soot levels, consistent with the HOV and viscosity effects mentioned previously. Soot emissions were not correlated with PMI

at any point in the sweep (see regression R^2 values in Table 14 and Figures 27a, 29a and 31a Emission Study Summary section below).

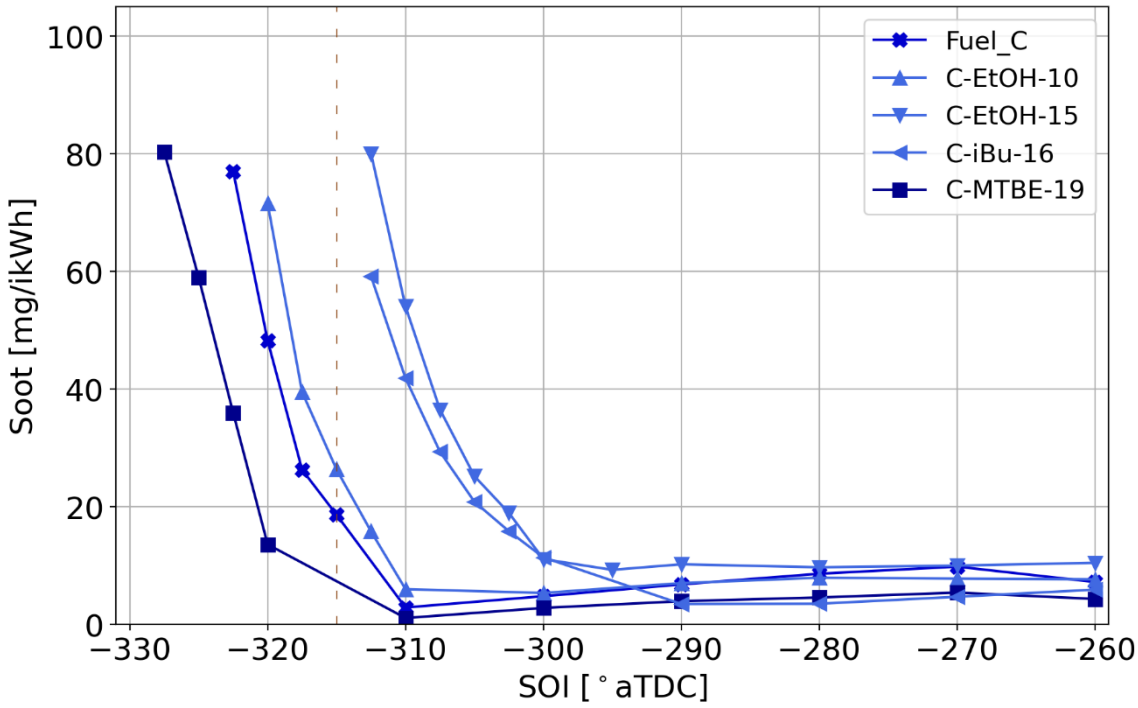

Figure 18. Soot emissions over SOI sweeps at condition B for Fuel C and blends.

Table 14. Analytical results from fuel C blends at condition B (95% confidence interval for soot based on 4 to 10 replications).

Fuel	PMI	-315° aTDC Soot (mg/ikWh)	Transition Point SOI (°aTDC)	-270° aTDC Soot (mg/ikWh)
C	1.21	19 ± 10	-311.3	9.9 ± 1.7
C-EtOH-10	1.11	26 ± 5	-310.7	7.8 ± 1.4
C-EtOH-15	1.05	106*± 10	-301.9	10.0 ± 1.1
C-iBu-16	1.06	77*± 9	-299.2	4.7 ± 0.4
C-MTBE-19	1.00	7± 4	-318.6	5.4 ± 0.9
PMI Regression R^2		<0.1	<0.1	0.36

*By extrapolation.

In the original CRC E-129 study these fuels were examined in four light-duty gasoline vehicles over the LA92 cycle. For change in PM emissions averaged over the fleet of cars relative to Fuel C the ranking of the fuels was: Fuel C ≈ C-EtOH-10 > C-EtOH-15 > C-MTBE-19 ≈ C-iBu-16 (*2*). For these results, taken over a drive cycle covering a wide range of speed load conditions and presumably a wide range of SOI values, the oxygenate dilution effect is observed for E15, isobutanol, and MTBE – but not for E10 where the relatively low level of dilution may have been too small to measurably reduce PM. In fact, on a molar basis the E15 blend dilutes the aromatics significantly more than the isobutanol or MTBE blends such

that if dilution were the only effect soot emissions should be lowest for E15. Apparently HOV/VLE effects are in competition with dilution effects for this fuel.

The present study examined the same fuels under a much narrower set of conditions: spray non-impinging and spray impinging conditions. For non-impinging conditions the fuel ranking is:

Condition A: Fuel C ≈ C-EtOH-15 ≈ C-EtOH-10 > C-iBu-16 > C-MTBE-19
Condition B: Fuel C ≈ C-EtOH-15 > C-EtOH-10 > C-iBu-16 ≈ C-MTBE-19

E15 has the highest dilution of aromatics on a molar basis for this set of blends, yet consistently produces just as much soot as the base fuel for non-impinging conditions – which we attribute to the HOV/VLE effect. E10, the isobutanol blend, and the MTBE blend all have similar levels of dilution on a molar basis, yet E10 has consistently higher soot emissions, likely for the same reasons as E15. These trends are not in line with PMI and given that these conditions do not involve deposition of fuel onto the piston, likely imply impacts on droplet evaporation leading to fuel rich regions at the time of combustion. We examined two additional PM metrics (NREL PMI and PME) that were designed to try to capture HOV/VLE effects for alcohols – but they also are not well correlated with the results, which is as expected given their high correlation with PMI.

For impinging conditions, we can (arbitrarily) use the soot emissions at -330° (A) or -315° (B) SOI for fuels comparison. This provides the following ranking:

Condition A: C-iBu-16 > Fuel C ≈ C-EtOH-10 > C-MTBE-19
Condition B: C-EtOH-15 > C-iBu-16 > Fuel C ≈ C-EtOH-10 > C-MTBE-19

The observation that the isobutanol blend moves from being one of the lowest soot forming fuels under non-impinging conditions to one of the highest soot forming fuels under impinging conditions clearly points to a change in the controlling physics for this fuel. Isobutanol's higher viscosity relative to other gasoline blending components and the significantly higher viscosity of the C-iBu-16 blend may be an important factor. This is also supported by the longer injection duration observed for C-iBu-16 in comparison to fuels with similar volumetric energy content (C-EtOH-10 and C-MTBE-19) as shown in Figure 19 for both conditions A and B. The figure also shows fuel volumetric energy content, where the E10, isobutanol, and MTBE blends are all similar and so should have similar injection duration, yet isobutanol's is significantly longer. Higher viscosity fuels will have lower fluid velocity in the injector nozzle at constant injection pressure and therefore require longer injection times (*34*,*35*). It is also interesting to note that C-iBu-16 has the highest density of the Fuel C group (Table 5). These factors may alter the fuel spray such that C-iBu-16 has the most retarded transition point of this group of fuels, for example by increasing spray penetration and reducing fuel atomization (or put another way, the range of SOI for non-impingement is smallest for the isobutanol blend). Fuel surface tension can also impact spray breakup and droplet formation but was not significantly different for these fuels.

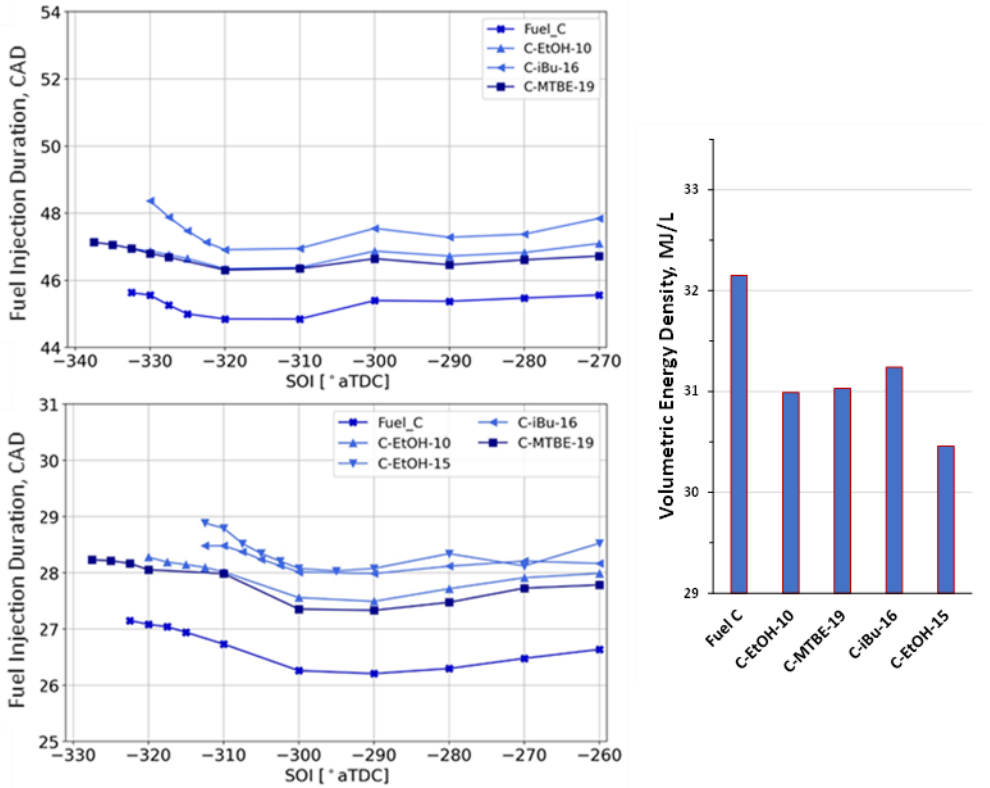

Figure 19. Injection duration for Fuel C and oxygenate blends for condition A (top) and condition B (bottom). Fuel volumetric energy content at right.

A detailed spray chamber and simulation study may be able to confirm this speculation. Another factor potentially increasing soot from C-iBu-16 under impinging conditions is chemistry. Isobutanol is known to form isobutylene during combustion (*36*,*37*) which has been observed in tailpipe emissions from vehicles (*38*). It therefore seems plausible that high concentrations of isobutylene arising from fuel film or pool fires may participate in soot forming reactions.

Fuel D Blends. Because of the large number of Fuel D blends studied, alcohol blends are discussed separately from ether blends. Results for alcohol blends in Fuel D at conditions A and B are shown in Figures 20 and 21, and Tables 15 and 16. For condition A – non-impingement zone, it is notable that overall soot emissions are almost twice as high as observed for the Fuel C fuels consistent with the more than doubling of the base fuel PMI. The two highest HOV fuels D-MeOH-10 and D-EtOH-15 show higher soot emissions than the other fuels which all have similar soot emissions, Table 15. These trends contradict the expectation that soot would decrease based on aromatics dilution and lowered PMI. The results overall are suggesting an HOV effect for all these alcohols with the effect being large enough for the high-level methanol and ethanol blends to increase soot formation.

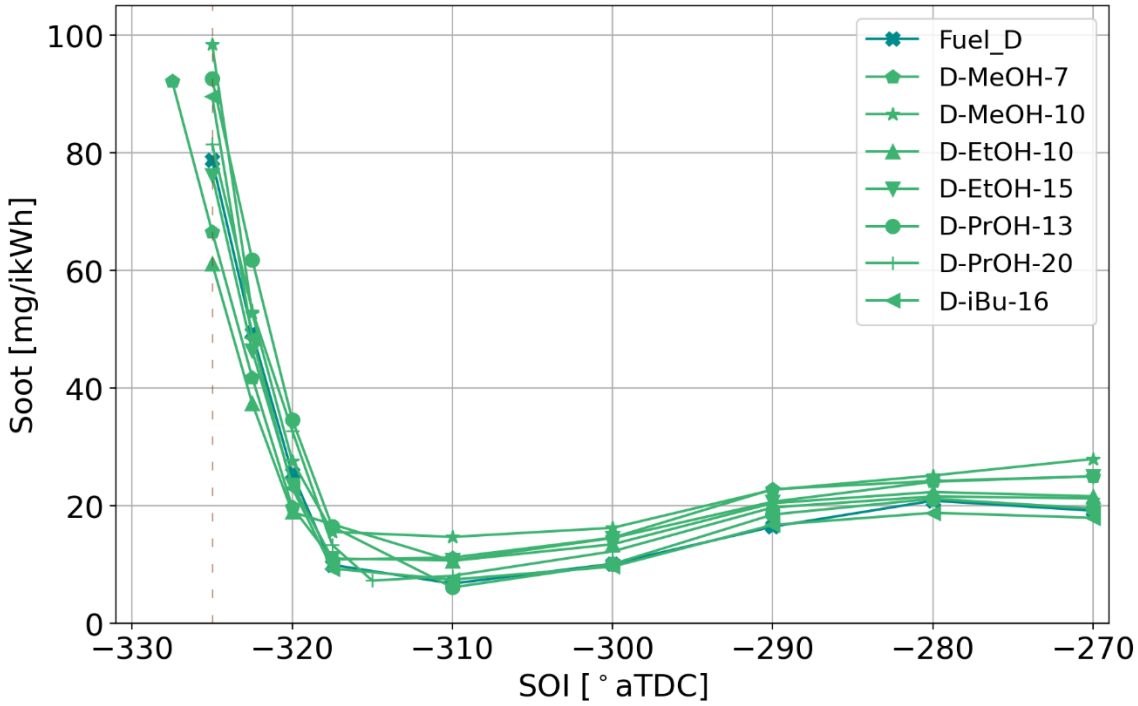

Figure 20. Soot emissions over SOI sweeps at condition A for Fuel D and alcohol blends.

One of the most notable observations from Figure 20 is that there is little differentiation between the fuels for transition point, as these are clustered in a narrow 1.9° SOI range. The transition points for all Fuel D fuels are 3° to 4° retarded from the most retarded Fuel C blend, again reinforcing the idea that harder to evaporate fuels have more retarded transition points. The isobutanol blend is not showing a more retarded transition for this set of fuels at condition A.

In the impingement zone at -325° SOI we see D-EtOH-10 lowering soot emissions, presumably by dilution of aromatics. The D-MeOH-7, D-MeOH-10, D-EtOH-15 and D-PrOH-20 blends have similar emissions (considering the confidence intervals) to the base fuel, indicating that HOV effects were more important than dilution effects. The E10 has similar HOV to these blends and its lower soot emissions seem to be an outlier. Higher soot emissions for D-PrOH-13 relative to the 20% propanol blend may be explained by dilution effects becoming dominant at the higher blend level.

Table 15. Analytical results from fuel D and alcohol blends at condition A (95% confidence interval for soot based on 4 to 10 replications).

Fuel	PMI	-325° aTDC Soot (mg/ikWh)	Transition Point SOI (°aTDC)	-280° aTDC Soot (mg/ikWh)
D	2.75	79 ± 9	-317.5	20.9 ± 0.6
D-MeOH-7	2.56	67 ± 19	-319.2	24.2 ± 3.9
D-MeOH-10	2.44	99 ± 12	-319.3	25.2 ± 2.3
D-EtOH-10	2.46	61 ± 3	-319.1	22.4 ± 1.6
D-EtOH-15	2.31	76 ± 3	-318.9	24.1 ± 0.4

D-PrOH-13	2.47	93 ± 1	-317.6	21.2 ± 2.0
D-PrOH-20	2.28	82 ± 4	-317.5	21.6 ± 1.2
D-iBu-16	2.34	90 ± 13	-319.0	18.8 ± 1.0
PMI Regression R^2		<0.1	<0.1	<0.1

Figure 21 shows that for condition B increasing volume percentages of alcohols reduce soot emissions through the impingement-free zone – consistent with the dilution effect – and shows some correlation with PMI (Table 16). Compared to condition A, Figure 21 shows there is much more differentiation among the alcohol blends in terms of transition point; these data are also tabulated in Table 16. D-iBu-16 showed the most retarded transition point, as was also observed for the Fuel C blends. D-MeOH-7 and D-EtOH-15 had the most advanced transition points, while all the other fuels had transition points very similar to that of Fuel D.

In the impingement zone a notable feature is the poor repeatability (large 95% confidence interval) observed for the methanol blends (this was also an issue for D-MeOH-7 at condition A). For these fuels the RVP values are about 10.8 psi or 75 kPa. It is possible that cylinder pressure during fuel injection could have dropped to below this level at condition B, leading to fuel flash boiling. If conditions reached these borderline limits, this could have caused instability in the soot results. Recall that for flash boiling to occur the ambient pressure must drop below the fuels saturation vapor pressure. The RVP for the other alcohol blends was at least 2 psi lower. The impingement zone results generally show significantly higher levels of soot for all the alcohol blends except D-MeOH-7 and D-EtOH-15.

Figure 22 shows injection duration for the Fuel D alcohol blends at conditions A and B, along with volumetric energy density for the fuels. Although less pronounced than for the Fuel C blends, the longest injection durations are for the lowest energy density fuels, plus D-PrOH-20 and D-iBu-16, consistent with the higher measured viscosity of these fuels.

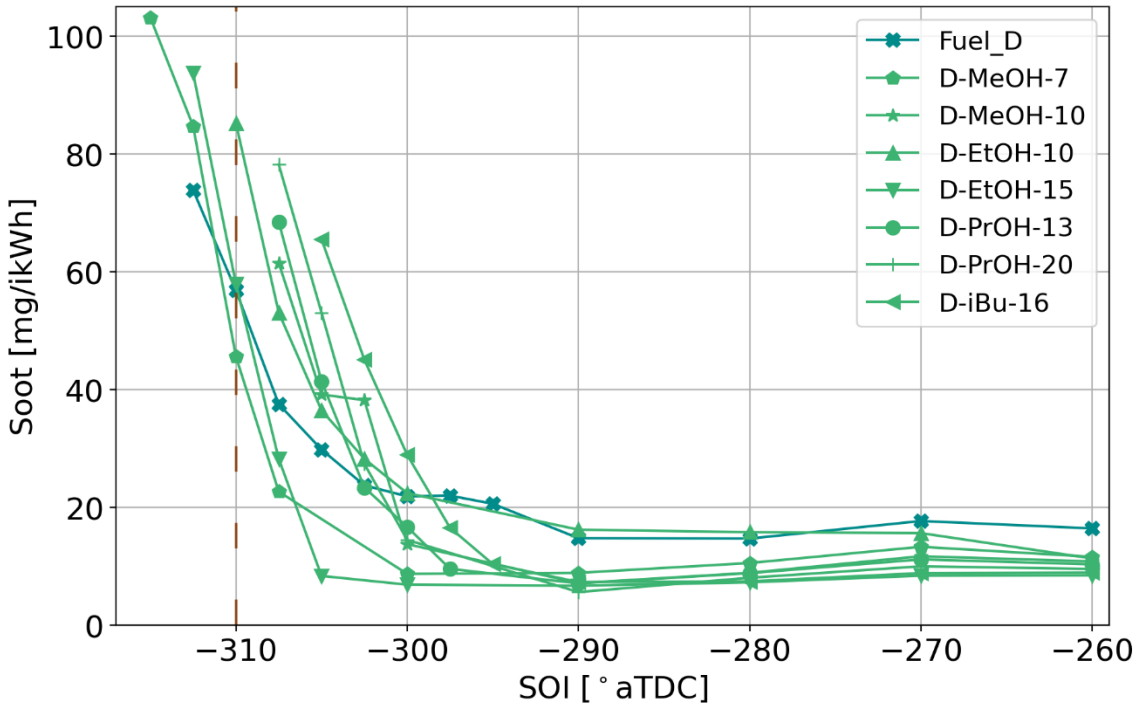

Figure 21. Soot emissions over SOI sweeps at condition B for Fuel D and alcohol blends.

Table 16. Analytical results from fuel D and alcohol blends at condition B (95% confidence interval for soot based on 4 to 10 replications).

Fuel	PMI	-310° aTDC Soot (mg/ikWh)	Transition Point SOI (°aTDC)	-270° aTDC Soot (mg/ikWh)
D	2.75	57 ± 7	-298.8	17.7 ± 1.1
D-MeOH-7	2.56	46 ± 23	-306.4	13.4 ± 0.9
D-MeOH-10	2.44	84*± 36	-298.8	11.8 ± 0.8
D-EtOH-10	2.46	85 ± 15	-300.2	15.7 ± 2.2
D-EtOH-15	2.31	58 ± 3	-305.2	8.5 ± 1.0
D-PrOH-13	2.47	96*± 6	-298.2	11.2 ± 1.3
D-PrOH-20	2.28	103*± 13	-299.4	10.0 ± 0.5
D-iBu-16	2.34	106*± 7	-295.3	8.9 ± 1.1
PMI Regression R^2		0.33	<0.1	0.77

*By extrapolation.

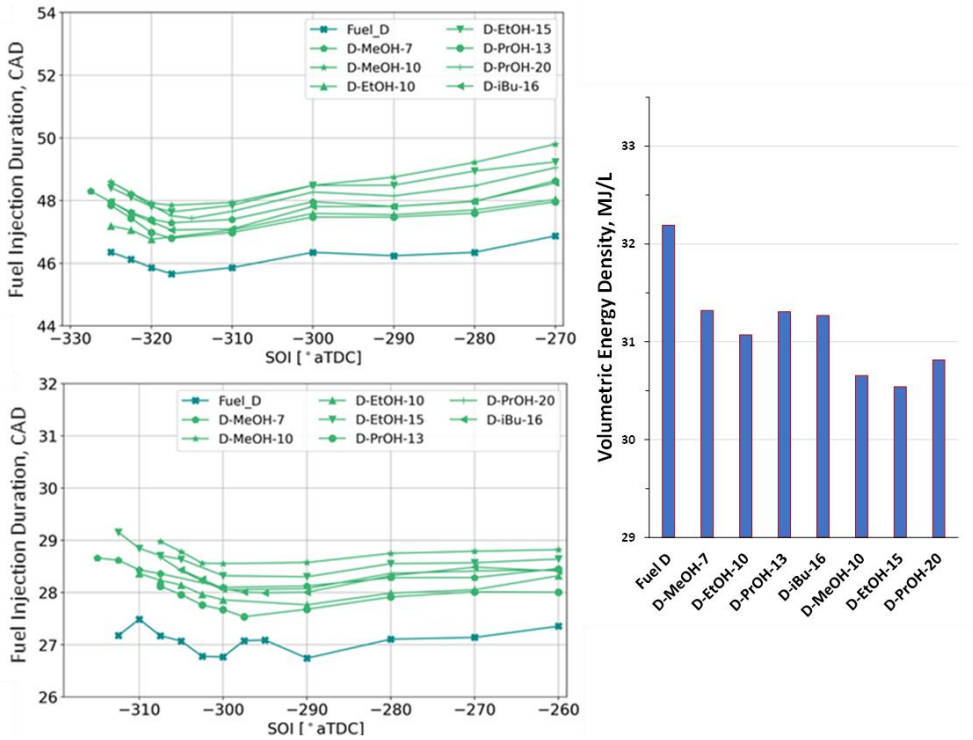

Figure 22. Injection duration for Fuel D alcohol blends for condition A (top) and condition B (bottom). Fuel volumetric energy content at right.

Soot emissions from the ether blends in Fuel D at conditions A and B are shown in Figures 23 and 24. The increase in soot emissions from the dimethoxymethane blends across the impingement-free zone is unexpected and the available fuel property data offer no obvious explanation. Both blends required retarded spark timing due to their knock tendency, however, it is not suspected that this is the reason for the elevated soot in the impingement-free zone (*19*). As shown in Figure 25, the D-DMM-12 blend had significantly longer injection duration than the lower DMM level blend, as well as the other ethers or alcohols used in this study. There is no obvious explanation based on fuel properties as the volumetric energy density of this fuel is similar to or higher than for several of the other ether blends. However, the boiling point for DMM is 42°C, lowest of all the oxygenates tested. Given that the surface temperature of the fuel rail was in the 38-45°C range, and the likelihood that the fuel in the injector was even hotter, spray collapse from flash boiling could have affected the entire fuel droplet breakup process and/or deposited more fuel on combustion chamber surfaces (*8*). The behavior of the tert-butyl ethers is more aligned with expectations based on dilution, although one might expect more significant soot reductions given that the ethers provide high levels of aromatics dilution and slightly lower the HOV of the blends. The range of transition point locations for condition A is again narrow, within 2° for most of the blends as shown in Table 17. Only the MTBE blend is significantly advanced from the base fuel. Notably the surface tension of the D-ETBE-35 blend is 5% lower than that of the base fuel (and the other fuel blends), but we cannot attribute any of the observations to this difference.

In the impingement zone at condition A all the ether blends reduce soot relative to the base fuel, with the MTBE blend having the greatest effect. This is not consistent with dilution as both ETBE blends have higher dilution levels. The DMM blends produced similar soot reductions as the ETBE blends despite being at the opposite end of the aromatic dilution ranking. These results are difficult to explain given that total oxygen content of the fuels was capped at either 3.7 or 5.5 wt%.

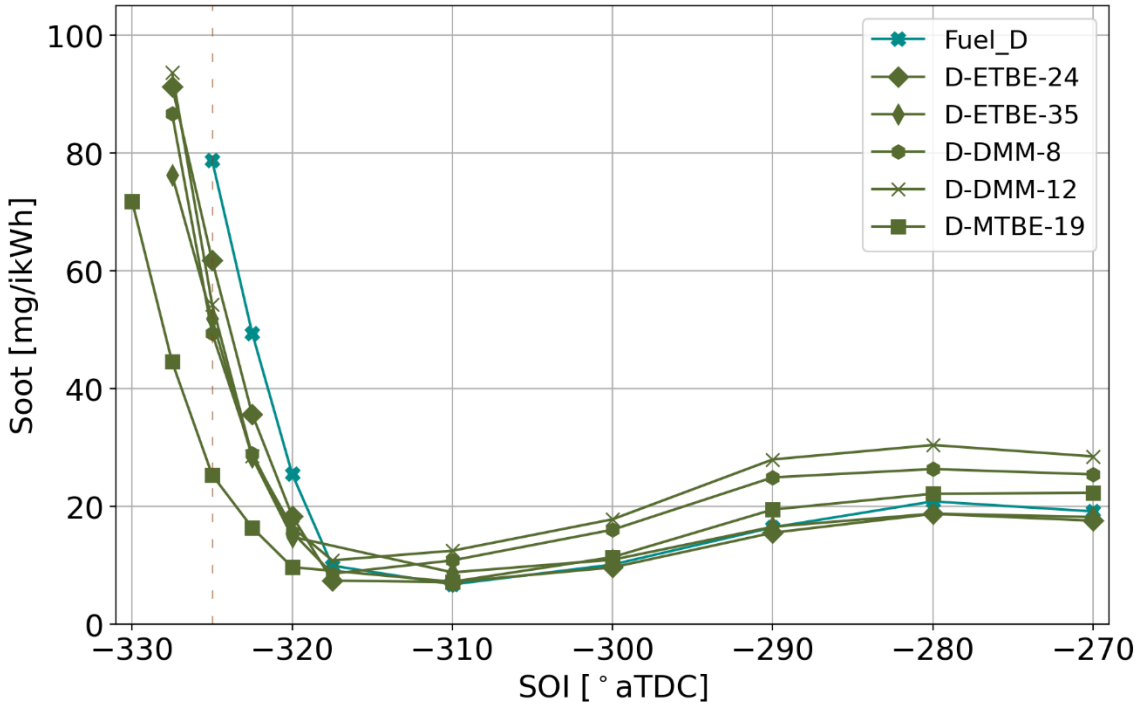

Figure 23. Soot emissions over SOI sweeps at condition A for Fuel D and ether blends.

Table 17. Analytical results from fuel D and ether blends at condition A (95% confidence interval for soot based on 4 to 10 replications).

Fuel	PMI	-325° aTDC Soot (mg/ikWh)	Transition Point SOI (°aTDC)	-280° aTDC Soot (mg/ikWh)
D	2.75	79 ± 9	-317.5	20.9 ± 0.6
D-ETBE-24	2.08	62 ± 8	-320.0	18.9 ± 1.0
D-ETBE-35	1.75	52 ± 3	-320.5	18.1 ± 0.7
D-DMM-8	2.47	49 ± 8	-318.7	26.6 ± 1.8
D-DMM-12	2.40	54 ±5	-321.3	30.5 ± 3.2
D-MTBE-19	2.08	25 ± 2	-323.2	22.2 ± 1.4
PMI Regression R^2		0.26	<0.1	0.24

At condition B non-impingement zone, the ETBE and MTBE blends show soot reductions consistent with aromatics dilution, see Figure 24 and Table 18. However, the DMM blends continue to behave

differently from the tert-butyl ethers. The 8% DMM blend is unique in that it matches the soot emissions from fuel D through the impingement-free zone, yet it is the only fuel in this set that retards the transition point. As observed for condition A, the DMM blends have significantly longer injection durations than other fuels. Nevertheless, there is an excellent correlation of impingement free zone soot with PMI. Similar to the condition A results, MTBE provided the largest advance in the transition point. In the impingement zone MTBE reduces soot emissions, D-DMM-8 increases them, while the other fuels provide results like the base fuel.

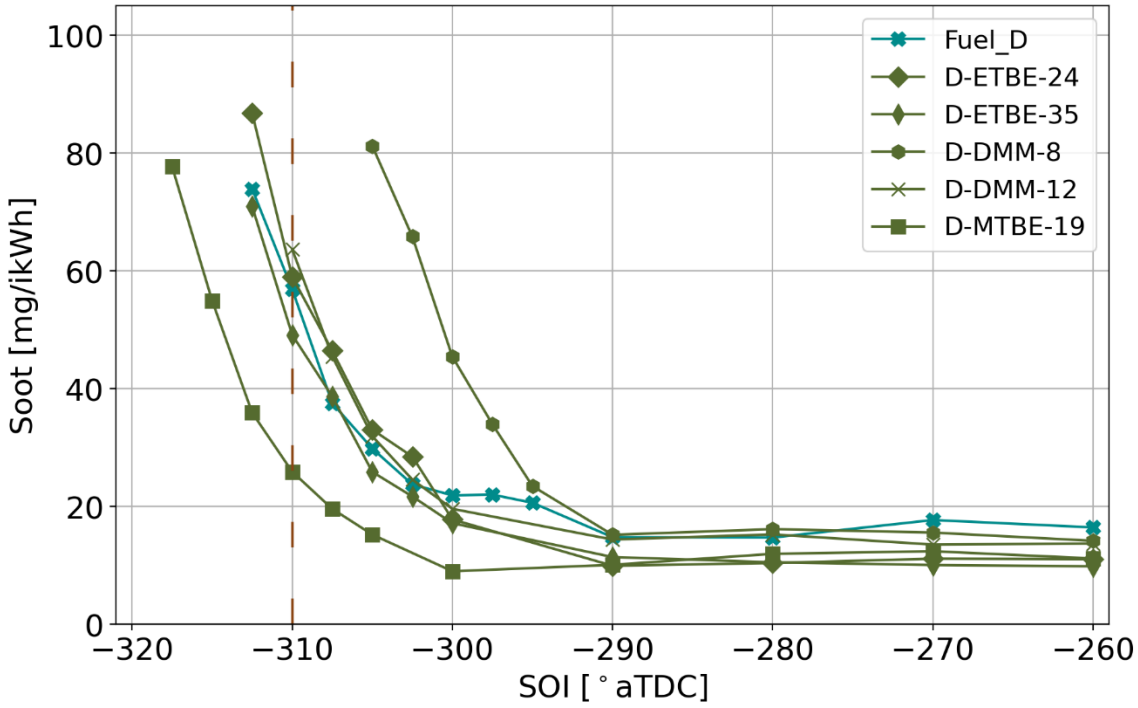

Figure 24. Soot emissions over SOI sweeps at condition B for Fuel D and ether blends.

Table 18. Analytical results from fuel D and ether blends at condition B (95% confidence interval for soot based on 4 to 10 replications).

Fuel	PMI	-310° aTDC Soot (mg/ikWh)	Transition Point SOI (°aTDC)	-270° aTDC Soot (mg/ikWh)
D	2.75	57 ± 7	-298.8	17.7 ± 1.1
D-ETBE-24	2.08	59 ± 6	-299.4	11.2 ± 0.5
D-ETBE-35	1.75	49 ± 12	-300.0	10.1 ± 1.4
D-DMM-8	2.47	112*± 18	-294.1	15.8 ± 1.1
D-DMM-12	2.40	64 ± 9	-299.8	13.6 ± 1.5
D-MTBE-19	2.08	26 ± 17	-305.3	12.4 ± 1.4
PMI Regression R^2		0.19	0.18	0.93

*By extrapolation.

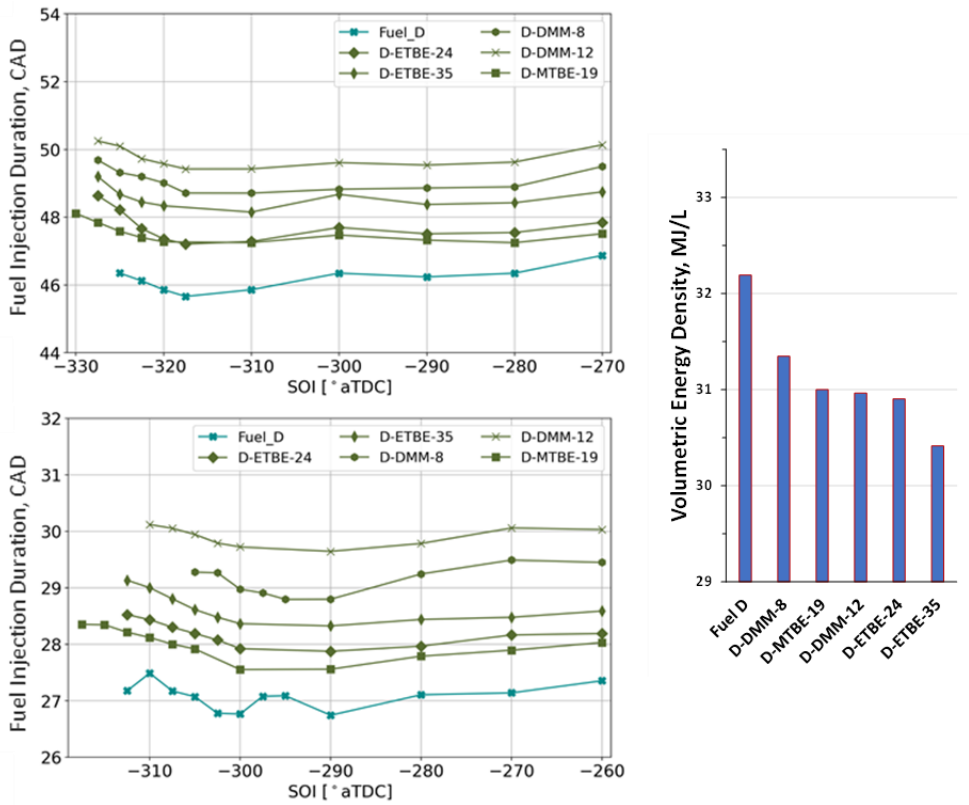

Figure 25. Injection duration for Fuel D ether blends for condition A (top) and condition B (bottom). Fuel volumetric energy content at right.

Emissions Study Summary. The three engine combustion metrics related to soot emissions that were examined in this study were soot emissions in the impingement zone, the SOI transition point between the impingement and non-impingement zones, and soot emissions in the non-impingement zone. Under the assumption that engine calibrations avoid spray impingement, results in the non-impingement zone may be most relevant.

For the hydrocarbon fuels soot emissions at both high speed and low speed conditions in both the non-impingement and impingement zones are well correlated with PMI. Fuel D exhibits a more retarded transition to spray impingement which appears to be related to its high T90 and final boiling point, and high aromatics content, than to physical properties that effect spray penetration or droplet size.

For alcohol blends (at condition A, 2500 rpm, 12.5 bar gIMEP non-impingement) we see all possible effects relative to the base fuel: soot increasing, staying the same, or decreasing. These effects can be rationalized as being caused by aromatics dilution (soot decreases) or by HOV/VLE effects (soot increases or stays the same). The highest HOV fuels generally caused soot to increase, however there is not a 1 to 1 correspondence between HOV and the magnitude of soot increase (correlation between soot and HOV or HOV per kg of stoichiometric mixture is poor). Except for DMM, ethers generally reduced soot (C-MTBE-19, D-ETBE-24, D-ETBE-35) or had no effect (D-MTBE-19). DMM blends significantly increased soot emissions in the non-impingement zone for condition A. We originally speculated that this could be caused by fuel properties that affect the fuel spray, however density, viscosity, and surface tension for the D-DMM-12 blend are fairly close to values measured for the base fuel.

Fuels that have the most retarded (latest) transition point usually have the highest soot emissions in the impingement zone. The hydrocarbon fuels correlated with PMI, with Fuel D having roughly five-times the emission level of Fuel C. C-iBu-16 showed the most retarded transition point and highest impingement soot emissions of the Fuel C blends, which is not explainable by its HOV, but may have been caused by the measurably higher viscosity of this blend relative to the base fuel possibly altering fuel spray parameters, droplet size, or other factors. Ethers reliably reduce soot emissions at this operating condition, however not in proportion to their concentration in the fuel. For example, ETBE blends did not reduce soot as much as MTBE blends even though they were present at higher mass or molar concentration – D-ETBE-24 had the same soot emissions level as Fuel D. Alcohol blends showed the full range of possible effects and results were not well correlated with fuel properties or dilution.

For the lower speed condition B (1500 rpm, 12 bar gIMEP) at non-impinging late injection, fuel dilution effects were dominant – in agreement with a prior study that proposed at low engine speed there was additional time for mixing, heat transfer, and evaporation (*5*). Of the 16 oxygenate blends tested, none caused soot to increase, 12 produced a soot reduction, and four caused no statistically significant change. In the impingement zone for the Fuel C blends, C-iBu-16 and C-EtOH-15 showed the most retarded transition and highest soot emissions. C-MTBE-19 had the most advanced transition and lowest soot. For the Fuel D alcohol blends the highest soot emissions were the isobutanol and propanol blends, followed by E10 and then the other fuels. The methanol blends showed significant variability (larger 95% confidence interval) that the other fuels. For the ethers D-DMM-8 showed the highest soot emissions and most retarded transition, while D-MTBE-19 showed the lowest soot emissions and most advanced transition. All other ether blends fell in between.

In prior studies using this engine under non-impinging conditions we have found correlation coefficients for PM in mg/m^3 versus PMI ranging from 0.53 (*5*) to 0.82 (*39*) for fuel sets containing ethanol and isobutanol among other blendstocks. Figures 26-31 show the relationship of the three PM indices PMI, NREL Index, and PME to the three engine soot emission metrics: impingement zone soot, transition point, and non-impingement zone soot. Examining correlation of these indices with the entire fuel dataset, the highest correlation observed ($r^2 > 0.7$) was for PME or PMI in predicting the SOI transition point at condition A. PMI and the NREL Index also predicted non-impingement zone soot at condition A

with r^2>0.7. For all other cases correlation coefficients are lower. However, as shown in Figure 31, for the lower engine speed condition B, correlations for just the ethers or just the Fuel D alcohol blends with PMI and the NREL Index were reasonably high. For ether blends the correlation with PMI or the NREL Index was r^2>0.9, while correlation of soot emissions with PMI for the Fuel D alcohol blends was r^2 =0.77. Under these low engine speed conditions dilution effects dominated and these are reasonably well captured by the PMI and the NREL Index. Nevertheless, to capture trends in PM emissions for the very wide range of oxygenate blends considered in this study indices that more accurately represent both HOV/VLE effects as well as fuel property effects on the fuel spray will need to be developed.

Note that examination of these data as percent change in soot relative to the base fuel resulted in markedly worse correlations with PM indices.

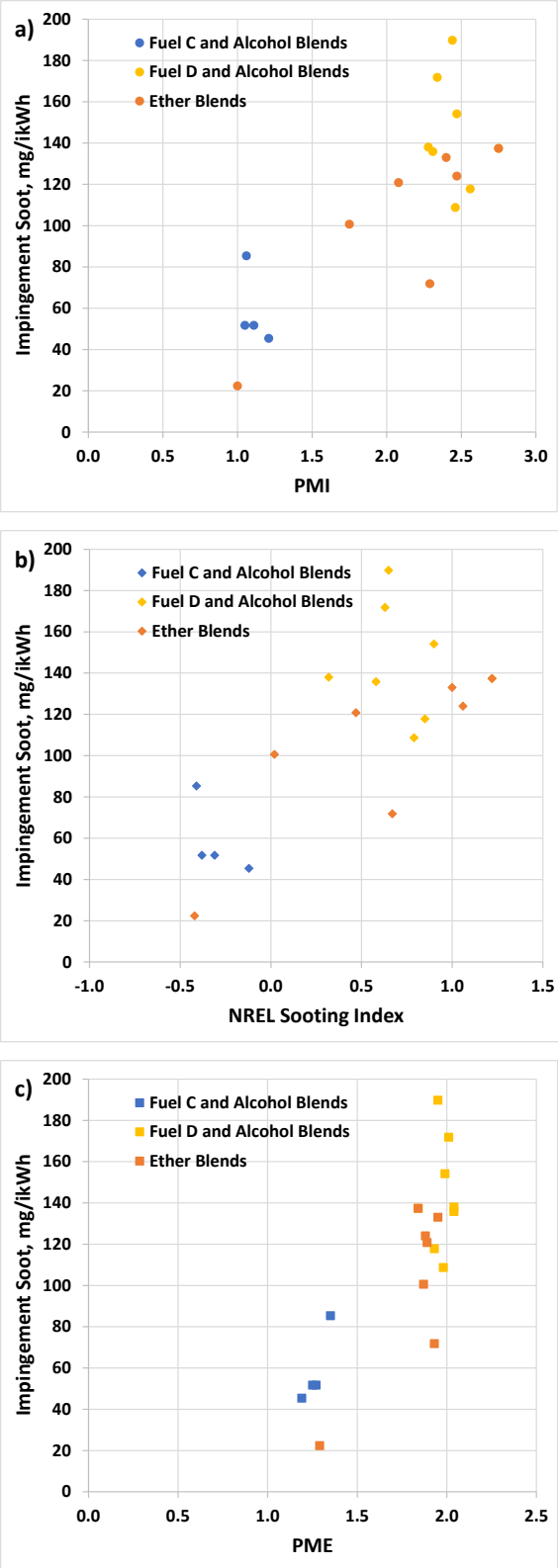

Figure 26. Impingement zone soot emissions, condition A, compared to a) PMI (r^2=0.67), b) NREL Index (r^2=0.54), PME (r^2=0.68).

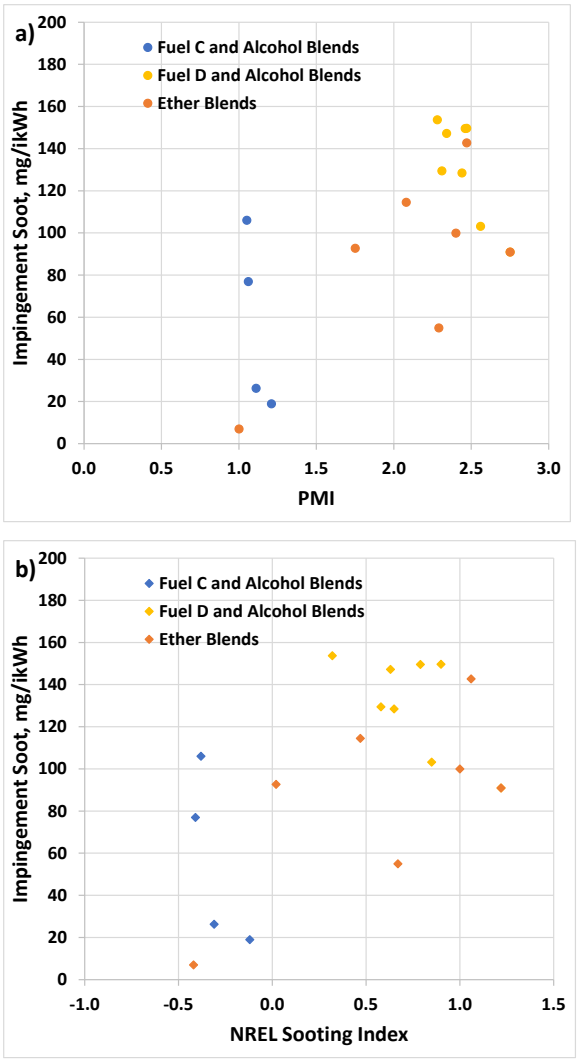

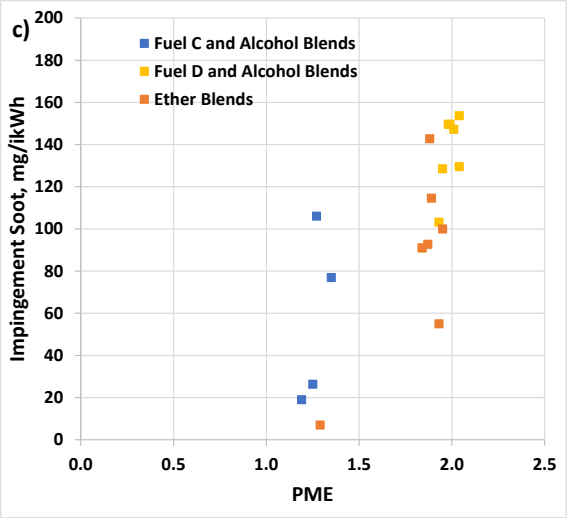

Figure 27. Impingement zone soot emissions, condition B, compared to a) PMI (r^2=0.51), b) NREL Index (r^2=0.40), PME (r^2=0.63).

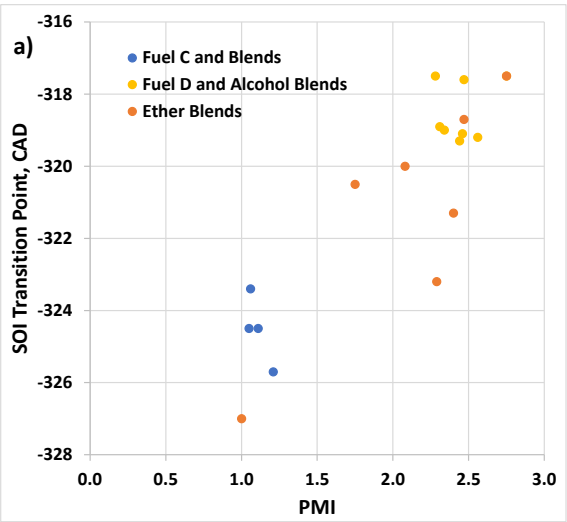

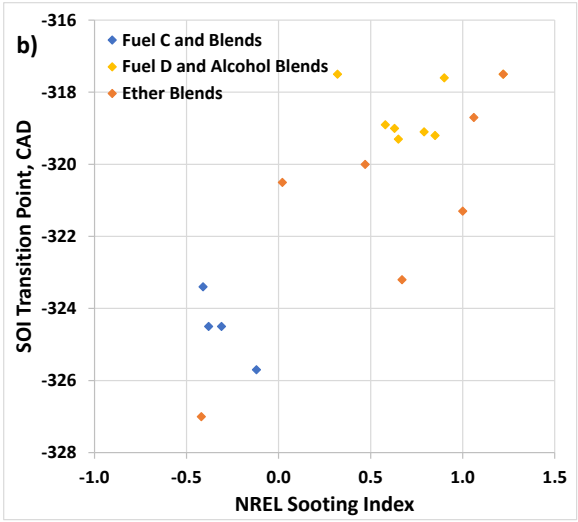

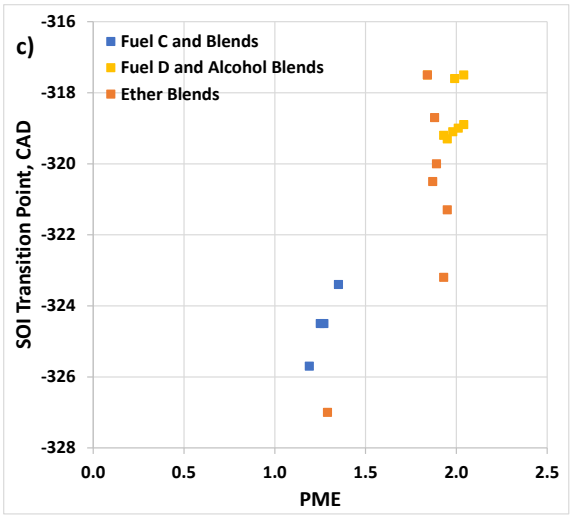

Figure 28. SOI transition point, condition A, compared to a) PMI (r2=0.76), b) NREL Index (r2=0.62), PME (r2=0.73).

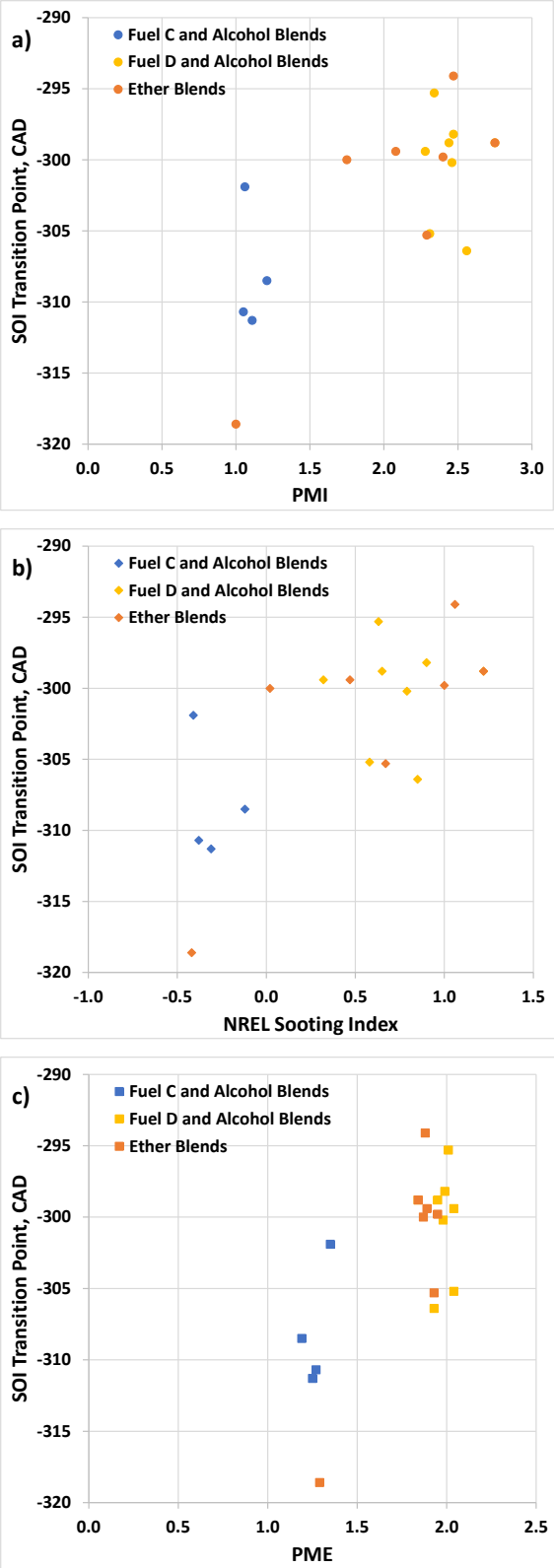

Figure 29. SOI transition point, condition B, compared to PMI (r2=0.37), b) NREL Index (r2=0.34), PME (r2=0.41).

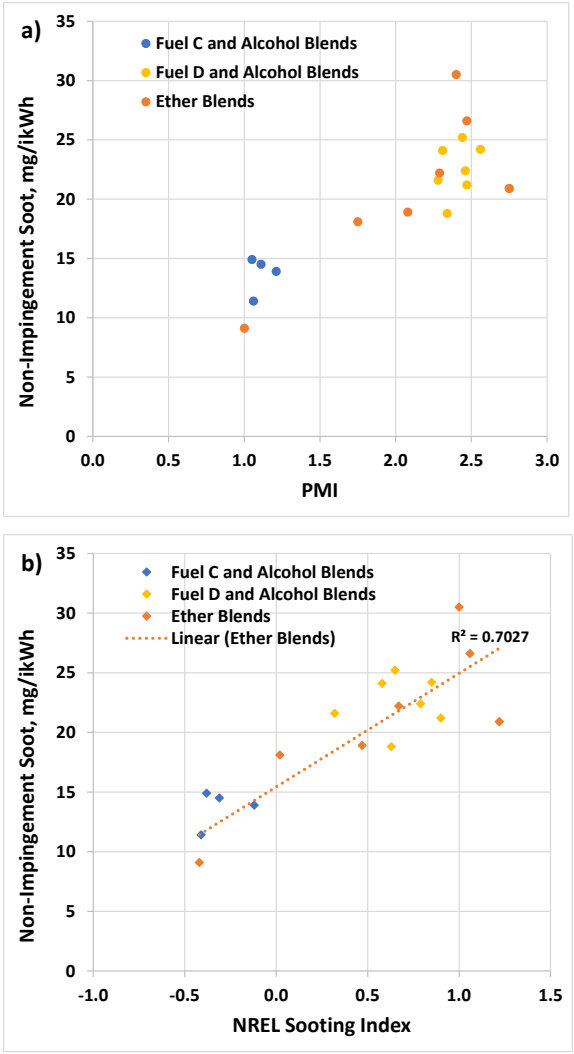

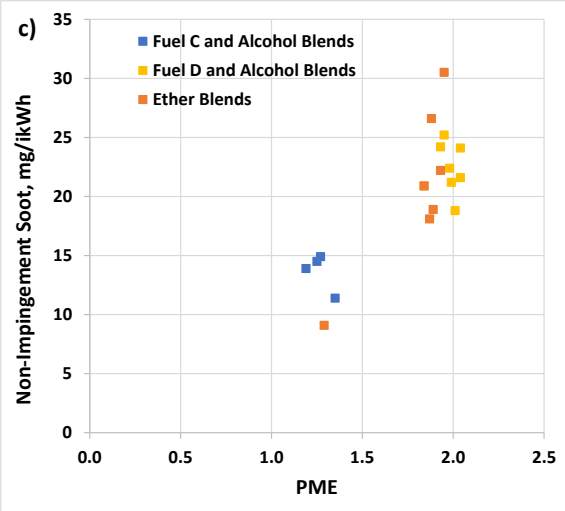

Figure 30. Non-impingement zone soot emissions, condition A, compared to a) PMI (r^2=0.72), b) NREL Index (r^2=0.71), PME (r^2=0.61).

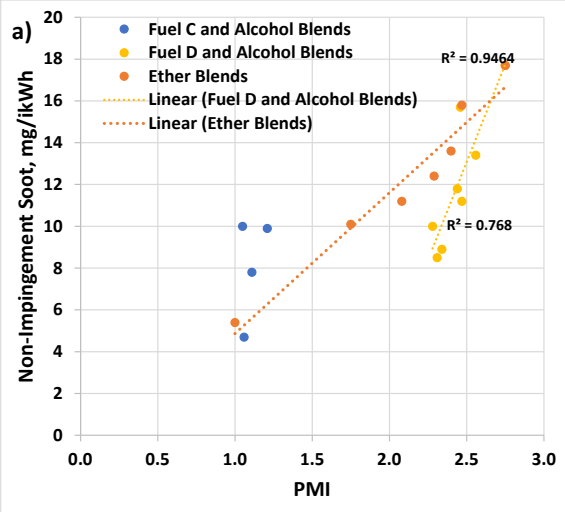

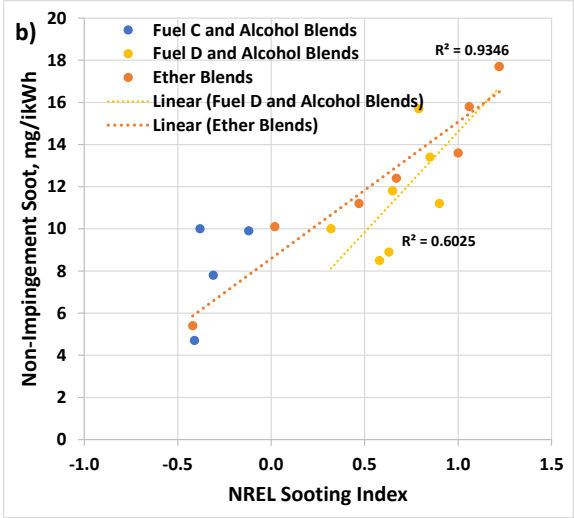

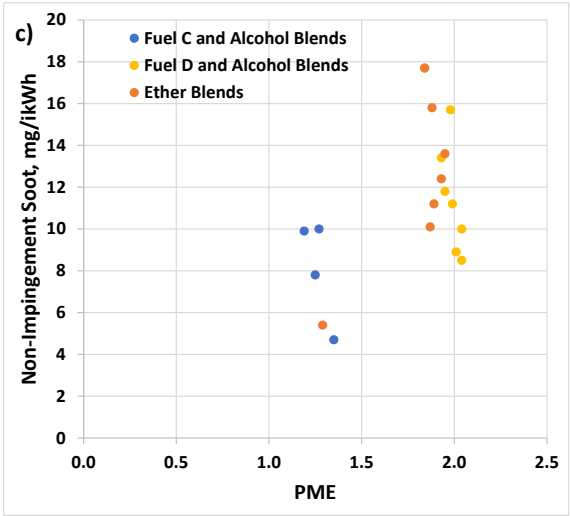

Figure 31. Non-impingement zone soot emissions, condition B, compared to a) PMI (r^2=0.52), b) NREL Index (r^2=0.61), PME (r^2=0.24).

Conclusions and Recommendations

The present study varied SOI to achieve both non-impinging and impinging conditions. If engine calibrators primarily avoid spray impinging conditions, results at non-impinging conditions may be more representative. For Fuel C blends with ethanol under this condition, E15 showed similar soot emissions to the base fuel, with E10 showing the same or lower emissions. These results imply that HOV/VLE effects can produce fuel rich zones even when the spray is not impinging on the piston. In the SCE study the spray may impinge on the cylinder liner, or HOV/VLE effects may be large enough to slow droplet evaporation to the point that fuel rich zones exist in the gas phase at the time the fuel is ignited. This contrasts with the dominance of dilution in the original E-129 study. For Fuel D ethanol blends soot emissions increased relative to the base fuel at the high engine speed condition. However, at the lower engine speed condition dilution effects dominated such that ethanol blends reduced soot formation. Taken together, these results show that both HOV/VLE and dilution effects can impact soot formation from ethanol blends, depending on engine operating conditions and the properties of the base fuel. Lower engine speeds that provide more time for heat transfer, evaporation, and mixing favor dilution effects and hence lower soot. Note that examination of these data as percent change in soot relative to the base fuel resulted in markedly worse correlations with PM indices.

The other oxygenates examined exhibited a wide range of behaviors. At the slow engine speed condition for non-impingement both alcohols and ethers showed a strong aromatics dilution effect to reduced soot formation, with moderate to strong correlations with PMI and the NREL Sooting Index. However, at high speed and non-impingement HOV/VLE effects appeared to be dominant for alcohols causing increased soot for methanol and ethanol or the same soot as the base fuel for propanol and isobutanol in Fuel D and a poor correlation with PMI. In the much lower PMI Fuel C, isobutanol showed dilution effects. These effects do not show a strong correlation with HOV, likely because dilution, HOV, and VLE effects are of a different magnitude for each alcohol, and all affect the results. For the ethers at high engine speed ETBE reduced soot, while DMM blends increase soot. Because these effects were not observed at low engine speeds, some aspects of ETBE and DMM properties appear to be inhibiting fuel evaporation and mixing enough to create fuel rich regions at high engine speed.

Similar to the results for this study, specific questions that arise from the prior E-129 and E-94-2 studies would appear to be explainable by the interplay between aromatics dilution and HOV/VLE effects in most cases. In particular:

- Why does 10% ethanol fuel increases PM emissions in comparison to E0 fuels of equal PMI value in E-94-2? This result was observed at both low (1.4) and high (2.6) PMI values (*1*).
    - For the vehicles and test conditions used in E-94-2 the results suggest that HOV/VLE effects were more important than dilution effects.
- Why does 15% ethanol fuel not display the same emissions behavior as 10% ethanol in the E-129 study? In the E-129 study 10% ethanol had no statistically significant effect on PM, implying that any dilution effect was too small to be measured or that HOV/VLE effects were dominant over dilution (*2*).

    - Ethanol blends containing 15% reduced PM significantly, but not as much as isobutanol and MTBE blends. The result for E15 appears to be caused by a combination of dilution (PM emissions went down) and HOV/VLE effects (i.e., based on molar dilution only, PM emissions should have been lower than observed for isobutanol and MTBE).
- Why do the 15% ethanol fuel and the fuels oxygenated with isobutanol and MTBE follow the PMI trend line for E0 fuels that was established in the prior CRC E-94-2 study, rather than being offset above like the 10% ethanol fuel?
    - The rationale is the same as for the question above. For E10 the effect of dilution is too small to see, or the result is dominated by HOV/VLE effects. While for E15 dilution effects reduce PM but not as much as expected because of HOV/VLE.

A recommendation for future studies of oxygenates blended into base fuels is to perform a DHA on the base fuels, and then for the oxygenate blends to carefully measure the oxygenate content using an oxygenate-specific method. The DHA of the oxygenate blends can then be calculated from a material balance. While this clearly requires significantly fewer resources than measuring DHA for a large fuel set, it may also be more accurate as hydrocarbon species at relatively low concentrations are diluted by blending the oxygenate, making them even harder to quantify in the oxygenate blends. In addition, this approach obviates the need to quantify oxygenates using the DHA, which can be fraught with challenges.

A second recommendation is to measure a complete set of fuel properties for the fuels used in future studies. Viscosity and surface tension can have a significant impact on fuel spray penetration, spray angle, and droplet mean diameter – all of which can impact spray impingement and fuel evaporation. Examination of how ethers impact aromatics evaporation may explain ether results that did not conform to the dilution theory. This could be conducted by DSC/TGA/MS, for example (*7*). Simulation of the evaporation of fuels from liquid films or pools with varying fuel properties may also provide insight.

The effects of much higher fuel injection pressure and split injections, which separately or combined can significantly reduce soot emissions, would be worthy of further investigation. Especially at condition A where high levels of methanol and ethanol increased soot relative to base fuel D and the ETBE blends did not significantly reduce soot. Similarly, condition B, where isobutanol retarded the transition point and increased soot in the impingement zone, may be beneficially impacted by changing these injection parameters. Another interesting study to consider is the independent effect of fuel temperature on soot emissions and the onset of flash boiling impacts on soot – flash boiling occurs when the cylinder pressure during fuel injection is below the saturation vapor pressure of the fuel, producing radically different fuel atomization and mixing than in a standard spray (*8*).

The complex nature of the interaction between flow in the injector, spray physics, fuel evaporation (HOV/VLE), and aromatics dilution may require development or application of a high-performance computational model of fuel injection and evaporation. Spray chamber studies may facilitate this research and facilitate the development of spray models. To predict trends in PM emissions for various oxygenate blends, indices that more accurately represent both HOV/VLE effects as well as fuel property

effects on the fuel spray need to be developed. We recommend developing correlations based on indicated soot mass emissions (mg/ikWh) instead of percent change in soot relative to the base fuel because this resulted in better correlations with PM indices.

It is important to note that this study was conducted using a warmed-up engine under steady-state conditions while real world vehicle operation, as well as emissions compliance testing, includes cold starting along with transient operation and complex speed-load changes. While the present results can provide insights into the physical phenomena governing fuel effects on soot emissions, predicted fuel impacts must be validated using full vehicle tests over complete driving cycles.

References

1. Coordinating Research Council. *CRC Report No. E-94-2: Evaluation and Investigation of Fuel Effects on Gaseous and Particulate Emissions on SIDI In-Use Vehicles;* www.crcao.org, 2017.

2. Coordinating Research Council. *CRC Report E-129: Alternative Oxygenate Effects on Emissions;* www.crcao.org, 2019.

3. St John, P.; Kim, S.; McCormick, R. Development of a Data-Derived Sooting Index Including Oxygen-Containing Fuel Components. *Energy and Fuels* **2019,** *33* (10), 10290-10296.

4. Coordinating Research Council. *CRC Report No. RW-107-2: An Improved Index for Particulate;*, 2021.

5. Ratcliff, M.; Windom, B.; Fioroni, G.; St John, P.; Burke, S.; Burton, J.; Christensen, E.; Sindler, P.; McCormick, R. Impact of Ethanol Blending into Gasoline on Aromatic Compound Evaporation and Particle Emissions from a Gasoline Direct Injection Engine. *Applied Energy* **2019,** *250,* 1618-1631.

6. Christensen, E.; Yanowitz, J.; Ratcliff, M.; McCormick, R. Renewable Oxygenate Blending Effects on Gasoline Properties. *Energy and Fuels* **2011,** *25,* 4723-4733.

7. Fioroni, G.; Fouts, L.; Christensen, E.; McCormick, R. Heat of Vaporization and Species Evolution During Gasoline Evaporation Measured by DSC/TGA/MS for Blends of C1 to C4 Alcohols in Commercial Gasoline Blendstocks. *SAE Technical Paper 2019-01-0014* **2019**.

8. Lacey, J.; Poursadegh, F.; Brear, M.; Gordon, R.; Petersen, P.; Lakey, C.; Butcher, B.; Ryan, S. Generalizing the behavior of flash-boiling, plume interaction and spray collapse for multi-hole, direct injection. *Fuel* **2017,** *200,* 345-356.

9. Leone, T.; Anderson, J.; Davis, R.; Iqbal, A.; Reese, R.; Shelby, M.; Studzinski, W. The Effect of Compression Ratio, Fuel Octane Rating, and Ethanol Content on Spark-Ignition Engine Efficiency. *Environmental Science and Technology* **2015,** *49,* 10778-10789.

10. U.S. Environmental Protection Agency. Control of Air Pollution From Motor Vehicles: Tier 3 Motor Vehicle Emission and Fuel Standards. *Federal Register* **2014,** *79* (81), 23414.

11. Chow, E.; Heywood, J.; and Speth, R. Benefits of a Higher Octane Standard Gasoline for the U.S. Light-Duty Vehicle Fleet. *SAE Technical Paper 2014-01-1961* **2014,** No. doi:10.4271/2014-01-1961.

12. Saliba, G.; Saleh, R.; Zhao, Y.; Presto, A.; Lambe, A.; Frodin, B.; Sardar, S.; Maldonado, H.; Maddox, C.; May, A.; Drozd, G.; Goldstein, A.; Russell, L.; Hagen, F.; Robinson, A. Comparison of Gasoline Direct-Injection (GDI) and Port Fuel Injection (PFI) Vehicle Emissions: Emissions Certification

Standards, Cold-Start, Secondary Organic Aerosol Formation Potential, and Potential Climate Impacts. *Environmental Science and Technology* **2017,** *51,* 6542-6552.

13. Fatouraie, M.; Wooldridge, M.; Wooldridge, S. In-Cylinder Particulate Matter and Spray Imaging of Ethanol/Gasoline Blends in a Direct Injection Spark Ignition Engine. *SAE International Journal of Fuels and Lubricants* **2013,** *6* (1), 1-10.

14. Velji, A.; Yeom, K.; Wagner, U.; Spicher, U.; al, e. Investigations of the Formation and Oxidation of Soot Inside a Direct Injection Spark Ignition Engine Using Advanced Laser-Techniques. *SAE Technical Paper 2010-01-0352* **2010**.

15. U.S. Energy Information Agency. Almost all U.S. gasoline is blended with 10% ethanol, 2016. Today in Energy. https://www.eia.gov/todayinenergy/detail.php?id=26092 (accessed October 17, 2021).

16. U.S. Environmental Protection Agency. Partial waiver for E15 use in MY 2001-2006 light-duty motor vehicles. *Federal Register* **2011,** *76* (17), 4662.

17. Butler, A.; Sobotowski, R.; Hoffman, G.; Machiele, P. Influence of Fuel PM Index and Ethanol Content on Particulate Emissions from Light-Duty Gasoline Vehicles. *SAE Technical Paper* **2015,** *2017-01-1072*.

18. Coordinating Research Council. *CRC Report E-94-3: Impacts of Splash-Blending on Particulate Emissions for SIDI Engines;* www.crcao.org, 2018.

19. He, X.; Ratcliff, M.; Zigler, B. Effects of Gasoline Direct Injection Engine Operating Parameters on Particle Number Emissions. *Energy & Fuels* **2012,** *26* (4), 2014-2027.

20. Chen, Y.; Zhang, Y.; Cheng, W. Effects of Ethanol Evaporative Cooling on Particulate Number Emissions in GDI Engines. *SAE Technical Paper 2018-01-0360* **2018**.

21. Sakai, S.; Rothamer, D. Effect of Ethanol Blending on Particulate Formation from Premixed Combustion in Spark-Ignition Engines. *Fuel* **2017,** *196,* 154-168.

22. ASTM International. *ASTM D6729-20 Standard Test Method for Determination of Individual Components in Spark Ignition Engine Fuels by 100 Metre Capillary High Resolution Gas Chromatography;* West Conshohocken, PA 19428-2959.

23. ASTM International. *ASTM D6730-21 Standard Test Method for: Determination of Individual Components in Spark Ignition Engine Fuels by 100-Meter Capillary (with Pre-column) High-Resolution Chromatography;* West Conshohocken, PA 19428-2959.

24. Coordinating Research Council. *CRC Report AVFL-29: ENHANCED SPECIATION OF;*, 2018.

25. ASTM International. *ASTM D4626-95(19) Standard Practice for Calculation of Gas Chromatographic Response Factors;* West Conshocken, PA 19428-2959.

26. ASTM International. *ASTM D7096-19 Standard Test Method for Determination of the Boiling Range Distribution of Gasoline by Wide-Bore Capillary Gas Chromatography;* West Conshocken, PA 19428-2959.

27. Aikawa, K.; Sakurai, T.; Jetter, J. Development of a Predictive Model for Gasoline Vehicle Particulate Matter Emissions. *SAE Technical Paper 2010-01-2115* **2010**.

28. Perry, R. G. D. *Perry's Chemiocal Engineers' Handbook;* McGraw-Hill, 1999; pp 2-346.

29. Yaws, C.; Satyro, M. *The Yaws Handbook of Physical Properties for Hydrocarbons and Chemicals, Chapter 1: Physical Properties - Organic Compounds;* Elsevier: Amsterdam, 2015.

30. American Petroleum Institute. *API Technical Data Book - Petroleum Refining;* American Petroleum Institute Publishing Services: Washington, DC, 1993.

31. Reid, R.; Prausnitz, J.; Poling, B. *The Properties of Gases and Liquids,* 4th ed.; McGraw Hill: New York, 1987.

32. Das, D.; St. John, P.; McEnally, C.; Kim, S.; Pfefferle, L. Measuring and Predicting Sooting Tendencies of Oxygenates, Alkanes, Alkenes, Cycloalkanes, and Aromatics on a Unified Scale. *Combustion and Flame* **2018,** *190,* 349-364.

33. Fioroni, G.; Hays, C.; Christensen, E.; McCormick, R. Reduced Sample Loss in DSC/TGA Measurement of Heat of Vaporization of Ethanol/Gasoline Blends by Differential Scanning Calorimetry/Thermogravimetric Analysis. *SAE International Journal of Fuels and Lubricants* **2021,** *14* (3), 175-276.

34. Zeng, W.; Xu, M.; Zhang, M.; Zhang, Y.; Cleary, D. Macroscopic characteristics for direct-injection multi-hole sprays using dimensionless analysis. *Experimental Thermal and Fluid Science* **2012,** *40,* 81-92.

35. Zigan, L.; Schmitz, I.; Flugel, A.; Knorsch, T.; Wensing, M.; Leipertz, A. Effect of Fuel Properties on Spray Breakup and Evaporation Studied for a Multihole Direct Injection Spark Ignition Injector. *Energy and Fuels* **2010,** *24,* 4341-4350.

36. McEnally, C.; Pfefferle, L. Sooting Tendencies of Oxygenated Hydrocarbons in Laboratory-Scale Flames. *Environmental Science and Technology* **2011,** *45,* 2498-2503.

37. Sarathy, S.; Osswald, P.; Hansen, N.; Kohse-Hoinghaus, K. Alcohol combustion chemistry. *Progress in Energy and Combustion Science* **2014,** *44,* 40-102.

38. Ratcliff, M.; Luecke, J.; Williams, A. C. E.; Yanowitz, J.; McCormick, R. Impact of Higher Alcohols Blended in Gasoline on Light-Duty Vehicle Exhaust Emissions. *Environmental Science and Technology* **2013,** *47,* 13865-13872.

39. Ratcliff, M.; Burton, J.; Sindler, P.; Christensen, E.; Fouts, L.; Chupka, G.; McCormick, R. Knock Resistance and Fine Particle Emissions for Several Biomass-Derived Oxygenates in a Direct Injection Spark-Ignition Engine. *SAE Int. J. Fuels Lubr.* **2016,** *9* (1), 59-70.

Appendix A: Injection Pressure and λ Sweep Results

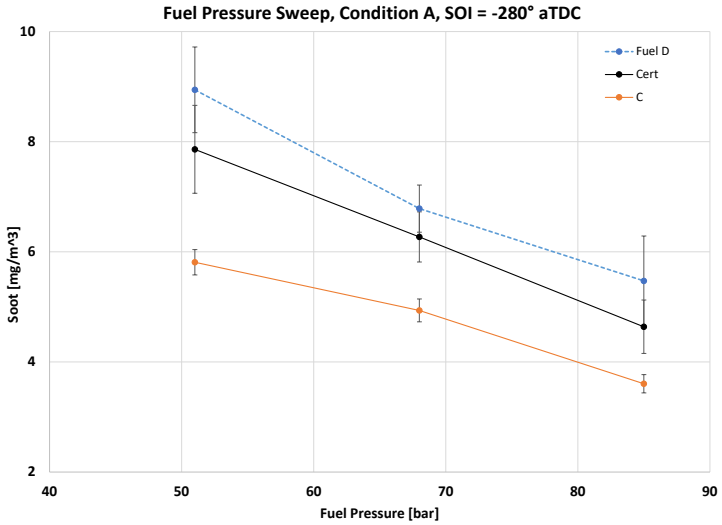

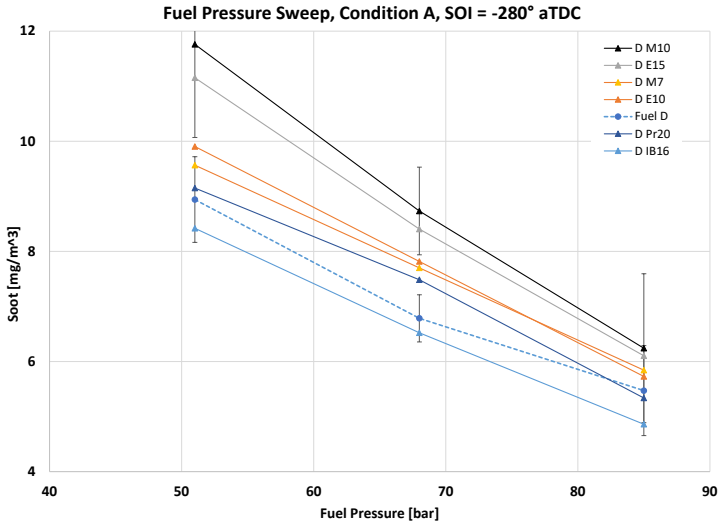

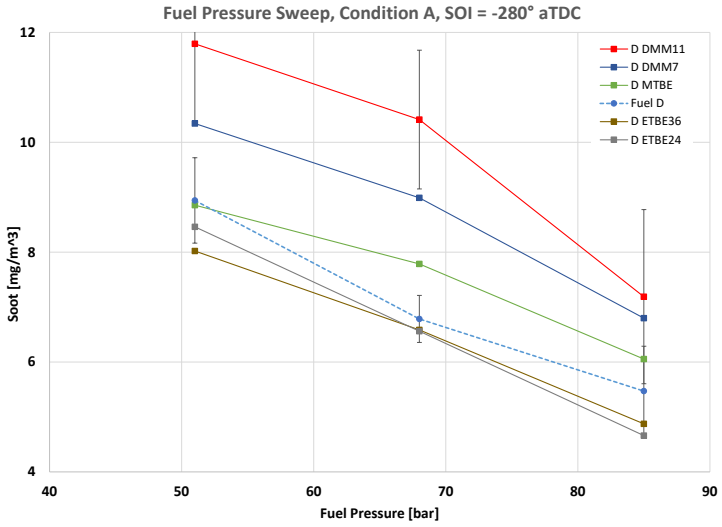
Fuel Pressure Sweep, Condition A, SOI = -280° aTDC
D DMM11
D DMM7
D MTBE
Fuel D
D ETBE36
D ETBE24
Soot [mg/m^3]
Fuel Pressure [bar]
12
10
8
6
4
40
50
60
70
80
90

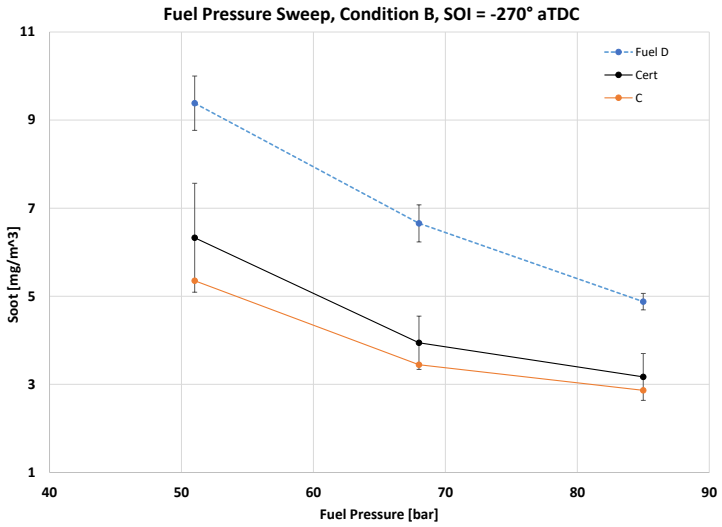
Fuel Pressure Sweep, Condition B, SOI = -270° aTDC
Fuel D
Cert
C
Soot [mg/m^3]
Fuel Pressure [bar]
11
9
7
5
3
1
40
50
60
70
80
90

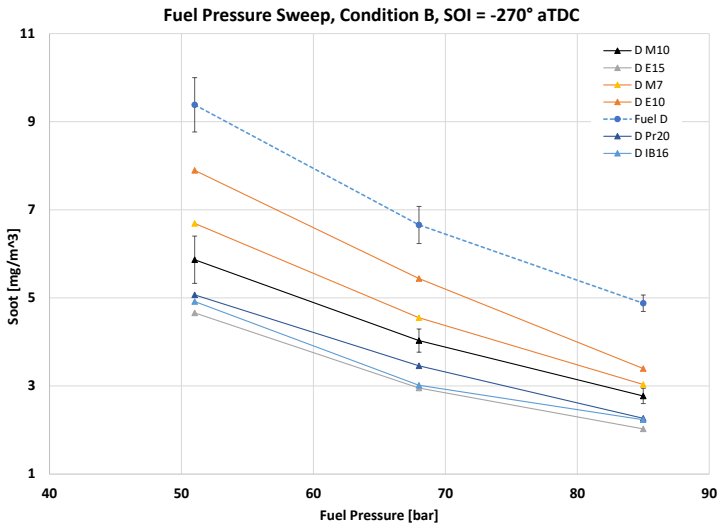
Fuel Pressure Sweep, Condition B, SOI = -270° aTDC
D M10
D E15
D M7
D E10
Fuel D
D Pr20
D IB16
Soot [mg/m^3]
Fuel Pressure [bar]
11
9
7
5
3
1
40
50
60
70
80
90

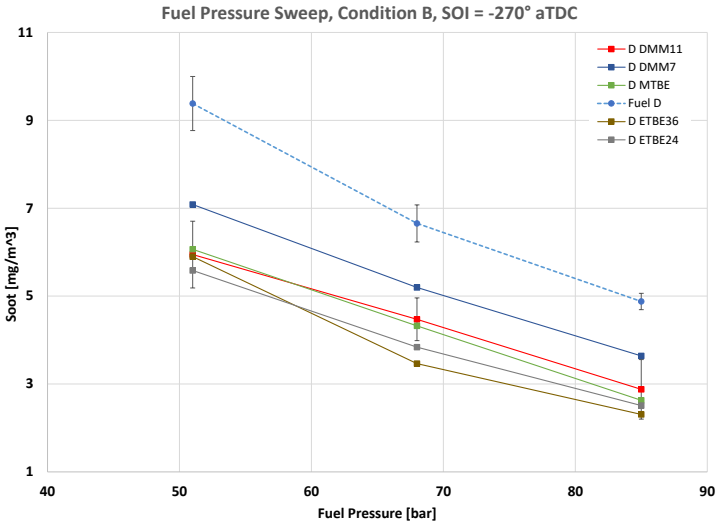
Fuel Pressure Sweep, Condition B, SOI = -270° aTDC
D DMM11
D DMM7
D MTBE
Fuel D
D ETBE36
D ETBE24
Soot [mg/m^3]
Fuel Pressure [bar]
11
9
7
5
3
1
40
50
60
70
80
90

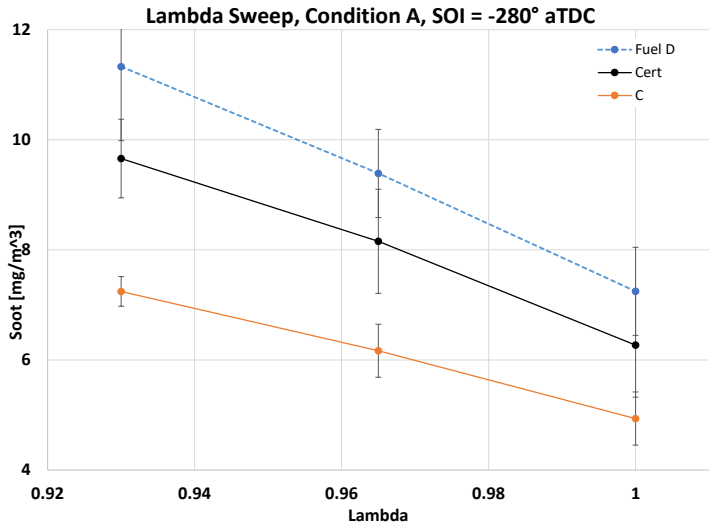
Lambda Sweep, Condition A, SOI = -280° aTDC
Fuel D
Cert
C
Soot [mg/m^3]
Lambda
12
10
8
6
4
0.92
0.94
0.96
0.98
1

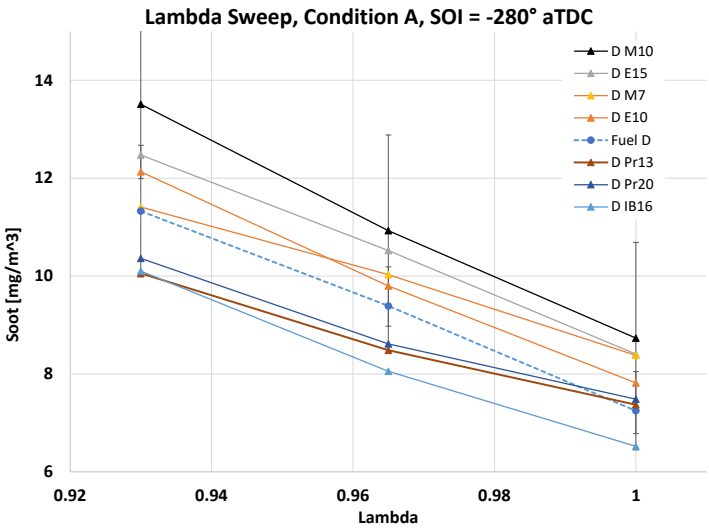
Lambda Sweep, Condition A, SOI = -280° aTDC
D M10
D E15
D M7
D E10
Fuel D
D Pr13
D Pr20
D IB16
Soot [mg/m^3]
Lambda
14
12
10
8
6
0.92
0.94
0.96
0.98
1

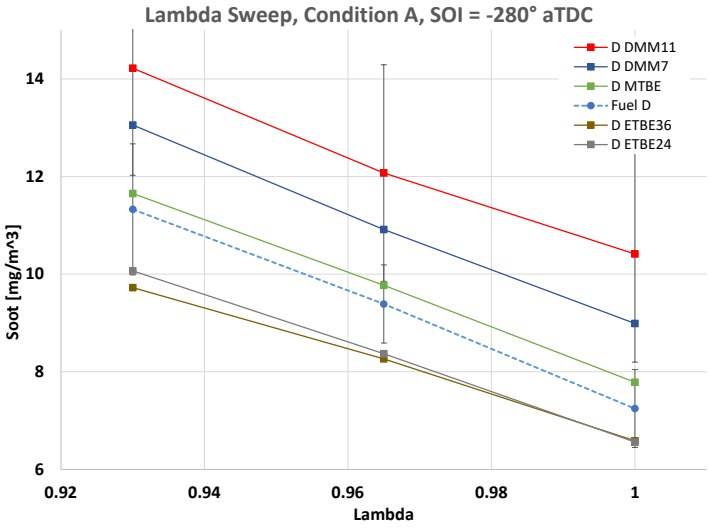
Lambda Sweep, Condition A, SOI = -280° aTDC
D DMM11
D DMM7
D MTBE
Fuel D
D ETBE36
D ETBE24
Soot [mg/m^3]
Lambda
14
12
10
8
6
0.92
0.94
0.96
0.98
1

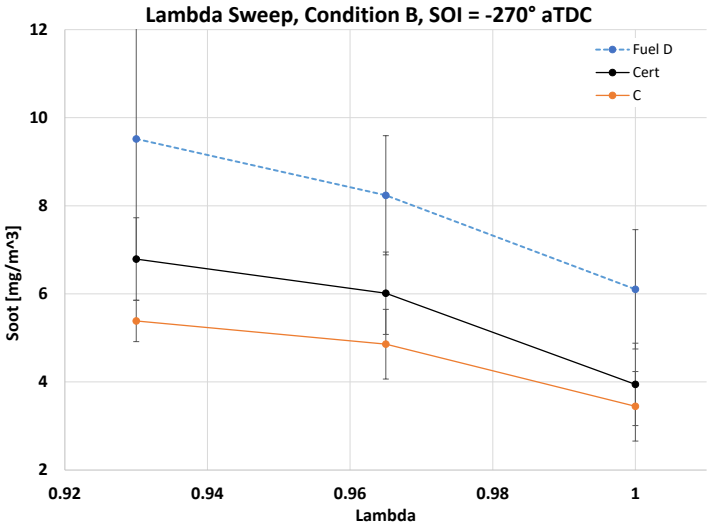
Lambda Sweep, Condition B, SOI = -270° aTDC
Fuel D
Cert
C
Soot [mg/m^3]
Lambda
12
10
8
6
4
2
0.92
0.94
0.96
0.98
1

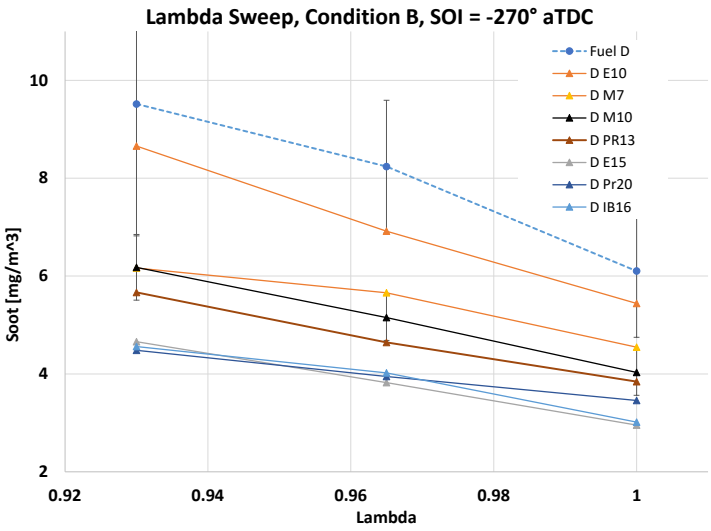
Lambda Sweep, Condition B, SOI = -270° aTDC
Fuel D
D E10
D M7
D M10
D PR13
D E15
D Pr20
D IB16
Soot [mg/m^3]
Lambda
10
8
6
4
2
0.92
0.94
0.96
0.98
1

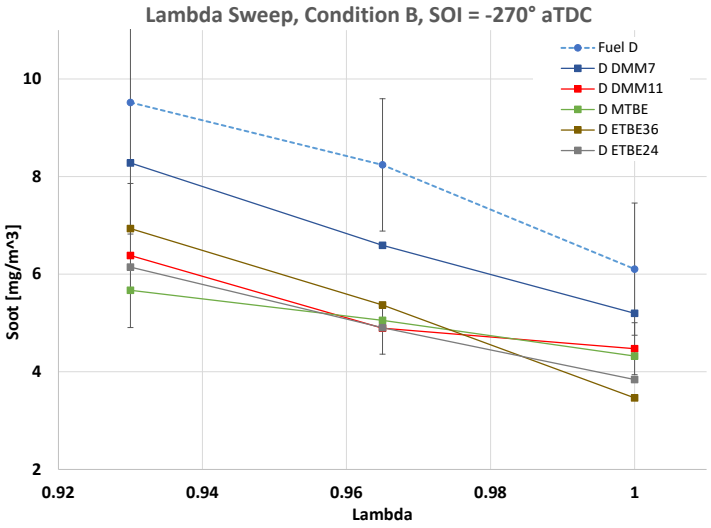
Lambda Sweep, Condition B, SOI = -270° aTDC
Fuel D
D DMM7
D DMM11
D MTBE
D ETBE36
D ETBE24
Soot [mg/m^3]
Lambda
10
8
6
4
2
0.92
0.94
0.96
0.98
1

Appendix B: Fuel Test Order

1	C-EtOH-15
2	Cert. Gasoline *
3	C-EtOH-10
4	C-MTBE-19
5	Fuel C
6	D-EtOH-10
7	D-EtOH-15
8	D-MeOH-10
9	Cert. Gasoline *
10	D-MTBE-19
11	D-MeOH-7
12	D-PrOH-20
13	D-PrOH-13
14	Fuel D *
15	D-ETBE-24
16	D-ETBE-35
17	D-DMM-12
18	D-DMM-8
19	D-iBu-16
20	C-iBu-16
21	Fuel D *
22	Cert. Gasoline *

*Fuels with replicates

Note: Fuel D was originally the first test fuel, however, the fuel injector was replaced part way through testing of the C-EtOH-15 fuel. After review, all data prior to the injector swap were removed from the analysis, including Condition A for C-EtOH-15.

Appendix C: Emissions Results Data

Fuel C Blends at Condition A

Non-Impingement Emissions @ -280° aTDC	**Cert. Gasoline**	**Fuel C**	**C-EtOH-10**	**C-EtOH-15**	**C-iBu-16**	**C-MTBE-19**
Soot, mg/ikWh	17.9 ± 1.3	13.9 ± 0.6	14. 5± 1.9	14.9 ± 1.1	11.4 ± 1.3	9.1 ± 0.4
NOx, g/ikWh	12.9 ± 0.2	12.6 ± 0.1	12.5 ± 0.1	12.5 ± 0.1	12.8 ± 0.2	12.3 ± 0.1
Total Hydrocarbons, g/ikWh	5.4 ± 0.2	5.0 ± 0.2	4.9 ± 0.2	5.0 ± 0.2	5.0 ± 0.3	4.1 ± 0.1
CO, g/ikWh	19.6 ± 1.0	19.8 ± 0.7	19.3 ± 0.8	17.5 ± 1.9	20.4 ± 0.8	19.9 ± 0.7
Impingement Emissions @ -330° aTDC						
Soot, mg/ikWh	69.8 ± 8.9	45.4 ± 6.3	51.7 ± 4.4	NA	85.4 ± 7.5	22.4 ± 5.3
NOx, g/ikWh	11.5 ± 0.1	11.5 ± 0.0	11.3 ± 0.0	NA	11.4 ± 0.0	11.3 ± 0.1
Total Hydrocarbons, g/ikWh	3.2 ± 0.1	3.0 ± 0.1	3.0 ± 0.1	NA	3.2 ± 0.2	2.3 ± 0.1
CO, g/ikWh	20.5 ± 0.5	19.0 ± 0.6	18.8 ± 0.4	NA	22.4 ± 0.4	18.2 ± 0.7
Transition Point , ° aTDC	-322.5	-325.7	-324.5	NA	-323.4	-327.0

Note: ± values are 95% confidence intervals

Fuel C Blends at Condition B

Non-Impingement Emissions @ -270° aTDC	**Cert. Gasoline**	**Fuel C**	**C-EtOH-10**	**C-EtOH-15**	**C-iBu-16**	**C-MTBE-19**
Soot, mg/ikWh	11.4 ± 2.0	9.9 ± 1.7	7.8 ± 1.4	10.0 ± 1.1	4.7 ± 0.4	5.4 ± 0.9
NOx, g/ikWh	13.1 ± 0.2	13.2 ± 0.2	12.8 ± 0.3	13.0 ± 0.2	13.4 ± 0.2	12.5 ± 0.2
Total Hydrocarbons, g/ikWh	5.6 ± 0.5	5.1 ± 0.2	5.0 ± 0.3	5.4 ± 0.2	5.1 ± 0.1	4.3 ± 0.2
CO, g/ikWh	17.6 ± 0.8	16.6 ± 0.7	17.9 ± 1.8	15.0 ± 1.3	18.5 ± 1.0	17.8 ± 1.3
Impingement Emissions @ -315° aTDC						
Soot, mg/ikWh	43.4 ± 11.8	18.7 ± 9.5	26.4 ± 5.3	106 ± 10*	77 ± 9*	7.4 ± 4.4*
NOx, g/ikWh	12.7 ± 0.2	12.9 ± 0.1	12.6 ± 0.1	12.9 ± 0.3*	12.8 ± 0.3*	12.4 ± 0.1*
Total Hydrocarbons, g/ikWh	4.1 ± 0.4	3.5 ± 0.2	4.0 ± 0.1	4.3 ± 0.1*	3.9 ± 0.2*	3.0 ± 0.2*
CO, g/ikWh	18.9 ± 0.8	17.6 ± 0.2	16.9 ± 0.8	14.6 ± 1.3*	19.2 ± 2.1*	17.2 ± 0.9*
Transition Point , ° aTDC	-308.5	-311.3	-310.7	-301.9	-299.2	-318.6

*Extrapolated or interpolated

Note: ± values are 95% confidence intervals

Fuel D Blends at Condition A

Non-Impingement Emissions @ -280° aTDC	**Fuel D**	**D-MeOH-7**	**D-MeOH-10**	**D-EtOH-10**	**D-EtOH-15**	**D-PrOH-13**	**D-PrOH-20**	**D-iBu-16**	**D-MTBE-19**	**D-ETBE-24**	**D-ETBE-35**	**D-DMM-8**	**D-DMM-12**
Soot, mg/ikWh	20.9 ± 0.6	24.2 ± 3.9	25.2 ± 2.3	22.4 ± 1.6	24.1 ± 0.4	21.2 ± 2.0	21.6 ± 1.2	18.8 ± 1.0	22.2 ± 1.4	18.9 ± 1.0	18.1 ± 0.7	26.6 ± 1.8	30.5 ± 3.2
NOx, g/ikWh	13.0 ± 0.1	13.1 ± 0.1	12.9 ± 0.1	12.6 ± 0.1	12.8 ± 0.1	12.9 ± 0.1	12.7 ± 0.1	12.9 ± 0.1	12.7 ± 0.1	12.8 ± 0.1	12.4 ± 0.1	13.1 ± 0.1	13.0 ± 0.0
Total Hydrocarbons, g/ikWh	6.0 ± 0.2	5.7 ± 0.3	5.8 ± 0.2	5.7 ± 0.1	5.6 ± 0.2	5.5 ± 0.2	5.4 ± 0.2	5.9 ± 0.1	5.4 ± 0.2	5.2 ± 0.2	5.1 ± 0.1	5.2 ± 0.3	5.8 ± 0.2
CO, g/ikWh	19.1 ± 1.6	19.1 ± 0.7	19.5 ± 0.5	19.5 ± 0.3	18.8 ± 0.8	19.1 ± 0.9	18.8 ± 0.6	18.9 ± 1.0	18.2 ± 0.6	17.9 ± 0.6	18.9 ± 1.0	19.0 ± 0.9	18.9 ± 0.4
Impingement Emissions @ -325° aTDC													
Soot, mg/ikWh	78.8 ± 9.1	66.6 ± 19.1	98.5 ± 12.1	61.2 ± 2.6	76.2 ± 2.9	92.6 ± 1.1	81.5 ± 3.6	89.7 ± 13.3	25.4 ± 2.2	61.8 ± 8.2	51.9 ± 3.0	49.4 ± 8.1	54.3 ± 4.9
NOx, g/ikWh	11.7 ± 0.2	11.9 ± 0.2	11.7 ± 0.1	11.6 ± 0.2	11.6 ± 0.1	11.4 ± 0.1	11.5 ± 0.1	11.6 ± 0.1	11.5 ± 0.1	11.3 ± 0.2	11.2 ± 0.2	11.5 ± 0.2	11.5 ± 0.2
Total Hydrocarbons, g/ikWh	3.6 ± 0.0	3.7 ± 0.2	4.4 ± 0.2	3.7 ± 0.1	4.0 ± 0.2	3.5 ± 0.1	3.5 ± 0.2	3.7 ± 0.1	3.3 ± 0.3	3.3 ± 0.1	3.3 ± 0.1	3.6 ± 0.1	3.7 ± 0.2
CO, g/ikWh	19.9 ± 1.8	17.5 ± 1.3	18.0 ± 0.8	17.4 ± 0.6	17.0 ± 0.9	20.9 ± 1.2	18.5 ± 1.1	19.8 ± 1.1	17.8 ± 1.0	20.6 ± 2.0	19.2 ± 1.4	23.0 ± 1.7	21.1 ± 2.2
Transition Point , °aTDC	-317.5	-319.2	-319.3	-319.1	-318.9	-317.6	-317.5	-319.0	-323.2	-320.0	-320.5	-318.7	-321.2

Note: ± values are 95% confidence intervals

Fuel D Blends at Condition B

Non-Impingement Emissions @ -270° aTDC	**Fuel D**	**D-MeOH-7**	**D-MeOH-10**	**D-EtOH-10**	**D-EtOH-15**	**D-PrOH-13**	**D-PrOH-20**	**D-iBu-16**	**D-MTBE-19**	**D-ETBE-24**	**D-ETBE-35**	**D-DMM-8**	**D-DMM-12**
Soot, mg/ikWh	17.7 ± 1.1	13.4 ± 0.9	11.8 ± 0.8	15.7 ± 2.2	8.5 ± 1.0	11.2 ± 1.3	10.0 ± 0.5	8.9 ± 1.1	12.4 ± 1.4	11.2 ± 0.5	10.1 ± 1.4	15.8 ± 1.1	13.6 ± 1.5
NOx, g/ikWh	13.6 ± 0.2	13.5 ± 0.2	13.1 ± 0.2	13.1 ± 0.3	13.1 ± 0.2	13.3 ± 0.2	12.9 ± 0.2	13.2 ± 0.2	12.9 ± 0.2	12.8 ± 0.3	12.9 ± 0.1	13.6 ± 0.2	13.6 ± 0.1
Total Hydrocarbons, g/ikWh	6.6 ± 0.3	6.2 ± 0.2	6.1 ± 0.2	6.3 ± 0.2	5.6 ± 0.2	5.9 ± 0.1	5.6 ± 0.1	6.4 ± 0.2	5.7 ± 0.1	5.7 ± 0.1	5.4 ± 0.2	6.7 ± 0.2	6.4 ± 0.1
CO, g/ikWh	16.1 ± 1.6	16.9 ± 0.8	18.7 ± 1.4	16.2 ± 1.1	16.9 ± 0.5	16.1 ± 0.6	17.9 ± 0.8	18.1 ± 0.7	16.6 ± 0.8	17.7 ± 1.7	16.4 ± 0.6	18.2 ± 1.3	18.0 ± 0.7
Impingement Emissions @ -310° aTDC													
Soot, mg/ikWh	56.9 ± 6.7	45.7 ± 22.6	84 ± 36*	85.3 ± 15.3	58 ± 2.9	96 ± 6*	103 ± 13*	106 ± 7*	25.9 ± 16.6	59 ± 5.8	49.2 ± 11.8	112 ± 18*	63.7 ± 9.3
NOx, g/ikWh	13.0 ± 0.2	13.0 ± 0.2	12.9 ± 0.3*	12.8 ± 0.2	12.8 ± 0.1	12.7 ± 0.2*	12.7 ± 0.1*	12.7 ± 0.2*	12.6 ± 0.3	12.6 ± 0.1	12.6 ± 0.2	12.9 ± 0.1*	13.3 ± 0.2
Total Hydrocarbons, g/ikWh	4.5 ± 0.4	4.7 ± 0.1	4.9 ± 0.4*	5.2 ± 0.2	4.5 ± 0.2	4.3 ± 0.2*	4.4 ± 0.1*	4.6 ± 0.2*	3.9 ± 0.2	4.6 ± 0.1	4.4 ± 0.2	4.8 ± 0.1*	4.4 ± 0.2
CO, g/ikWh	18.1 ± 1.2	16.6 ± 1.3	17.6 ± 1.9*	16.2 ± 1.2	15.9 ± 0.3	16.8 ± 0.8*	17.9 ± 1.3*	19.5 ± 0.9*	15.9 ± 1.9	16.4 ± 0.7	16.3 ± 1.2	16.8 ± 0.2*	17.0 ± 1.5
Transition Point , °aTDC	-298.8	-306.4	-298.8	-300.2	-305.2	-298.2	-299.4	-295.3	-305.3	-299.4	-300.0	-294.1	-299.8

*Extrapolated or interpolated

Note: ± values are 95% confidence intervals

Appendix D: Discussion of Gaseous Emissions

Tabulated in Appendix C are the measured exhaust gas emissions from the fuels at selected non-impingement and spray impingement SOIs, for both engine operating conditions A and B. For reader convenience the appendix tables also include the corresponding soot emissions and transition point locations, but these were already discussed previously. Note that NOx, CO and total hydrocarbon (THC) emissions are reported on a gram per indicated kWh basis (g/ikWh), whereas the soot results reported here (and through this report) are on a milligram per indicated kWh (mg/ikWh) basis. The reported errors are 95% confidence intervals. Note also that CO exhibited higher variability than NOx and THCs, as indicated by much larger 95% confidence intervals for CO.

Hydrocarbon base fuels. At non-impingement SOIs, NOx emission rates were essentially the same (≈13 g/ikWh) across these fuels at both conditions A and B. The NOx range limits observed were 12.6 ± 0.1 g/ikWh from fuel C at condition A and 13.6 ± 0.2 g/ikWh from fuel D at condition B, indicating no significant fuel effects on NOx. At the selected spray impingement SOIs, overall NOx rates were lower, especially at condition A (≈11.5 g/ikWh), but again no significant differences between the hydrocarbon fuels were observed.

THC emissions exhibited fuel effects– fuel D produced higher emission rates at both operating conditions using non-impingement SOIs. For example, at condition B rates of 6.6, 5.6 and 5.1 g/ikWh were measured from fuel D, certification gasoline and fuel C, respectively. The higher THC emissions are correlated to higher final boiling points– 212°C, 199°C, and 193°C, respectively, and to a lesser extent with higher distillation T90s (see Table 4). At spray impingement SOIs, the overall THC emissions trend repeats, albeit at significantly lower rates. Comparisons of soot and THC trends among these base fuels show that these emissions are correlated. No statistically significant fuel effects on CO emissions were observed at non-impingement or spray impingement SOIs, or when comparing A and B conditions. Condition A produced slightly higher CO rates than condition B.

Fuel C blends. No large fuel effects on NOx emissions were observed, C-MTBE-19 produced 3-5% lower NOx at non-impingement SOIs at operating conditions A and B. The impingement SOI at condition B produced 2-4% lower NOx from C-EtOH-10 and C-MTBE-19, relative to fuel C.

C-MTBE-19 produced about 20% lower THC emissions than base fuel C at condition A using both impingement and non-impingement SOIs. But no effects from the alcohols were observed. At condition B, C-MTBE-19 alone produced slightly lower THCs at non-impingement SOI. Interestingly, impingement SOIs at condition B produced about 20% higher THC emissions from the ethanol blends, while C-MTBE-19 produced slightly lower emissions.

No statistically significant fuel effects on CO emissions were observed at non-impingement SOIs for conditions A and B. The averages suggest that C-EtOH-15 may reduce CO emissions and C-iBu-16 may increase CO emissions, relative to fuel C. However, the larger errors associated with the CO values make discernment of any fuel effects difficult. Similar observations arise from inspection of the impingement data.

Fuel D alcohol blends. No significant fuel effects on NOx were observed at condition A, with or without spray impingement SOI. Slightly lower (3-5%) NOx emissions were observed from most alcohol blends at condition B with non-impingement SOI. All alcohol blends produced slightly lower THC emissions relative to fuel D for non-impingement SOIs at conditions A and B, however, many were within measurement error. Notable exceptions include D-EtOH-15 and the n-propanol blends at condition A (7-10% lower THC), as well as D-EtOH-15 and D-PrOH-20 at condition B (15% lower THC). Most alcohol blends using spray impingement SOIs showed no fuel effects on THC emissions. However, at condition A, D-MeOH-10 and D-EtOH-15 increased THC emissions by 22% and 11%, respectively, while D-EtOH-10 increased THC emissions by 16% at condition B.

No fuel effects on CO emissions were observed from non-impingement SOIs at condition A, while many blends at condition B appeared to slightly increase CO relative to fuel D. However, larger CO errors mean most values are statistically the same. The exception is that CO emissions significantly increased from D-MeOH-10 (16%) at condition B.

Fuel D ether blends. The MTBE and ETBE blends reduced NOx emissions 4-5% at conditions A and B with non-impingement SOIs, and somewhat smaller reductions were observed from impingement SOIs at condition B. In contrast the DMM blends had no effect on NOx. Similarly, the MTBE and ETBE blends lowered THC emissions 10-18% at conditions A and B with non-impingement SOIs. Smaller and less consistent reductions were observed using impingement SOIs. The DMM blends did not impact THC emissions within the measurement errors.

No statistically significant fuel effects on CO emissions were observed at non-impingement SOIs for conditions A and B. The averages suggest that D-MTBE-19 and D-ETBE-24 may reduce CO emissions relative to fuel D at condition A, and that D-ETBE-24, D-DMM-8 and D-DMM-12 may increase CO at condition B. However, the larger errors associated with the CO values make discernment of actual fuel effects difficult. Similar observations arise from inspection of the impingement data.

Key summary observations-

- Among the hydrocarbon base fuels THC and soot emissions are correlated
- MTBE and ETBE blends slightly reduced NOx emissions
- MTBE and ETBE blends significantly reduced THC emissions at non-impingement SOIs
- Some ethanol and n-propanol blends in fuel D modestly reduced THC emissions at non-impingement SOIs
    - Thus, competing dilution and HOV effects may impact THC emissions
- Some methanol and ethanol blends in fuel D increased THC emissions at spray impingement SOIs